

INAUGURAL - DISSERTATION
zur
Erlangung der Doktorwürde
der
Naturwissenschaftlich - Mathematischen Gesamtfakultät
der
Ruprecht - Karls - Universität Heidelberg

Vorgelegt von:

Dipl.-Chem. Stefan V. W. Gräter

aus Esslingen a.N.

Tag der mündlichen Prüfung: 19.07. 2006

Design of Artificial Modular Extracellular Matrices

Gutachter: Prof. Dr. Joachim P. Spatz
Prof. Dr. Martin Möller

I.	Summary – Zusammenfassung	1
II.	Introduction and Motivation	5
III.	Theory and background	9
III.1.	Extracellular matrix	9
III.1.1.	What is the extracellular matrix?	9
III.1.2.	Components of the ECM	10
III.2.	Cell surface receptors.....	14
III.2.1.	Transmembrane receptors, and their various functions	15
III.2.2.	The integrin family of adhesion receptors	16
III.2.3.	L1 of the immunoglobulin family.....	18
III.3.	Interactions between cells and the ECM.....	19
III.3.1.	Mechanical interactions between cells and the ECM	19
III.3.2.	Chemical interactions between cells and the ECM.....	22
III.3.3.	Structural interactions between cells and the ECM.....	22
III.4.	Design of an artificial extracellular matrix	24
III.4.1.	Approaches used to mimic the extracellular matrix	24
III.4.2.	Concept of synthetic modular ECMs.....	30
IV.	PEG-based supports with tunable mechanical properties	32
IV.1.	Tuning the mechanical properties of PEG hydrogels	32
IV.1.1.	Crosslinking reaction of PEG-DA	32
IV.1.2.	Crosslinking parameters and mechanical properties.....	34
IV.2.	Characterizing the mechanical properties of a hydrogel.....	36
IV.2.1.	Determination of the mesh size, swelling and gel content.....	36
IV.2.2.	Measuring elasticity at the nanoscale	37
IV.3.	Experiments, results and discussion	39
IV.3.1.	Crosslinking of PEG	39
IV.3.2.	Gel content and swelling ratio	41
IV.3.3.	AFM Indentation.....	44
IV.4.	Conclusion	45
V.	Nanostructured polymeric supports	46
V.1.	Nanostructures	46
V.1.1.	Different nano-structuring approaches	46
V.1.2.	Block copolymer micelle nanolithography	47
V.1.3.	Preparation of gold nanopatterned substrates	51

V.2.	Transfer nanolithography.....	53
V.3.	Transfer of gold clusters to different polymers.....	54
V.3.1.	Linker system: Experiment and characterization.....	55
V.3.2.	Transfer of the gold particles: Experiments and results.....	59
V.4.	Conclusion	66
VI.	Preparation of patterned hydrogel channels.....	68
VI.1.	Decoration of non-planar glass structures.....	68
VI.2.	Transfer lithography for non-planar substrates.....	72
VI.3.	Conclusion	74
VII.	Chemical modification of PEG hydrogels.....	76
VII.1.	Introduction.....	77
VII.1.1.	Chemical properties of PEG hydrogels.....	77
VII.1.2.	Bio-molecules for surface activation	78
VII.2.	Bio-functionalization of gold particles on hydrogels.....	82
VII.2.1.	Binding of RGD peptides to the gold particles.....	83
VII.2.2.	Binding of proteins to the gold particles via a nickel-NTA complex..	84
VII.3.	Biofunctionalization of PEG hydrogels	87
VII.3.1.	Copolymerization of carboxyethylacrylate to the PEG-DA	88
VII.3.2.	Binding of peptides to the hydrogel.....	90
VII.3.3.	Binding of proteins to the hydrogel via a Nickel-NTA complex.....	91
VII.4.	Conclusion	94
VIII.	Cell response to various hydrogel modules	96
VIII.1.	Cell culture protocols.....	96
VIII.1.1.	Standard culture conditions.....	96
VIII.1.2.	Cell experiments on hydrogels.....	97
VIII.2.	Cells on biofunctionalized hydrogels.....	98
VIII.3.	Conclusion	105
IX.	Conclusion and future plans	107
X.	Materials.....	111
XI.	Acknowledgments	113
XII.	Bibliography	115

I. Summary – Zusammenfassung

Summary

Cellular functions such as cell growth, adhesion and differentiation are essentially controlled by the surrounding extracellular matrix (ECM). The mechanical, chemical and structural properties of the ECM are consequently crucial for the selection of cells at interfaces and the formation of tissues.

The objective of this thesis was to develop an artificial ECM to determine and control the parameters influencing the crosstalk between cells and their surroundings on a molecular level. Artificial ECMs which mimic the natural environment of cells enable precise insights into cell-ECM crosstalk; ultimately, we aim to trigger the crosstalk, such that specific cell functions are provoked. To this end, a modular ECM system was developed, consisting of (i) poly(ethylene glycol) (PEG) as the basic material, (ii) gold nano-particles as the structuring component, and (iii) bioactive molecules which are immobilized on the basic material and on the nano-structure, to equip these modules with a biological function. The mechanical, structural, and chemical properties of the artificial ECM, as defined by the respective modules, can be tuned independently from one another, enabling the customized tailoring of the artificial ECM for specific applications.

PEG hydrogels, used as both the basic material and first module of the artificial ECM, were chosen because of their resistance to protein adsorption, as well as their elastic and swelling properties, which partly mimic the hyaluronan material surrounding the cell membrane. A photo-initiated crosslinking reaction of PEG macromers was used to obtain hydrogels with well-controlled physical properties, characterized in terms of the gel content, swelling ratio, and mesh size. Elasticity at the nanoscale was assessed by an indentation method using atomic force microscopy (AFM). In this way, we were able to prepare hydrogel surfaces covering the biologically relevant range of elasticities.

Structuring the hydrogel substrates with nanoscale gold patterns as the second module of the artificial ECM was achieved by means of a newly-developed transfer lithography method. Gold particles of a particular size, and separated by a defined distance were obtained by using block copolymer micelle nanolithography, which itself is restricted to solid, inorganic, and planar surfaces such as glass slides; the gold particles are transferred to polymers by means of a thiol-gold coupling scheme. Depending on the polymer to be gold-decorated, an appropriate thiol linker molecule was incubated on the gold-patterned glass surface, and crosslinked to the PEG hydrogel during polymerization. The transfer resulted in a complete and accurate transfer of the nano-pattern to the polymer surface. Cryo-electron microscopy was used for structural characterization of the resulting surfaces, including water-containing soft hydrogels.

The transfer nano-lithography technique is the first method to successfully nanostructure soft and polymeric materials with metal structures on a large scale, and can in principle be applied to the structuring of any organic planar and non-planar surface. The structural properties of the artificial ECM, controlling, e. g., the clustering of receptors at adhesion sites of adhering cells, can be adjusted by choosing the particle size and distance of the original gold pattern. Another structural parameter can be introduced by the non-planarity of the surfaces. Hydrogel-based micro-channels have been developed that were internally decorated with gold nanoparticles, resulting in nanopatterned, tube-shaped artificial ECMs surrounding the cell in three dimensions, mimicking, for example, blood vessels.

As a third module of the artificial ECM, the nanostructured hydrogel surfaces were chemically modified to provide the cell with biofunctions. Proteins were coupled to the gold particles or the hydrogel surface via Ni(II)-NTA complexes, and peptides were coupled to the gold particles via thiol groups, or to the hydrogel surface via amino groups. The four different schemes were developed to specifically couple the bioactive molecules at well-defined orientations and in their native conformation to either the hydrogel surface or the gold moieties, without introducing either cytotoxicity or loss of biocompatibility. The selective functionalization was tested for representative biomolecules, the adhesion receptor-binding peptide RGD, the cell-cell adhesion protein L1, and the green fluorescent protein. This concept enables selective modification of the gold particles or the inter-particle surface by coupling virtually any biomolecule to the aforementioned domains of the artificial ECM.

The functionality of the three different components of the artificial ECM was tested in cell experiments. Experiments using substrates with various inter-gold particle spacing, biofunctionalizations, and cell types, demonstrated the applicability of the artificial ECM as such. Most importantly, for the first time, nanopatterned hydrogels were shown by cryo-SEM to be deformed by the adhering fibroblasts, thereby revealing the direct crosstalk between the cell and the ECM mimic on the molecular level. In addition, the functionality of non-planar substrates for cell experiments was demonstrated by means of micro-channels.

In conclusion, the modular artificial ECM, as developed in this research project, meets the mechanical, structural, and biological requirements necessary to serve as a versatile and adjustable tool to investigate and provoke specific cell-surface interactions. The artificial ECM provides a useful means by which to influence cell adhesion and function, thereby enabling systematic selection of cell types for biotechnological and medical applications.

Zusammenfassung

Zellfunktionen wie Wachstum, Adhäsion oder Differenzierung werden nachhaltig durch äußere Faktoren wie die mechanischen, chemischen und strukturellen

Eigenschaften der Extrazellulären Matrix (ECM) bestimmt. Damit nehmen diese Parameter eine entscheidende Rolle bei der Bildung von Geweben und der Selektion von Zellen an Grenzflächen ein.

Das Ziel dieser Arbeit war die Entwicklung einer künstlichen ECM, die es erlaubt die entscheidenden Parameter für den gegenseitigen Einfluss von Zellen und ihrer Umgebung auf molekularer Ebene zu kontrollieren. Eine solche künstliche Matrix erlaubt die Untersuchung der Wechselwirkungen zwischen Zellen und ihrer Umgebung und ermöglicht schliesslich die gezielte Kontrolle von Zellfunktionen durch äußere Einflüsse. Dafür wurde ein modulares System entwickelt bestehend aus (i) dem Basismaterial Poly(propylenglykol) (PEG), (ii) Gold-Nanostrukturen als strukturgebende Komponente und (iii) biologisch aktiven Molekülen, die auf dem nano-strukturierten Trägermaterial angebunden werden und diesen Modulen biologische Funktionalität verleihen. Die mechanischen, strukturellen und chemischen Eigenschaften, die durch die jeweiligen Module bestimmt werden, lassen sich unabhängig voneinander einstellen und für ausgewählte Anwendungen aufeinander abstimmen.

PEG Hydrogel wurde auf Grund seiner Resistenz gegen Proteinadsorption, den Elastizitäts- und Quelleigenschaften als Basismaterial gewählt, um das in der natürlichen ECM vorkommende Hyaluronan zu imitieren. Die photoinduzierte Vernetzungsreaktion der PEG Makromere zur Formung eines Hydrogels eignet sich gut um Eigenschaften des Hydrogels wie Gel Gehalt, Quellrate und Maschengröße zu kontrollieren. Die Elastizität der Oberflächen wurde auf Nanometer Skala mit einem Rasterkraftmikroskop bestimmt. Das System ermöglichte es uns, Hydrogele mit Elastizitäten im biologisch relevanten Bereich herzustellen.

Die Übertragslithographie wurde entwickelt, um die Hydrogele mit Gold-Nanostrukturen zu versehen, das zweite Modul der künstlichen ECM. Die Goldstrukturen bestehend aus Goldpartikeln mit definierten Größen und Abständen wurden mit Hilfe der auf anorganische feste Oberflächen beschränkten Mizellaren Blockcopolymer Nanolithographie hergestellt. Diese Strukturen wurden auf Polymere, u. a. PEG Hydrogele übertragen, die auf die Nanostrukturen aufgetragen und dort vernetzt werden. Ein Linker, der für jedes Polymer speziell ausgewählt wurde, verbindet dabei die Nanogoldpartikel mit dem Polymer. Das Ablösen des Polymers vom ursprünglichen Träger der Nanostruktur führte zu einer vollständigen Übertragung der Nanostruktur auf das Polymer. Mit einem Cryo-Rasterelektronenmikroskop (REM) wurden die Strukturen auf den Wasser enthaltenden Hydrogelen charakterisiert. Die Übertragslithographie ist die erste Methode, um großflächig planare und unplanare weiche Polymeroberflächen mit metallischen Nanostrukturen zu dekorieren. Die strukturellen Eigenschaften der künstlichen ECM, die z.B. das Gruppieren von Adhäsionsproteinen in Adhäsionskomplexen der adhärierenden Zellen beeinflussen, können durch Variationen der Goldpartikelabstände und -größe modifiziert werden. Ein weiterer

struktureller Parameter besteht in der Krümmung der Oberfläche. Zur Kontrolle dieses Parameters wurden PEG Hydrogel Röhren entwickelt, deren Innenwand mit Gold-Nanopartikeln dekoriert ist. Mit diesen nanostrukturierten künstlichen ECMs, die röhrenförmig die Zellen umschließen, lassen sich z.B. Blutgefäße imitieren.

Das dritte Modul der künstlichen ECM umfasst biologisch aktive Moleküle, die an die Goldpartikel oder das PEG Hydrogel angebunden werden, um diesen beiden Modulen biologisch zu funktionalisieren. Peptide und Proteine wurden entweder über Thiolbindungen an die Goldpunkte gebunden oder mit primären Aminogruppen direkt an die Hydrogel-Oberfläche gekoppelt. Während die Peptide direkt über eine Amino- bzw. Thiolgruppe an die Oberflächen gebunden wurden, wurden Proteine über einen Ni(II) Histidin Komplex an ein Linkersystem angebunden. Diese Methoden wurden entwickelt, um eine spezifische Ankopplung von biologisch aktiven Molekülen mit definierter Orientierung und natürlicher Konformation an entweder das Hydrogel oder die Goldpartikel zu binden. Dabei musste darauf geachtet werden, dass keine zelltoxischen Substanzen im Hydrogel zurückbleiben oder das Gel seine Resistenz gegen Proteinadsorption verliert. Das selektive Anbinden von Biomolekülen wurde mit repräsentativen Bio-Molekülen, dem Adhäsionsrezeptor bindenden Peptide RGD, dem Zell-Zellkontakt vermittelnden Protein L1 und dem grünen Fluoreszenzprotein GFP. Ergebnisse wurden anhand von Zellexperimenten und Fluoreszenzmikroskopie untersucht. Die Methode erlaubt eine selektive Biofunktionalisierung der Nanostruktur und der Bereiche dazwischen durch die Anbindung von nahezu beliebigen biofunktionalen Gruppen an diese Module der künstlichen ECM.

Die Funktionalität der drei Komponenten, dem PEG Hydrogel, der Nanostruktur und der chemischen Funktionalisierung wurde durch Zellexperimente getestet. Experimente mit Substraten unterschiedlicher Festigkeit, mit unterschiedlicher Biofunktionalisierung, unterschiedlichen Goldpunktständen und unterschiedlichen Zelltypen zeigen die grundsätzliche Eignung der Module für die Verwendung in einer künstlichen ECM. Mit dem Cryo-REM konnte gezeigt werden, dass nanostrukturierte Hydrogele von Fibroblasten auf molekularer Ebene deformiert werden können, was das direkte mechanische Wechselspiel von Zellen mit ihrer Umgebung auf molekularer Ebene zeigt. Zusätzlich konnte die Funktionalität von nicht planaren Systemen in Form von nanodekorierten Hydrogelröhren für Zellexperimente gezeigt werden.

Zusammengefasst kann gesagt werden, dass die modulare System, das in dieser Arbeit entwickelt wurde, den Anforderungen einer künstlichen ECM entspricht, und ein bewegliches, flexibles Instrument darstellt, um die Zell-Oberflächen Wechselwirkungen zu untersuchen und zu kontrollieren. Die künstliche ECM bietet die Möglichkeit zur Beeinflussung der Zelladhäsion und Zellfunktion und erlaubt damit die gezielte Selektion von Zelltypen.

II. Introduction and Motivation

Motivation

The basic unit of living organisms is the cell. Cellular functions are highly diverse, as reflected by the variety of organisms – from plants to mammals – and of different tissues – from bones to neuronal tissue. One of the amazing features of life is the organization of this variety of cells into organisms in a highly spatially and temporarily coordinated fashion. Every cell knows exactly how to communicate and interact with its surroundings. It knows when to proliferate, how to specialize and grow, and when to die. It is the communication between the intracellular and the extracellular machinery that allows cells to perform their particular functions in a complex multicellular organism. The properties of the extracellular machinery control cellular functions such as cell differentiation, growth, adhesion, motion. In return, cells control their environment by secreting and structuring it.

The mutual control of cells and their environment forms the basis for the hierarchical organization and formation of tissue, organs, and ultimately organisms. The cellular environment influences the development and function of tissues mainly by two basic mechanisms.¹ Firstly, certain functions of cells are triggered by the environment by means of external signals. This has been impressively demonstrated by stem cell experiments, in which the development of muscle cells from stem cells was stimulated by mechanical signals.² Similarly neuronal stem cells are differentiating into either neurons or glial cells depending on the addition of external signaling molecules.³

The second mechanism by which tissue formation is externally guided is the discrimination of tissues between cell types. Tissues selectively support the growth of compatible cell types while obstructing the growth of others. Each of the tissues in an organism features properties which are highly specific for certain cell types and functions. External factors of the tissue preferentially stimulate growth of these cell types relative to others. Thus, in addition to the influence of the cell environment onto cell function, the extracellular matrix also discriminates between different cell types. This has been shown previously for neurons and glial cells on soft and stiff surfaces, respectively.⁴

Understanding the molecular mechanisms of the crosstalk between cells and the environment is an important task in medicine and biology. Such understanding will enable cell function and behavior to be steered. This will provide new medicinal and biotechnological tools. This will ultimately help to prevent malformation of tissues, to develop new strategies to fight cancer, to improve medical implants, and to tailor cell culture conditions for specific cell types.

The unnatural mechanical and chemical properties of artificial implants play a crucial role in the differentiation and selection of cells at the cell-implant interface.⁵ The design of modern implants incorporates signals from the surface to the adhering cells by appropriate modifications of the implant surface. The embedding of the implant into the surrounding tissues is thereby accelerated, the rejection reaction is much reduced, and the adhesion of specific cell types is enhanced. Neurons, for example, are suppressed by other cell types at the interface to artificial electrodes of neuronal implants. Conventional electrodes show preferential growth of invading adverse cell types, whereas implants with surfaces specifically tailored for neuronal tissue can selectively enhance neuron cell adhesion and growth at the interface.⁶ Another potential application for directed cell control with external signals is the stimulation of adult stem cells to migrate into tissue. This will accelerate the wound healing process after surgery or around implants, and also might help to suppress cancer tissue.⁷

A major challenge in cell biology is to culture stem cells. Here, the crucial role of cell-environment interaction is particularly evident, since stem cells react highly sensitively towards external stimuli. In vitro, stem cells are conserved in so called stem cell niches, a phenomenon far from being widely understood. Stem cell niches represent a microenvironment in which stem cells are surrounded by niche cells allowing a long-term persistence of the stem cells. The niche cells provide a sheltering environment that holds off differentiation stimuli, apoptotic stimuli, and other stimuli that would challenge the stem cell reserves. In artificial environments, stem cells differentiate after a short period and lose their function as stem cells. Up to now, it has not been possible to keep stem cells for a longer period in culture. The highly sensitive interaction between stem cells and their environment poses various questions regarding cell-matrix interactions and a challenge for the design of an adequate artificial environment.⁸ A first task is to understand the interaction between niche cells and stem cells embedded in the niche, in the hope of being able to culture stem cells in vitro.

The above examples demonstrate the importance of a profound understanding of the common principles and particularities of the interaction between cells and the environment, in particular, the extracellularmatrix (ECM). The ECM is a complex network composed of a variety of macromolecules. It is characterized by its mechanical (elasticity, tensile strength, compressibility etc.), structural (fibrillar organization versus highly crosslinked networks), and chemical (polysaccharide and protein contents like ligands for cell adhesion) properties. These properties of the ECM determine the particular cell types embedded, which in turn control the organization of the ECM. Questions to be addressed are as follows. How does a cell respond to mechanical stimuli such as external force or the softness of its environment? How does the biochemical environment alter the short-term and long-term cell behavior? Answering these questions is a prerequisite for rationally influencing and modifying the interaction, and for ultimately steering cells in terms of

their differentiation and function. Can the differentiation of stem cells to a certain tissue be provoked? Can wound healing be accelerated? Or can the protein expression profile of a cell be altered by providing the cell with an artificial surrounding mimicking the *in vivo* situation?

A starting point to address these questions is a model system that mimics the ECM and allows the precise control of the properties of this artificial matrix. Recent advances have been made in the development of surfaces for cell adhesion. Among others, hydrogel-based materials with different adhesion properties, eventually carrying adhesion receptor molecules, have been applied to study cells in artificial environments.⁹ Typically, certain properties such as ligand type or the elasticity of the matrix can be controlled. Nanopatterned glass surfaces have been applied to control adhesion on a molecular level. A quantitative understanding of the different biochemical and mechanical levels of cell-ECM interaction, however, requires precise and, more importantly, independent control over the major properties of the ECM that influence cell functions, namely the mechanical, structural and chemical properties.

Aim of this thesis

The aim of this research is the modular design of an artificial extracellular matrix. Modularity enables the independent tuning of the structural, mechanical and chemical properties of the matrix offered to the cell at the molecular level. The three modules can be flexibly combined to yield an artificial cell matrix as illustrated in Fig. 1, the basic concept of which will be introduced in Chapter III. First, for the basic material, or support, of the ECM, polyethylene glycol was chosen (Chapter IV). This hydrogel enables the adjustment of the mechanical properties of the ECM. The network structure, the elasticity, and the water content of the artificial ECM can be controlled by the polymerization conditions, as required. The modular system can be also extended to other types of polymers. Secondly, the structural properties of the ECM can be controlled by patterning the hydrogel surface (Chapter V). Structuring materials on the molecular, i. e. nanoscale, is essential for directing the positioning and function of single cell receptors and thus, the molecular biology of the cell. By means of block copolymer micelle nano-lithography, gold nanoparticles are transferred to the surface. Each gold nanoparticle on the surface is a potential candidate for immobilizing molecules or proteins. The particle size and the distance of the regular pattern on the hydrogel are adjustable by the processing conditions. As the third module of the artificial ECM, selected chemical and biochemical components can be added to the surface (Chapter VII). The modular design of the ECM permits two complementary chemical modifications, either modification of the hydrogel itself at well-defined crosslinking sites, or by immobilization of molecules such as adhesion peptides or other proteins, on the gold nanoparticles. In combination, the choice of the chemical components arranged in a regular pattern and distributed

on a molecular level in a mechanically well-defined environment yields the artificial ECM of choice as required for the stimulation of a cell in a particular way.

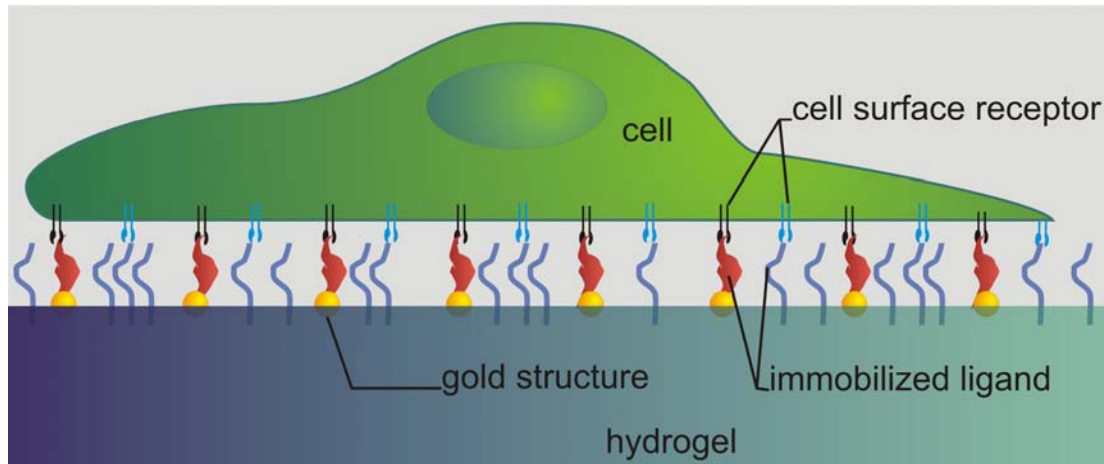


Fig. 1: The modularly-designed artificial ECM consists of several tools: the basic material (hydrogel), the structuring components (gold structure) and the chemical modifications of the basic material and the structure (immobilized ligands).

Outline of this thesis

As a first step in the design of modular ECMs, this thesis describes the design and analysis of the three modules described above, both separately and in combination. The formation of nanopatterned hydrogel channels, a variation of the two-dimensional basic structure, will be described in Chapter VI. We thereby have a quasi three-dimensional ECM at hand, in order to mimic the channel system of blood vessels. Finally, Chapter VIII demonstrates how the newly-developed modular ECM may be applied to cell experiments. As a proof of concept, the hydrogel stiffness, the inter-ligand distance, and the bio-functionalization were varied, and the corresponding cell behavior was monitored, by means of light- and electron microscopy.

A major achievement of this work arises from the fact that all three modules - the hydrogel, the gold pattern, and the chemical modification - can in principle be combined to form an artificial ECM of which the mechanical, structural and chemical properties can be independently and precisely modified. Therefore, this thesis paves the way toward the future development of the modular ECM system, possible variations on the system and potential applications, as outlined in more detail in the final chapter of the thesis.

III. Theory and background

III.1. Extracellular matrix

Natural tissues consist of more than just cells. The cells are surrounded by, imbedded in, and attached to a meshwork of various cell-secreted molecules (Fig. 3). This assembly of proteins and polysaccharides is known as the extracellular matrix (ECM). The aim of the work presented herein is to set up an artificial ECM system by mimicking key components of the natural ECM. the specific questions being addressed are the following: How can the various components of the natural ECM be mimicked by synthetic materials? Moreover, how can these components be combined to form artificial ECMs with adjustable properties, in order to specifically address cell behavior and function?

III.1.1. *What is the extracellular matrix?*

On the one hand, **ECM molecules are expressed and oriented by the cells** (Fig. 2). In other words, cells can condition their environment to their particular needs.¹⁰

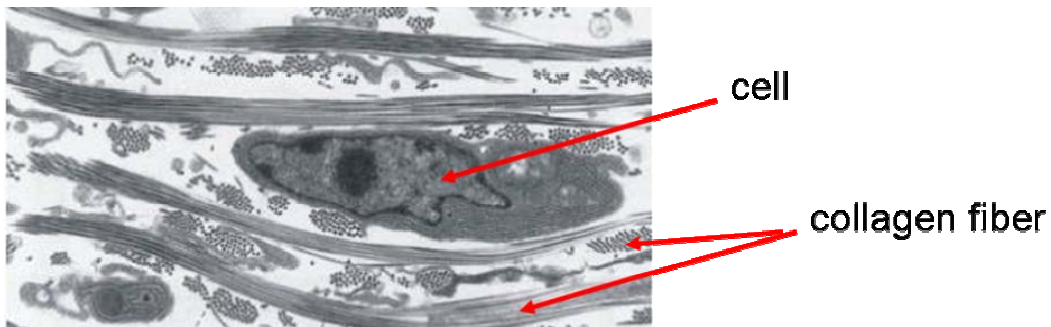


Fig. 2: Transmission electron microscopic image of a fibroblast embedded in a collagen matrix. The collagen fibers are oriented either in parallel or orthogonal to each other.¹⁰

On the other hand, the **ECM defines the chemical, structural and mechanical properties** of the cellular environment through its composition, and the arrangement of diverse proteins and polysaccharides. Variations in the composition and organization of the ECM molecules lead to the amazing diversity of ECM forms, all of which are tailored to the specific function of the particular tissue involved. For example, the ECM can be calcified for the hard structure of a bone, or take on the rope-like structure which is responsible for the tendons' enormous strength. The ECM thereby regulates the behavior of the cells contacting it, including such aspects as cell survival, development, differentiation, migration, proliferation, shape, and function.

The interaction, or crosstalk, between cells and the cellular environment is, by its very nature, complex¹¹ (Fig. 3; discussed in detail in Section III.3). Thus, the ECM plays a key role in the formation of tissues and organs.

Though the ECM takes different forms in the various types of tissues, its components can be roughly divided into two main classes of molecules:

- **Fibrous proteins¹²** such as collagen (Fig. 3), fibronectin, laminin, and elastin, assemble in fibers and give the ECM its structure and mechanical stability. They also offer the cells structurally defined and chemically specific adhesion sites, as illustrated by means of multiadhesion proteins illustrated in Fig. 3.
- The polysaccharide chains of the group known as **glycosaminoglycans (GAGs)** are unbranched polymers of periodically repeating disaccharides.¹³ As shown in Fig. 3, except in the case of the GAG hyaluronan, the GAGs (yellow) are covalently bound to core proteins (red) to form proteoglycans. The GAGs form a hydrated, gel-like “basic material” in the ECM. These gels resist compressive forces on the tissue, and control the release and the diffusion of nutrients, hormones, and metabolites between the blood and the cells. They also embed other tissue components such as cells and fiber-like proteins.

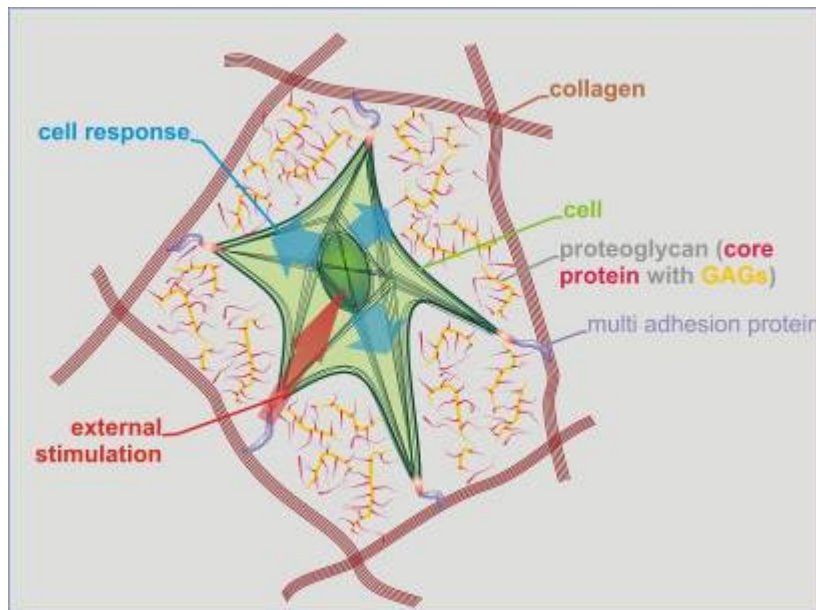


Fig. 3: Illustration of a cell in an extracellular matrix, showing the basic ECM components.

III.1.2. Components of the ECM

In the following section, five representative ECM molecules with different tasks, representing the two ECM molecule families, fibrous proteins and polysaccharides, are described.

Collagen

Collagen, the major component of the ECM and the most abundant protein in mammals, belongs to the group of fibrillar ECM proteins. Typically, collagens consist of a long, stiff triple-stranded helical structure with a length of 300 nm and a thickness of 1.5 nm. Three of the so called α -chains (Fig. 4a) are wound around each other to form this rope-like superhelix, as shown in Fig. 4b. At least 20 different types of collagen are known, consisting of a triple helix formed by the 25 different types of α -chains. The way in which a given collagen is arranged in fibers and networks (Fig. 4d) depends not only on the types of α -chains in the fibril, but also on the collagens or other proteins associated with the fibrils. The actual arrangement of the collagen in the tissue is influenced by the cells embedded within, which crawl over it and pull on the ECM components (Fig. 2).¹⁰

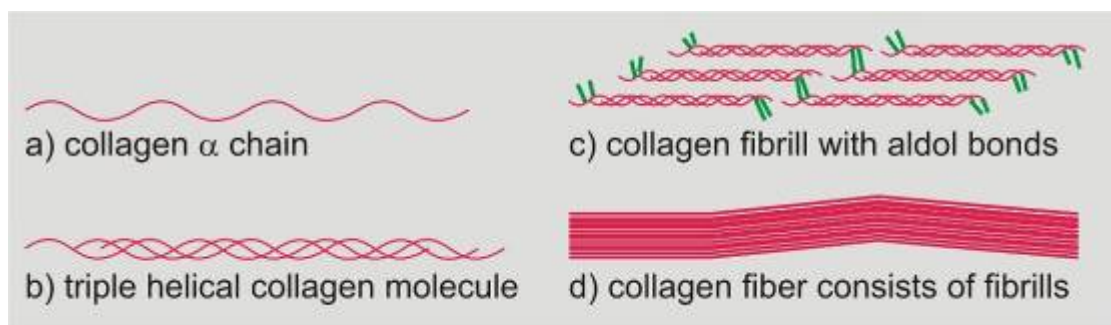


Fig. 4: Schematic drawing of a collagen fiber of collagen type I (d) formed out of a single collagen polypeptide (a) which aggregates to triple helices (b). The triple helices form fibrils (c)

Most common are the collagen types I-III, which form three-dimensional networks. Collagen type I, for example, achieves intermolecular crosslinking via aldol bonds between the amino acids hydroxylysine and lysine at its peptide termini, resulting in fibrils (Fig. 4c). The fibrils have diameters of 10-300 nm, are hundreds of micrometers in length, and have regular band patterns with a periodicity of 62 nm.¹⁴ Several crosslinked fibrils aggregate, in turn, to fibers of up to 300 nm in diameter.

The most remarkable property of collagens is their resistance toward strong tensile forces. The collagen matrix functions as the major structural element of the ECM, thereby providing the ECM with mechanical stability. In the artificial ECM developed in this project, the function of the collagen was implicitly mimicked by the tunable mechanical properties, as defined by the hydrogel material (Chapter IV) and the nano- and microscale structuring (Chapter V).

Fibronectin

Fibronectin is a non-collagen representative of the fibrillar ECM proteins. It is a dimeric glycoprotein 60-70 nm in length and consisting of two polypeptide chains, each of which contains approximately 2,500 amino acids arranged in five to six

domains of varying function. The two subunits are crosslinked by two disulphide bonds at their termini (Fig. 5).¹⁵

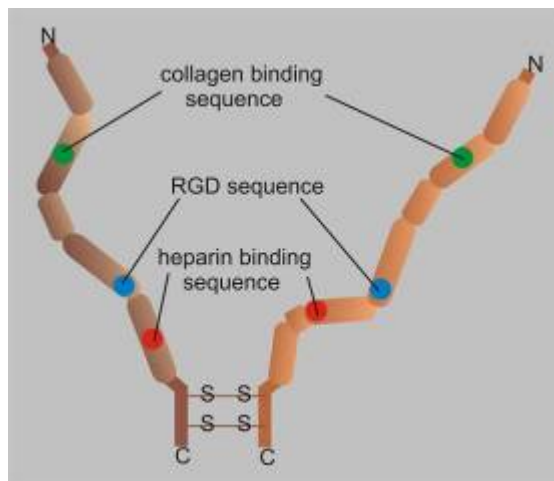


Fig. 5: Fibronectin molecule with collagen, integrin and heparin binding sequences¹⁵.

Fibronectin belongs to the group of multi-adhesion proteins of the ECM (Fig. 3). Multi-adhesion proteins consist of multiple domains, each with specific binding sites for both other matrix molecules, and for cell surface receptors. Fibronectin can show a solvable isoform which circulates in blood or it aggregates to fibrils. Fibronectin contains an RGD sequence,¹⁶ a tripeptide sequence consisting of arginine (R), glycine (G), and aspartate (D). This simple peptide structure specifically binds transmembrane receptors such as integrins.¹⁷ The RGD peptide sequence in the fibronectin is located in the so-called type III unit, with a periodical appearance within the fibronectin fiber. Immobilizing RGD sequences, which are responsible for the affinity to integrins on a surface (Section III.2.2) enables mimicking the presence of fibronectin, and stimulating cell adhesion.¹⁸ In solution, these peptides compete with a fibronectin-containing tissue matrix, thereby inhibiting the adhesion of cells to the tissue.¹⁹ Previous studies showed that the conformation of the RGD sequence in the proteins of the ECM determines the specific binding of different integrin subtypes.²⁰ Recent FRET experiments revealed a conformational change in fibronectin upon fibril formation, leading to the hypothesis of a mechanically-triggered exposure of the RGD binding site for integrin binding.^{21,22} With another binding site beside the RGD, the fibronectin binds to collagen fibrils of type I, II, III, and V. Thereby it connects the cell membrane to the collagen matrix. By establishing the mechanical link between the cell and the ECM, fibronectins play a major role in cell adhesion.²³ As that part of fibronectin forming the specific contact to integrins, the RGD sequence was extensively utilized for the artificial ECMs in this research, as further described in Section VII.1.2.

More recently, cell-reorganized fibronectin fibrils were shown to form assemblies with a characteristic spacing of 71 nm, as given by the spatial arrangements of the

protein interaction sites.²⁴ This finding shows that nanoscale periodic patterns play a crucial role in molecular assemblies of focal adhesion sites. They can be mimicked in the artificial ECMs by assembling, e.g., RGD sequences on gold nano-patterns (Chapter V).²⁵

Hyaluronan

Within the family of glycosaminoglycans (GAGs), the hyaluronan, consisting of up to 25,000 non-sulphonated, periodically arranged disaccharide units, is the simplest. In contrast to other GAGs, hyaluronan is not covalently bound to proteins, it contains no sulphonated unit, and all the disaccharide subunits are identical. Hyaluronan is present in all tissues and fluids in animals, where it appears as a hydrogel containing a huge amount of water. As a result, it can act as space filler, and shows a strong resistance to compressive force. Depending on its chain length and specific water content, its mechanical properties may vary. It is even capable of forcing changes in the tissue when a certain amount of waterlogged hyaluronan expands with additional water to occupy a large volume (Fig. 6). In cell migration, hyaluronan acts as a lubricant. Besides its mechanical role in the ECM, hyaluronan has various other functions, based on its specific interactions with other GAGs, growth factors, and cell receptors. It has been suggested that hyaluronan-mediated events play a major role in the early stages of cell attachment *in vivo*.²⁶ Early, adhesion at the hyaluronan coat is followed by the formation of stable focal adhesion sites via integrin.²⁷ The water-filled highly elastic hyaluronan polymer can be mimicked in a straightforward way by PEG hydrogel, as detailed in Chapter IV .

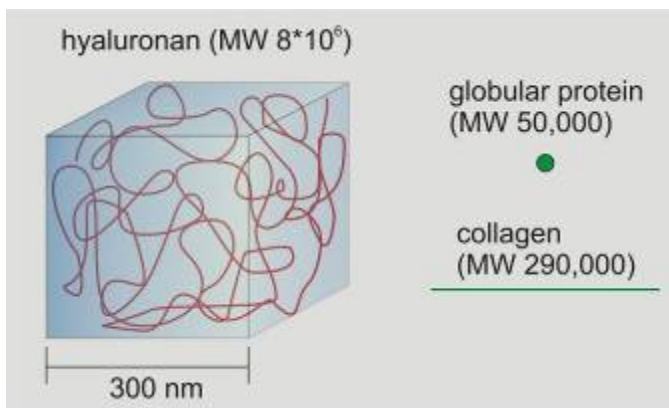


Fig. 6: Comparison of the size of a swollen hyaluronan molecule, a representative globular protein, and a collagen triple helix.

Proteoglycans

Proteoglycans consist of a linear core protein, to which GAGs or other polysaccharides are attached (Fig. 3). They can have a mass up to $3 \cdot 10^6$ Dalton, display a wide range of sizes, and are difficult to identify or classify, due to their

strongly heterogeneous composition. Thus, it is probably best to regard proteoglycans as a diverse group of highly glycolated glycoproteins, whose functions are mediated by both their core proteins and their GAG chains. Beyond the mechanical tasks of the simple hyaluronan, the complicated and diverse proteoglycans, in combination, can act as sieves, forming hydrogels with specific pore sizes and charge densities, according to which they regulate the release and diffusion of molecules and cells. Moreover, proteoglycans play a major role in cell signaling by binding specific growth factors or growth factor receptors on cells. They are thus able to regulate the signaling activity of the growth factors. In the present study, the incorporation of signaling and adhesion proteins into the ECM meshwork is achieved by chemically coupling peptides and proteins with biofunctions of choice, to the surface (Chapter VII).

Elastin

Elastin is a highly hydrophobic protein, 750 amino acids in length. Directly after secretion by the cells, tropoelastin molecules become highly crosslinked to one another, forming a network of elastin fibers and sheets. Elastin appears in elastic tissues such as arteries and skin, and is responsible for the elasticity of the ECM. As in synthetic rubber, crosslinked elastin fibers adopt a random, coil-like structure, which makes the network stretchable and retractable (illustrated in Fig. 7). AFM and sound absorption experiments revealed the entropic nature of elastin elasticity.²⁸ Elastin can in principle be mimicked by dextrane molecules, which could be crosslinked to the hydrogel.

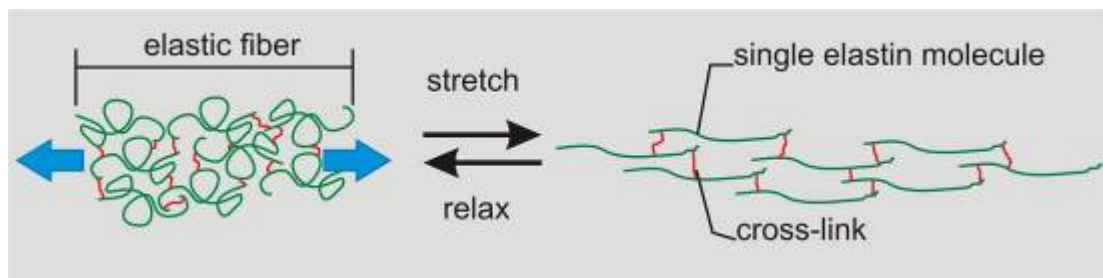


Fig. 7: Elastin fiber consisting of cross-linked elastin molecules in a relaxed and stretched state.

III.2. Cell surface receptors

Cell surface receptors play a major role in the reaction of cells to external influences, such as the properties of the extracellular matrix, or the presence of external signaling molecules. Adhesion receptors can be selectively addressed by receptor-binding molecules: for example, the highly selective binding of various polymer-linked RGD derivatives to members of the integrin family has been demonstrated.³¹ With regard to the aim of generating an artificial environment by means of which cell behavior could

be understood and controlled, the functional principles of the cell receptors with which cells sense external stimuli are detailed herein. The key questions are: What are the principles underlying the ability of cells to sense their environment? Furthermore, how specifically are the receptors addressed in the natural environment, and what role do they play in the interactions of cells with the ECM, and subsequent tissue formation?

III.2.1. *Transmembrane receptors, and their various functions*

Transmembrane receptors are proteins with both an intracellular and an extracellular domain. The extracellular domain of the receptor can bind to a ligand in a highly specific manner (Fig. 8 A). In turn, the intracellular domain, once stimulated, can trigger intracellular signaling cascades by changing its conformation and/or binding to other proteins (Fig. 8 B).

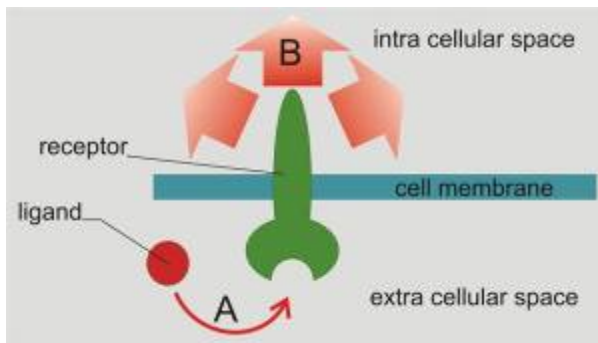


Fig. 8: Scheme of the general function of a transmembrane receptor.

According to their function, the cell surface receptors can be separated into two main groups, the cell adhesion molecules (CAMs; shown in Fig. 9) and the cell signaling receptors. In the case of signaling receptors, the ligands can be either hormones or growth factors, and can be presented to the cell in solution or, in some cases, bound to the ECM or to a signaling cell. In contrast, the ligands for adhesion receptors are already bound, or have a binding site which enables them to connect to the ECM or another cell surface. Those receptors binding ligands attached to the ECM or to cells show remarkable differences to those binding ligands in solution: Receptors for signaling molecules bound to ECM components or other cells, and adhesion receptors, show a much lower affinity to the ligand than receptors for soluble molecules. Otherwise, the cells become irreversibly bound to surfaces.

The density of one type of adhesion receptors on a cell surface is up to a hundredfold higher than the density of a signaling receptor. The large number of weak adhesions formed by adhesion receptors between cells and the ECM adds to a strong yet reversible adhesion along the lines of a Velcro fastener.

Adhesion receptors can be further classified into receptors mediating cell-ECM contacts, such as integrins, and receptors for cell-cell contacts, including cadherins and immunoglobulins (Fig. 9). Adhesion receptors are used by cells not only to link the cell to the ECM or other cells, but also to sense the conditions of the ECM. The adhesion receptors are triggering in turn signaling pathways within the cell, which ultimately enable the cell to respond to the network to which it is bound.

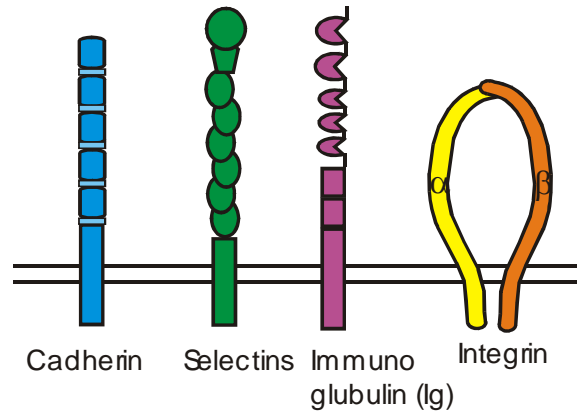


Fig. 9: The families of the cell adhesion molecules (CAMs).

III.2.2. *The integrin family of adhesion receptors*

The most important group of adhesion receptors is the large family of the integrins (Fig. 9). Integrin receptors mediate cell-ECM interactions. In the present study, the adhesion receptor $\alpha_v\beta_3$ integrin was targeted with a specific RGD ligand. It thereby illustrates the general mechanism by which receptors can sense the chemistry of a ligand, and react to the structure and rigidity of the extracellular matrix.

General structure of integrins

Integrins are composed of two noncovalently-linked transmembrane protein subunits called α and β . The extracellular parts of the subunits show a globular domain, which contains the ligand-binding sites (Fig. 11).^{29,30} In humans, the variety of integrins is formed by 9 types of β subunits, and 24 types of α subunits. Different combinations of integrin subunits lead to integrins with diverse specificities to ECM proteins. For example, eight different integrins bind fibronectin, and five target laminin. In many cases, the integrins bind specifically to RGD peptide sequences, depending on their conformation, orientation, and chemical side groups.³¹

Integrin function and integrin-mediated adhesion complexes

Integrin receptors are activated when their extracellular domain binds to a ligand. When an integrin is activated, the intracellular domains are splayed apart (Fig.

10).^{32,33} Under certain conditions (see below), activated integrins start clustering together. The clustering of integrins was also demonstrated *in vitro*, where they form homodimers and homotrimers (Fig. 10).³⁴

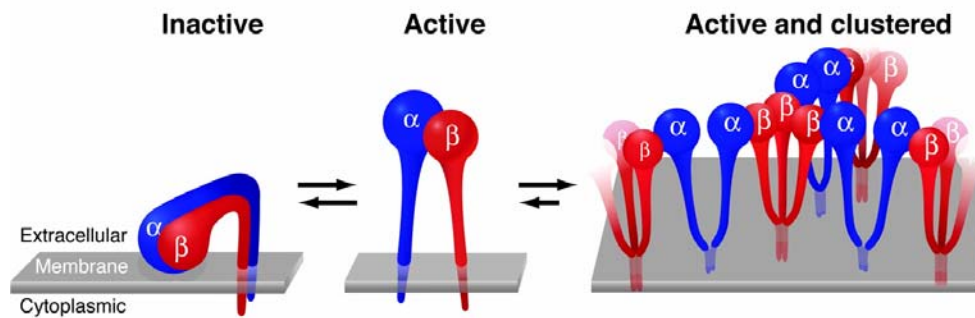


Fig. 10: Image adopted from reference 35, showing the activation and hypothesized clustering mechanism of activated integrin.³⁵

Similarly, cell experiments showed that once an integrin is activated, it associates with different intracellular adhesion molecules (iCAMS) such as vinculin or actin, and forms clusters; i.e., different kinds of integrin-mediated adhesion complexes³⁶ such as fibrillar adhesions, podosomes, focal complexes, or focal adhesions, with the principle structure shown in Fig. 11.

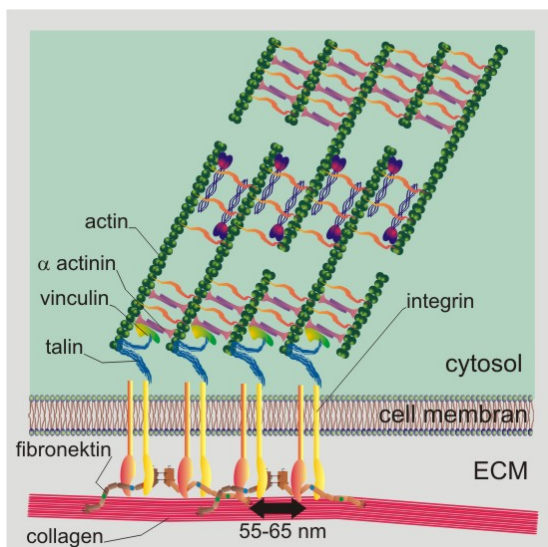


Fig. 11: Schematic drawing of an integrin-mediated adhesion complex.

The assembly of focal adhesions is based on the activation and clustering of ligand-occupied integrins. Within the context of the extracellular matrix, specific integrins are recruited to the focal adhesion site. Fibronectin, for example, mainly occupies the integrins $\alpha_5\beta_1$, whereas vitronectin is binding to the $\alpha_v\beta_3$ receptor.³⁷ While the periodically-arranged integrins in the focal adhesion bind to ligand molecules of the ECM with their extracellular domain, the cytosolic domain forms a protein cluster

with associated proteins, linking the ECM components to the intracellular fiber network. This transforms the integrin-mediated adhesion sites into anchoring junctions transmitting mechanical signals from the ECM into the cell⁴⁵ and vice versa,³⁸ helping the cell to migrate and functioning as biochemical signaling complexes. These adhesion sites are multifunctional sensors and actuators, taking part in mechanical, structural and chemical events between the cell and the ECM. In my model, integrin was addressed on the artificial ECM by means of immobilized RGD sequences on the hydrogel surface and on gold particles (Chapter VII).

III.2.3. *L1 of the immunoglobulin family*

L1 is a representative of the immunoglobulin-like protein family. The immunoglobulin family, together with the cadherins, belong to the group of cell adhesion molecules mediating cell-cell adhesion contacts (Fig. 9). Immunoglobulin proteins are a family of protein building blocks, occurring in protein adhesion molecules such as antibodies and major histocompatibility complex (MHC) proteins involved in the cellular immune response..

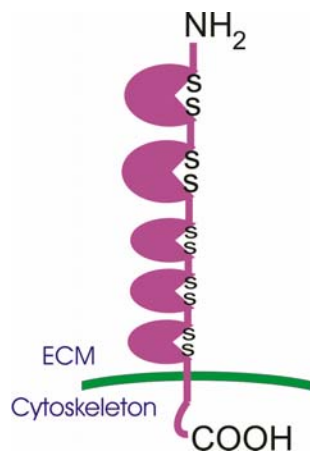


Fig. 12: Schematic drawing of the transmembrane protein L1, comprising the extensive extracellular N-terminal domain, and consisting of several immunoglobulin-like domains, a transmembrane part, and a short cytosolic C-terminal domain.

In this work, L1 was chosen to represent the immunoglobulin family, and used to mimic cell-cell adhesion sites in artificial ECMs (Section VII.2.2) depicted schematically in Fig. 12. L1 is an integral membrane protein (150 kDa) which plays a role in axonal growth. L1 proteins form cell-cell contacts by clustering at contact sites, thereby enhancing the adhesion strength and stability of the contact. Clustering activates the accumulation of ankyrin at the site of the adhesion contact. The binding of ankyrin to spectrin couples the L1 protein to cytosolic actin fibers, thus establishing a strong, direct linkage between cells and the cytoskeleton.

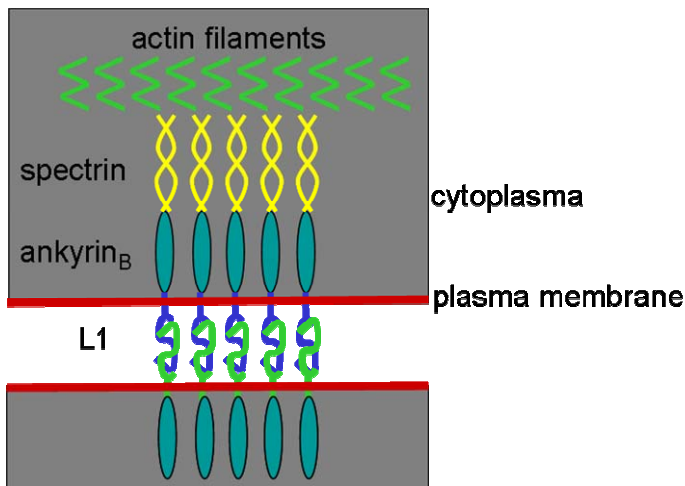


Fig. 13: Scheme of a cell-cell adhesion complex formed by a cluster of L1-L1 complexes in between the cells, which in turn are coupled to the actin cytoskeleton via ankyrin and spectrin linkages.

III.3. Interactions between cells and the ECM

As described in Section III.1.1, the ECM and the cells embedded within it display a highly complex network of interactions. In the following sections, various examples are used to demonstrate the complexity and diversity of the interactions. Most experiments were carried out on artificial surfaces, in order to exclude overlapping influences of different parameters of the ECM. It should be pointed out that *in vivo* the various interactions herein listed separately are, in fact, strongly interdependent.

III.3.1. Mechanical interactions between cells and the ECM

Mechanical interactions between the cell and the extracellular matrix are manifold. Most of them are related to integrin-mediated cell adhesions, due to the fact that integrins connect mechanical components from the cytoskeleton with mechanical components of the ECM (discussed in Section III.2.2). Even though these interactions are interdependent, it is instructive to look at them separately.

First, the cells can deform and rearrange the ECM by means of tensile forces.³⁹ Fig. 14 shows two pieces of embryonic chicken heart cultured for four days on a collagen gel. The fibroblasts in the explants aligned the collagen fibers in between both tissue pieces.⁴⁰

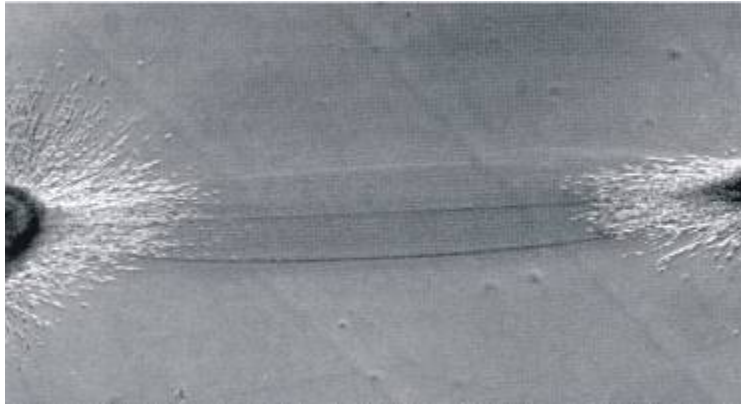


Fig. 14: The image, taken from Ref. 40, shows how cells from two tissue pieces initiate the alignment of collagen.

Secondly, cells react to the rigidity of the ECM in a highly sensitive manner. Whereas, for example, fibroblasts prefer a tissue with a Young's modulus higher than 3 kPa,⁴¹ neurons, in contrast, naturally prefer soft surfaces, with a softness of 0.1 - 1 kPa.⁴²

In a mathematical model⁴³ the isotropic extracellular matrix material can be described as a spring constant (Fig. 15), which is proportional to the Young's modulus. The model thereby explains the relationship between the rigidity of a substrate surface and a cell attaching to it. It also demonstrates that cellular reactions to surface rigidity are just another illustration of the fact that cells deform their surfaces with traction forces generated by the mechanical components of the cytoskeleton.⁴¹ As a consequence, both the arrangement of the mechanical components of the cytoskeleton and cell spreading show a strong dependency on substrate elasticity.⁴³ An experiment with fibroblasts on both rigid and soft gels shows remarkable differences in the behavior of the actin network (Fig. 16) and focal adhesion formation (Section III.2.2).⁴⁴

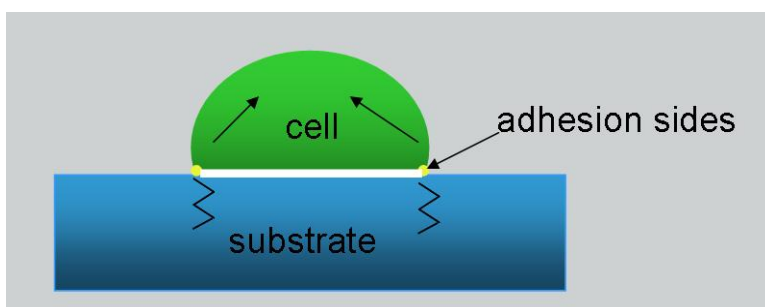


Fig. 15: An isotropic extracellular matrix material can be mathematically described as a spring with a certain spring constant. Cells are able to sense the substrate stiffness by pulling on this spring on the adhesion sites.

Diverse experimental setups have been developed, to quantify the pulling forces on the adhesion sites. The reactions of various cell types such as fibroblasts,⁴⁴ endothelial cells,⁴¹ neurons,⁴² and epithelial cells⁴⁴ to surfaces with defined elasticity, and coated

with cell adhesion-supporting ligands, have been tested. Traction forces have been visualized by patterning soft surfaces, attaching various types of cells to these surfaces, and observing the resulting deformation of the patterns.^{45, 46}

Furthermore, the process of cellular differentiation is also influenced by substrate stiffness. Breast epithelial cells, for example, differentiate into tubules only when they are cultured on a soft collagen matrix, and not on rigid matrices.⁴⁷

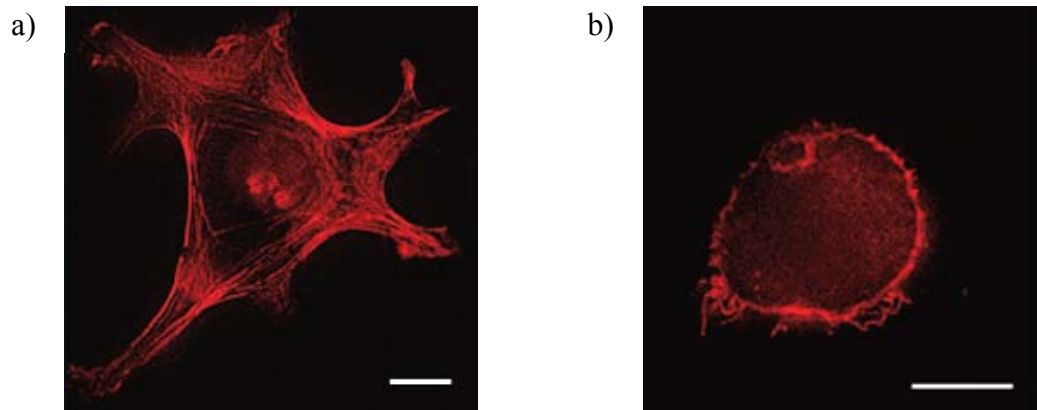


Fig. 16: Images adopted from Ref. 44 show the cytoskeleton of fibroblasts on a rigid (a) and a soft (b) substrate.

Thirdly, cells react to applied mechanical stress. Active mechanical stimulation of cells results in changes in the mechanical components of the cytoskeleton, and can have an influence on their differentiation.⁴⁸ Prodcytes seeded on a silicon rubber base, which was stretched periodically with 0.5 Hz and 5% of linear strain over 3 days, show a remarkable difference in the actin network, compared to non-stressed prodcytes (Fig. 17).⁴⁹ The influence of static and dynamic mechanical stress on osteoblast differentiation was also demonstrated in mechanically stressed three-dimensional collagen matrices.⁵⁰

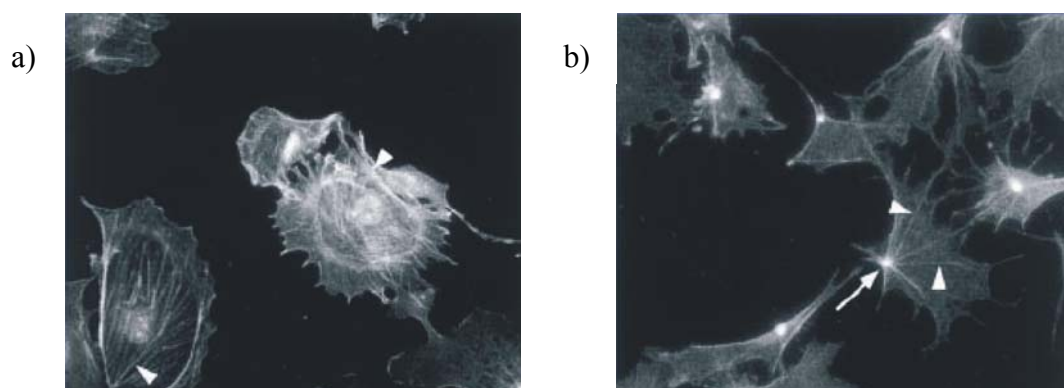


Fig. 17: Images taken from Ref. 49 show the actin network of prodcytes on a permanently relaxed (a) and on a periodically stretched (b) surface.

III.3.2. Chemical interactions between cells and the ECM

The field of chemical interactions between cells and the extracellular matrix is immense. As described in Section III.2.1, chemical signals can be transmitted via cell surface receptors reacting to specific ligand molecules. Other means of signaling, which will not be discussed in this section, involve gradients in ion concentrations.

In the case of adhesion receptor-transmitted chemical signals, the combination of receptor-specific ligands and their concentrations differs for each cell type, and each cellular function. Osteoblasts display a different migrating behavior on a surface coated with an osteopontin-derived peptide (DVDVPDGRGDSLAYG) than on a surface coated with a GRGDS peptide at the same concentration. Due to the varying combinations of integrin receptors on the surface of fibroblasts, the receptors show an inverse behavior.⁵¹ Besides the type of the adhesion molecule involved in the cell – ECM interaction, its concentration at which it is offered to the cell plays an important role in steering the cell behavior. The influence of the adhesion molecule density on the cell was also demonstrated in osteoblasts, which migrate faster on surfaces with higher GRGDS density.⁵¹

Other external stimuli include signaling molecules which bind to cell surface receptors, and initiate signaling cascades within the cells. In this case, concentration gradients in the signaling molecules also play an important role, in controlling cells. Directed cell movement toward small molecule ligands is a central function of many cell types, and plays a key role in diverse biological processes.⁵² Furthermore, some signals activate cells to express ECM components, thereby modifying the chemical composition of their own environment. The epidermal growth factors (EGF), for example, which bind to the EGF receptor of astrocytoma cells, are important regulators of the plasminogen activation system and therefore, influence the turnover of extracellular matrix compounds.⁵³

III.3.3. Structural interactions between cells and the ECM

The ways in which cells determine the structure and arrangement of their micro- and nano-scopic environments was discussed in Section III.3.1. In turn, the given chemical or mechanical patterns of the ECM influence cell behavior.

Cell adhesion, for example, is altered by a change in the chemical pattern of the environment, by means of adhesion receptor ligands in the ECM. This phenomenon was demonstrated on artificial nano-structured surfaces with RGD sequences offered to the cell with varying periodicity. In the case of a 58 nm periodicity, cells can form focal adhesion sites (Fig. 18 a), corresponding to the regular appearance of the RGD sequence in fibronectin fibers *in vivo*, as described in Section III.1.2 (Fig. 11). In case, the distances of the adhesion molecules offered to the cells is larger than 73 nm,

integrins become incapable of clustering to form focal adhesions (Fig. 18 b).⁵⁴ These experiments demonstrate that it is not the average density of the available ligands, but rather the nanoscopic distance between single RGD sequences that controls integrin function. The case of integrin thus shows that molecular arrangements in the ECM can support or inhibit protein function and assembly. In this study, corresponding experiments were performed on hydrogel-based nanopatterned surfaces (Chapter VIII), and yielded results similar to those shown in Section III.4.1.

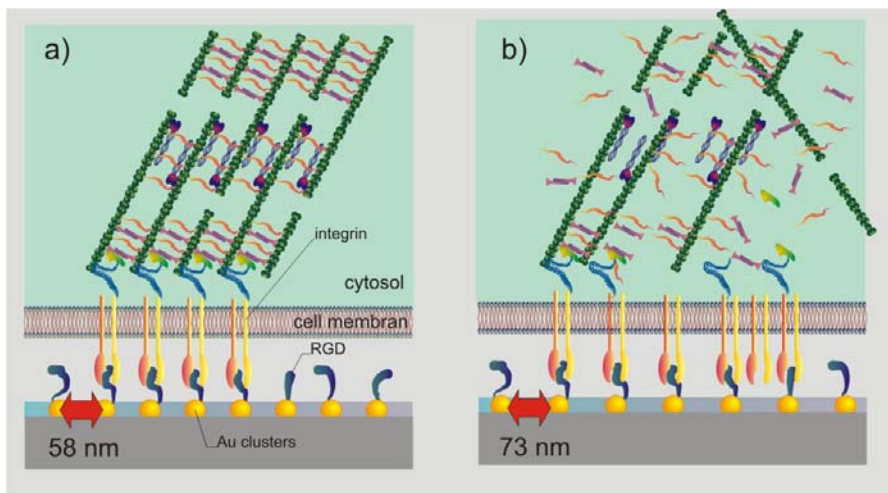


Fig. 18: Integrin binding to a periodical arrangement of RGD peptides. RGD distances of 58 nm allow integrins to cluster (a), whereas integrins binding to RGDs separated by 73 nm or more are incapable of clustering (b).⁵⁴

In another study, the influence of the topography of the extracellular environment on the cell behavior of macrophages was illustrated. Plated on a surface with a nanoscopic topography in the range of 30 to 280 nm, activated cell growth and spreading, as well as an increase in the number of protrusions on cells, were observed⁵⁵.

The influence on the micrometer scale can be more easily observed, and is therefore well-studied. On hydrogels with varying degrees of stiffness in a micrometer pattern, mimicking softer and harder regions in natural tissue, the migration and orientation of smooth muscle cells can be controlled.⁵⁶ By culturing neurofibromin 1-melanocytes with more than two dendrites on a surface with linear three-dimensional micrometer structures, the melanocytes are forced by the mechanophysical signals to reduce the number of dendrites to two.⁵⁷

Besides the influence of topographic and rigidity patterns, chemical patterns also influence cellular behavior. The patterning of the ECM for adhesion at the nanoscale is one example of a chemical influence (described above, in this Section). Similarly, the shape and the spreading behavior of fibroblasts on surfaces chemically pre-structured at the micrometer level depend on the availability, number, size, and

distribution of the adhesion sites.⁵⁸ Fig. 19 shows how the arrangement of artificial adhesion sites can influence the cell shape.

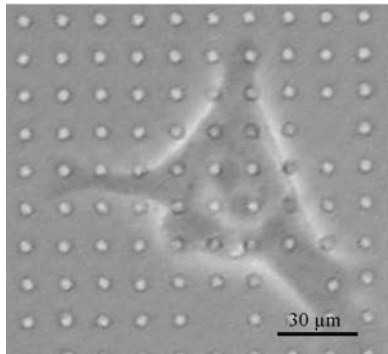


Fig. 19: Fibroblast on a μm patterned PEG hydrogel. The amount of cell spreading is controlled by the adhesive spots on the gel.

III.4. Design of an artificial extracellular matrix

The previous sections (III.1, III.2, III.3) explain the interplay between cells, and the various components of the extracellular matrix. In this section, the technical approaches used to offer cells tailored artificial environments for cell studies and for applied purposes, such as the development of medical devices such as implants, will be described. How is it possible to design synthetic components which could mimic the activities of single ECM components? Moreover, how can cell receptors be specifically targeted to direct cell function and to select cell types at interfaces? Is there a way to fool cells with synthetic components, such that they feel like in their natural environment? Established techniques will first be briefly reviewed, followed by a description of the modular ECM concept developed in this project.

III.4.1. Approaches used to mimic the extracellular matrix

In various experiments, cells have been cultured on surfaces such as stainless steel, titanium, metals, metal oxides,⁵⁹ and both biodegradable as well as undegradable polymers.⁶⁰ These studies aimed at an understanding of how cells interact with implant surfaces and how to design new implant materials, or improve existing ones. However, mimicking the natural environment of cells such that specific cellular functions are provoked; e.g., wound healing is accelerated, or drugs may be produced *in vitro*, has yet to be accomplished. The design of “intelligent” materials which could mimic the functioning of the ECM in turn requires a better understanding of cell – ECM interactions.

Most of the experiments described in Section III.3 showed that synthetic tools have been designed to control the mechanical, chemical and structural conditions of the artificial cellular support, and to reduce the interactions of the cell and its environment

to a controllable minimum. This work aims at the development of a novel modular ECM system combining properties and advantages of previously described approaches for artificial ECMs.

Concepts to bind adhesion receptor ligands to supports

To control cell adhesion, the chemical properties of the artificial ECMs, as provided by the type and density of biologically active adhesion receptor ligands, must be controlled (Section III.1.). A major task is to offer adhesion receptor ligands to cells in such a way that the ligand is attached to the artificial support at defined densities, and without losing or changing its biological function. In Chapter VII will be explained how this goal will finally be achieved for the artificial ECMs considered here. In this paragraph, the basic principles, some of which will be applied later, are comprehensively described.

The simplest way to immobilize biological active molecules on surfaces is by direct adsorption of proteins to a surface by incubating the surface in a physiological solution of cell adhesive proteins. With few exceptions, proteins adsorb to almost all kinds of artificial surfaces⁶¹ in a nonspecific manner. The disadvantages involved in such a system are that non-specific adsorption does not enable control of the orientation⁶² and spatial distribution of the cell adhesion domains. In addition, protein adsorption can involve changes in the protein's conformation⁶³ and biological function and, ultimately, in its partial denaturation.⁶⁴ This phenomenon leads to unknown biological activity at the surface and to the unspecified behavior of cells on these surfaces. Experiments performed on surfaces with unspecifically adsorbed fibronectin, for example, illustrate the irreproducibility of the adsorption process, as well as the effect of such fibronectin on changes in cell behavior.^{65,66,67}

In contrast, covalent binding of proteins, in regards to their spatial distribution and orientation to surfaces, is more easily controlled. Common reactions for binding a linker to a support surface (Fig. 20) include the N-hydroxysuccinimide ester (NHS ester)-amine coupling,⁶⁹ the binding of thiols to gold⁶⁸ or, in the case of polymeric supports, radical copolymerization reactions with acrylates and methacrylates.⁹ The literature describes a strong effect caused by the distance from an adhesion receptor ligand to the support surface, and its availability for adhesion receptors.⁶⁹ A small distance between the ligand and the surface can eventually lead to the partial unfolding of the covalently bound protein. Therefore, spacers are commonly introduced between the protein and the support surface (Fig. 20) which, at one end bind to the support, and at the other end bind, directly or indirectly, to the protein.⁷⁰

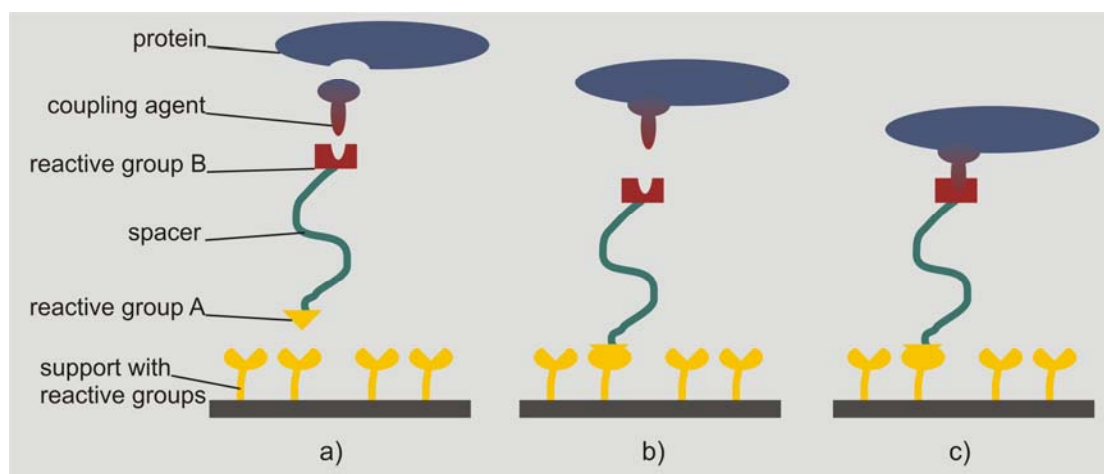


Fig. 20: A common approach to the immobilization of proteins on a support, via a spacer and coupling system. (a) Components of the coupling system. (b) In the first step, a spacer is linked to the substrate surface and a coupling agent is bound to the protein. (c) In the next step, the protein binds to the linker via the coupling agent.

In contrast to smaller peptides without well-defined tertiary structures, proteins are often unable to resist the harsh reaction conditions of chemical linking reactions, so that they lose their biological activity. Another disadvantage of the chemical linkage of proteins to surfaces via amine or thiol linkages is the non-specific binding of one of the several amine or thiol groups in a protein, resulting in an uncontrolled orientation of the protein. Again, these findings do not apply to the same extent to peptides, due to their lower number of chemically reactive groups. The coupling of the protein to a spacer (Fig. 20 b) circumvents these problems.

Coupling systems, with standardized procedures and simple chemical reactions under mild conditions and selectively on surfaces, have been developed to immobilize all kinds of proteins. These coupling systems all follow the same principle: A hetero-bifunctional coupling agent is bound to the protein under mild and simple conditions. Next, the protein with the coupling agent is immobilized on a substrate surface coated with binding sites specific for that agent (Fig. 20 c). A common coupling system is the histidine tag, which binds to the protein and forms a stable octahedral complex with nitrilotriacetic acid and Ni(II) as the central ion.⁷⁰ For proteins, this coupling scheme is the method of choice for the artificial ECM design, and in the present study, was applied as described in Sections VII.2.2 and VII.3.3. Another often used linker involves the use of the small avidin protein, binding to the target protein⁷¹ and coupled to the surface by its binding with very strong affinity⁷² to several immobilized biotin molecules.⁷³

Fig. 21 summarizes the advantages and disadvantages of the various ways to immobilize proteins on surfaces. The uncontrolled chemical linkage via covalent binding is strong but non-specific, because more than one site of the protein can react with the functionalities of the surface. Chemical linkage can be associated with

denaturation of the protein due to the small protein-surface distance, and often leads to random relative orientations. The use of peptide fusion tags circumvents these problems, by providing one specific linkage site for the protein. Linkers also guarantee a sufficiently large distance between the protein and the surface. However, fusion tags block both peptide termini of the protein, and require additional steps in the coupling procedure for tagging.

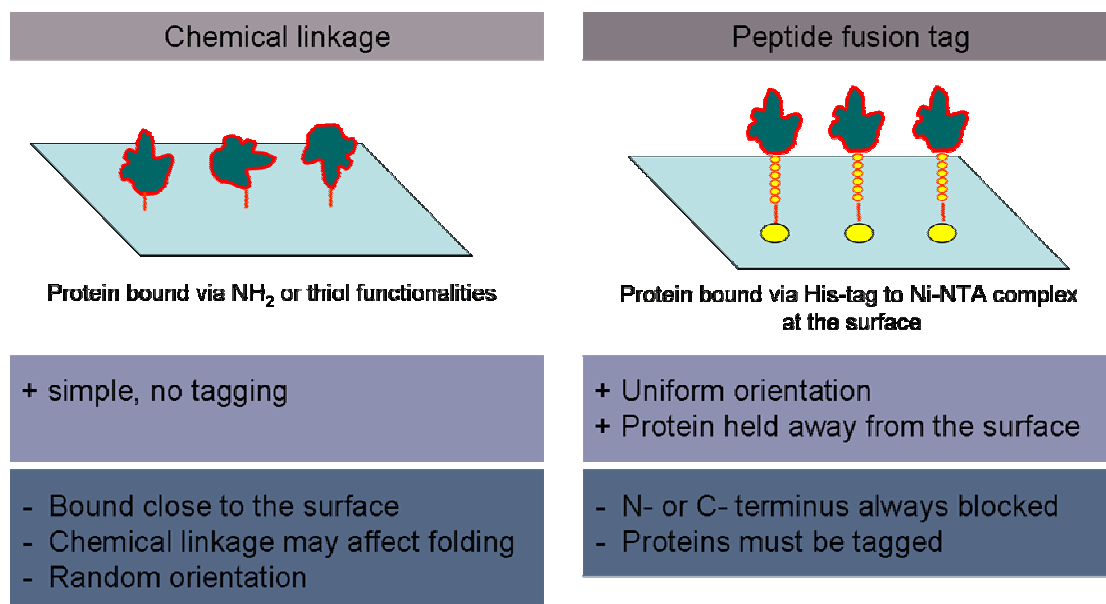


Fig. 21: Advantages and disadvantages of the various systems used to covalently couple proteins to surfaces: (a) the unspecific chemical linkage, and (b) specific linkage via peptide fusion tags.

Instead of immobilizing the entire adhesion-mediating protein, the immobilization of only the peptide sequences of interest enables even more stringent control of the adhesion properties. Various ways to immobilize adhesion peptides to surfaces via common linking reactions have been described (Fig. 22).³¹ These include the attachment of thiolated peptides to gold or silver surfaces,⁷⁴ and the coupling of active esters to amino-terminated peptides.⁷⁵ In the present study, the thiol-gold coupling method was chosen to immobilize RGD peptides on gold particles (Section VII.2.1), and the amide bond formation of amino-terminated RGD was utilized for coupling to hydrogel surfaces (Section VII.3.2).

Non-specific adsorption of the peptides and proteins can be inhibited by grafting polymeric monolayers which resist protein adsorption⁷⁶ onto the substrate surfaces, or by directly using polymeric substrates with this property.⁷⁷ Only a few synthetic polymers with protein adsorption-resisting properties like those of hyaluronan have been described to date, such as poly(ethylene glycol) (PEG) and polyhydroxyethyl methacrylate (PHEMA).⁷⁸

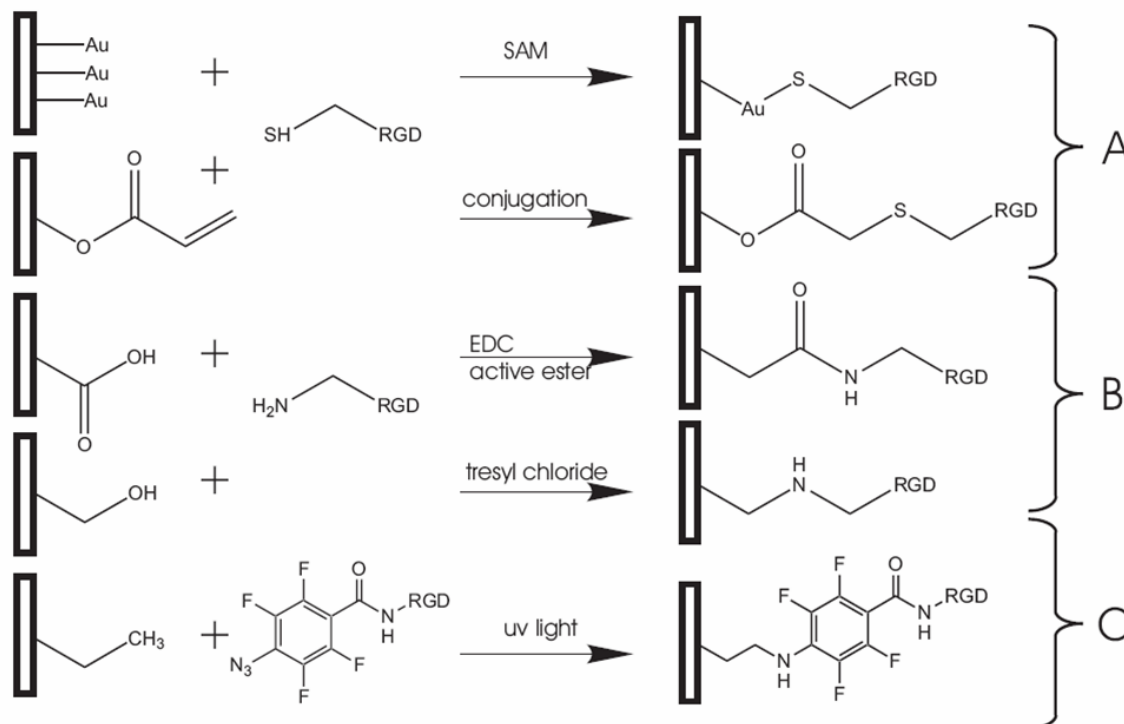


Fig. 22: Scheme adapted from Ref. 31 showing various methods used to couple thiolated (A), aminated (B), and light-sensitive (C) RGD peptides to pre-modified surfaces.

Choice of materials for artificial ECM supports

Cell behavior reflects and can be influenced by the mechanical and chemical consistency of the natural or, in this instance, artificial, ECM basic material, as demonstrated in Section III.3. Therefore, the material from which an artificial ECM is constructed should resemble, insofar as is possible, the complex natural ECM, with properties ranging from elastic and water-containing hydrogels to hard structures, from gels supporting cell attachment to those inhibiting cell growth, and from gels with high pH to those with low pH. Thus, polymers of choice are hydrophilic polymers forming three-dimensional networks capable of swelling by taking up large amounts of water, thereby exhibiting the desired chemical properties; e.g., biocompatibility, high permeability, resistance to non-specific protein adsorption (the so-called “anti-fouling property”) and the capacity for crosslinking to peptides or proteins (see previous Section).⁷⁹

Depending on their applications, hydrogels can be crosslinked either reversibly, leading to degradable hydrogels,⁸⁰ or irreversibly, yielding chemically stable materials.⁸¹ Various hydrogel systems have been tested in cell culture experiments based on macromers with at least one crosslinkable group; e.g., polyvinyl alcohol (PVA) derivatives,^{82,83} hydroxyethyl methacrylate (HEMA) crosslinked with ethylene glycol dimethacrylate (EGDMA),⁸¹ or various PEG derivatives.⁷⁸

Concerning the design of an artificial ECM which is, chemically, highly specific, PEG-based hydrogels seem to be optimal candidates. As the synthetic polymer with the highest protein adsorption resistance,⁸⁴ PEG offers the possibility of designing materials with a high specificity for cell attachment, by copolymerizing adhesion receptors of choice to the network.

Regarding the mechanical properties of the ECM, PEG hydrogels feature excellent similarities to the hyaluronan found in the natural ECM. In PEG hydrogels, mechanical properties such as elasticity can be defined by the polymerization conditions.⁸⁵ More precisely, the molecular weight of the macromer, the crosslinking density, and the reaction conditions are all factors influencing the polymer mechanics. This is further detailed in Chapter IV. As in the case of a natural ECM, the molecular network of elastin (Section III.1.2), a macromer network composed of the coil-like dextran molecules, can increase the elasticity of an artificial ECM.⁸⁶

Generating structured surfaces

ECMs are structured on the micro- to nanometer scale by various components, namely the collagen matrix, the ligand distribution as adhesion anchors, or the intermolecular distances of RGDs in the fibronectin (discussed in Section III.1). These chemical, mechanical and topographical structures in the ECM influence cell behavior (Section III.3.3), and can be controlled in artificial ECMs.

Techniques used to structure materials on the micrometer scale are mainly based on photolithography. They mimic the distribution of adhesive islands in the ECM by immobilizing adhesion receptor ligands, either directly on surfaces patterned with photolithography, or indirectly, on surfaces structured via imprint techniques, using a stamp generated by photolithography.^{87,58} By means of molds, also generated by photolithography, surfaces with topographic structures for cell adhesion experiments can be formed.⁸⁸ In addition, the surface material can be patterned in terms of elastic properties by using micro-structured masks for the photoinduced polymerization.⁵⁶

In general, nanometer-scale structuring of surfaces for cell experiments is achieved by different kinds of self-organization processes. Other nanostructuring techniques are limited in the size of the structured area to which they may be applied. A structure of self-assembled nanofibers was used to control the differentiation of neural progenitor cells.⁸⁹ To stimulate the growth of macrophages, nanoscopic topography at dimensions of between 30 and 280 nm was generated by etching the structures in a silicon support.⁵⁵ In the present study, block-copolymer micelle nanolithography⁹⁰ was applied, as described in Chapter V, below. Both, the ligand density, and the ligand distance can be defined at the scale of the resulting nanopattern.⁵⁴

Approaches to synthetic ECMs

The combination of bio-functionalization, polymeric supports and various structuring techniques has led to the preparation of different types of synthetic ECMs.⁹¹

The immobilization of RGD peptides on surfaces following one of the reactions (Section III.1.2.; illustrated in Fig. 22) leads to a well-defined ligand density and peptide orientation.⁹² RGD peptides can also be copolymerized in a PEG hydrogel network.⁹³ The passivating properties of PEG can thereby be specifically altered by the density of added biofunctions on the surface, while the mechanical properties of the PEG can be independently tuned. By immobilizing different peptide sequences on a patterned gold surface using photochemical activation reactions, the distribution of ECM proteins *in vivo* can be mimicked on an artificial surface.^{94,95}

The change in micro-scale elasticity of ECMs in tissues was mimicked by preparing hydrogels with an elasticity gradient. This was accomplished by means of photo-initiated polymerization and patterning, to modulate cell migration.⁵⁶ Recently, a synthesis route toward self-assembled monolayers of star-shaped PEG hydrogels was developed, that enables the coupling of peptides and proteins at a well-defined density.⁷⁶ Similarly, comb copolymer films were prepared, and the tails functionalized with RGD sequences, resulting in peptide nanoclusters.^{96,97} New approaches to the formation of three-dimensional gels with micro- or nanopores from peptides or PEG hydrogels enable the design of artificial ECMs in three dimensions.⁹⁸

III.4.2. *Concept of synthetic modular ECMs*

As mentioned above, the aim of this work is the development of a variety of synthetic modules which can be flexibly combined to form artificial ECMs with required properties. Such a system, which allows the simple tailoring of an ECM by combining standardized tools, would serve as a powerful instrument in experiments focusing on the interactions between the ECM and cells. The concept of the system developed and described herein, includes three basic modules (Fig. 23) which, to some extent, were previously described in the literature (Section III.4.1).

Chapter IV will describe the **basic material** used for the artificial ECM. In brief, this material consists of a crosslinked poly(ethylene glycol) (PEG) hydrogel with mechanical properties that are tunable by varying the polymerization conditions⁸⁵ and combinations with other macromers such as dextran.⁸⁶ It mimics the mechanical properties of the polysaccharide network including the hyaluronan, elastin and the proteoglycans of the ECM, and can be formed into microscopic topographic structures (e.g., tubes or pillars). Furthermore, the material is a protein adsorption-resistant hydrogel; thus, its chemical behavior toward cells is inert.⁸⁴ PEG hydrogels are well-known, and commonly used for the design of artificial ECMs.

Chapter V describes the **structuring component**, which consists of gold micro- and nano-structures on the hydrogel surface. These gold structures function as a chemical pre-structure, used to immobilize various biological active molecules via a thiol group. They successfully mimic the chemical structures in the ECM, ranging from the nanoscopic localization of single peptides, to the microscopic distribution of adhesion sites. The gold structures used in this study provide binding sites for cell receptor-binding molecules, thereby providing a means by which to direct the assembly of transmembrane proteins, enabling control over protein interactions and function. While gold micro- and nanostructures on solid inorganic supports are well-known, a novel technique for the generation of ordered gold binding sites on hydrogel surfaces has been developed in this study. **Chapter VI** describes how these modules cannot only be applied to planar surfaces, but to **non-planar surfaces** as well. The resulting nanopatterned hydrogel channels provide structural elements in three dimensions.

The **chemical modification** of the artificial surface discussed in **Chapter VII** includes a linker system, which enables the specific immobilization of diverse biologically active molecules like peptides or proteins on either the gold structures or on the hydrogel. A grafting system was developed herein, which enables the immobilization of various proteins to the hydrogel.

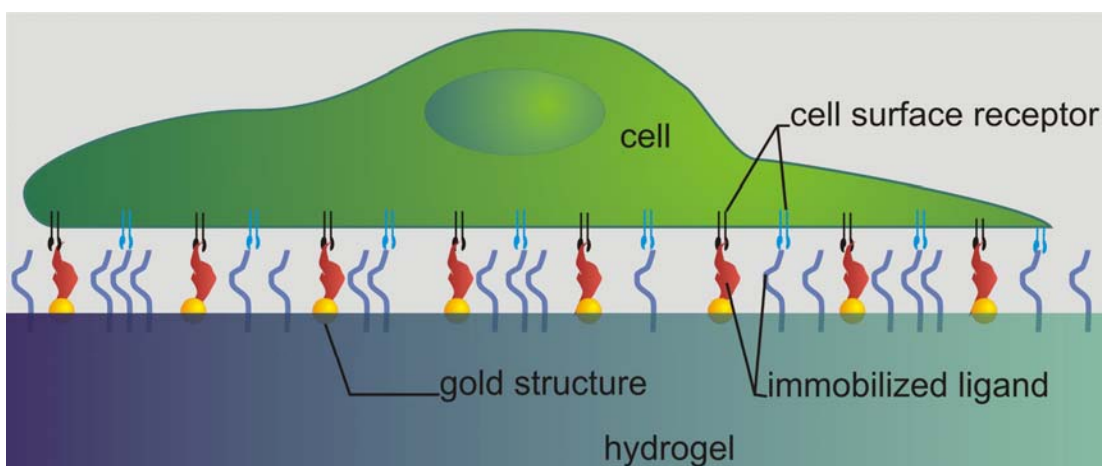


Fig. 23: The modularly-designed artificial ECM consists of several different tools: the basic material (hydrogel), the structuring components (gold structures) and the chemical modifications of the basic material and the structures (immobilized ligands).

IV. PEG-based supports with tunable mechanical properties

To mimic the cellular environment in terms of mechanical properties, a polymeric system is required, with mechanical properties close to those of the hydrogel system found in the complex water-containing polymeric network which forms the natural ECM. Such a hydrogel can be mimicked by poly(ethylene glycol) (PEG) macromers, which form a meshwork once they are crosslinked via functional end groups. It is then necessary to control the elasticity of the PEG, and to characterize its nature. The PEG hydrogel system was chosen because of its resistance towards protein adsorption and its elastic properties, both of which are comparable to those of the natural ECM. The system was selected in such a way that the crosslinking conditions responsible for the resulting hydrogel were easily controllable. The characterization of the gels was performed with an atomic force microscope (AFM). The aim was to develop standard protocols for the crosslinking of hydrogels with Young's moduli, ranging from 1 kPa to a value higher than 1000 kPa. This is the range within which cells react to changes in surface rigidity, as described in Section III.3.1.^{41,42}

IV.1. Tuning the mechanical properties of PEG hydrogels

The elasticity of a crosslinked synthetic hydrogel depends on its crosslinking density which, in turn, depends on the crosslinking reaction conditions and on the choice of the macromer. To obtain hydrogels with defined elasticities, these reaction conditions must be controlled.

IV.1.1. Crosslinking reaction of PEG-DA

By modifying the end groups of the poly(ethylene glycol) (PEG) macromers to crosslinkable groups such as isocyanates, methacrylates or acrylates, the macromers can be crosslinked to form hydrogels. A light-induced crosslinking reaction via acrylate groups was chosen for this study, because it is easily controllable. The corresponding macromer used for this research was poly(ethylene glycol) diacrylate (PEG-DA). PEG-DA Macromers with molecular weights of 700 g/mol, 4,000 g/mol, 10,000 g/mol, 20,000 g/mol were used and termed in the following as PEG 700, PEG 4,000, PEG 10,000 and PEG 20,000.

Most photo-polymerizations are induced by the cleavage of a photoinitiator. The initiator undergoes photo cleavage to form two radicals upon exposure to a special light wave length, which promotes the polymerization reaction. In this work, the photoinitiator 2-hydroxy-4'-(2-hydroxyethoxy)-2-methylpropiophenone was used, which is cleaved upon radiation with at a wavelength of 365nm (Fig. 24). The reasons

for this choice of initiator were threefold: In contrast to most other photoinitiators (e.g., 2,2-dimethoxy-2-phenylacetophenone, triethanolamine or isopropyl thioxanthone) it is **not cytotoxic**.⁹⁹ Moreover, it allows the usage of **water as solvent**, and it can also be **precisely dosed**, due to its small yet sufficient solubility in water.⁹⁹

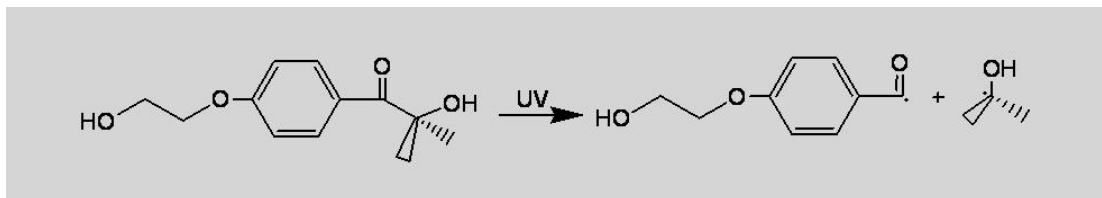


Fig. 24: Photocleavage of the photoinitiator 4-(2-hydroxyethoxy)phenyl-(2-propyl)ketone, used in this study to form two radicals for initiating the photopolymerization.

In the primary reaction which is initiating the polymerization, the radical attacks the terminal acrylate groups of the macromer, resulting in the formation of a macromer radical (chain start reaction, Fig. 25). The chain reaction continues, if the PEG-DA radicals react with PEG-DA macromers (chain growth reaction, Fig. 25). These steps do not involve a change in the radical concentration. The chain reaction terminates when the two radicals react with each other (Fig. 26). The photopolymerization results in a crosslinked PEG. Due to the tendency of oxygen to form radicals, the radical crosslinking reactions have to be carried out in an inert gas atmosphere, to avoid non-specific reactions of the acrylate groups with oxygen.

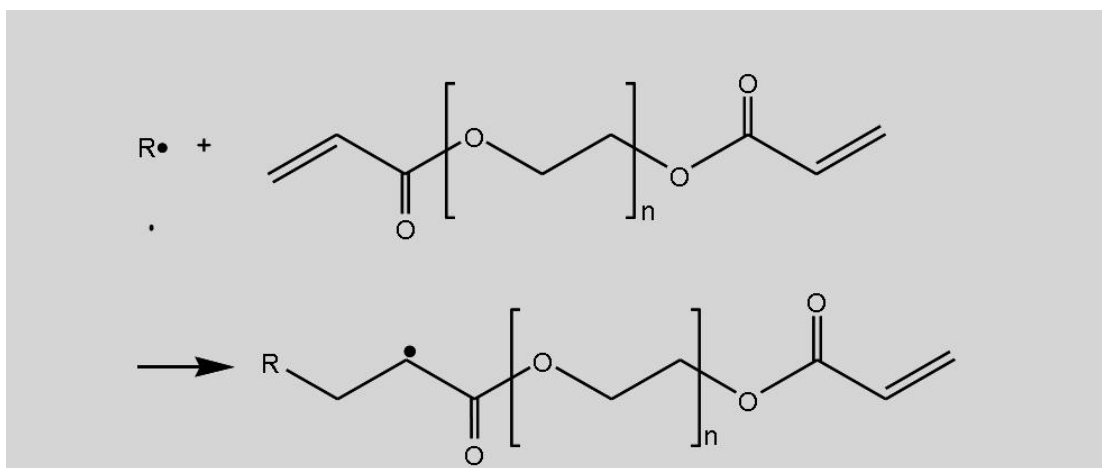


Fig. 25: Chain start reaction and chain growth reaction. The chain reaction is initiated by the reaction of the initiator radical (R) with a PEG-DA monomer. Repeated crosslinking of PEG-DA macromers occurs as the PEG-DA radicals (R) react with further PEG-DA macromers.

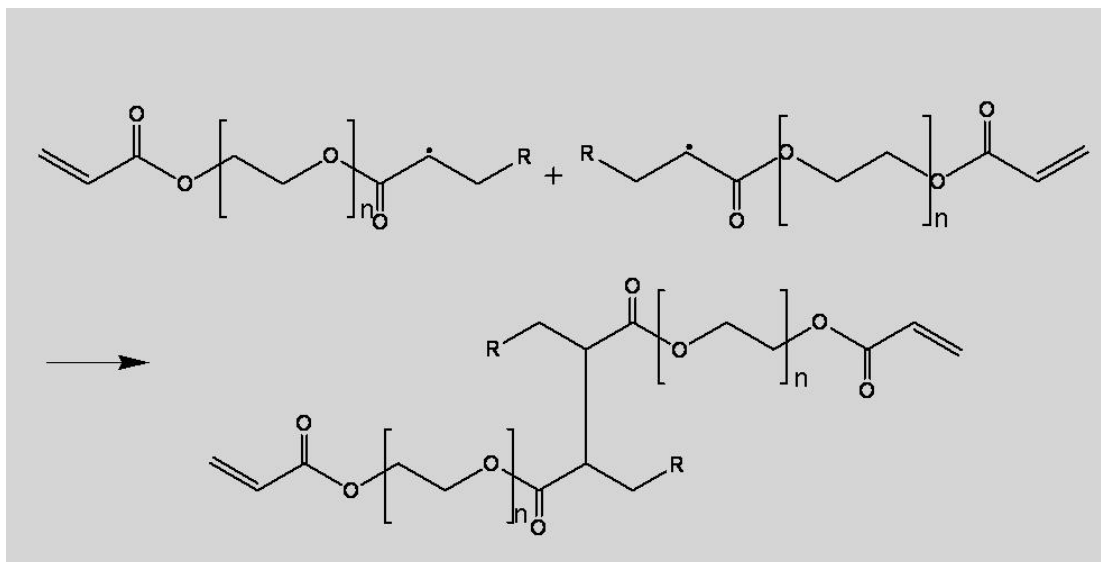


Fig. 26: Chain formation interruption reaction. The polymerization reaction ends when two radicals react with each other to form a non-reactive product, the crosslinked PEG hydrogel.

IV.1.2. Crosslinking parameters and mechanical properties

The mechanical properties of crosslinked polymer networks, such as their elasticity, swelling ratio in a solvent, and gel content, which define the percentage of non-crosslinked polymer chains remaining after the crosslinking reaction, are highly dependent on their crosslinking density.¹⁰⁰ The crosslinking density may be defined as the number of crosslinks per molecular weight (Fig. 27). In the following sections, the molecular weight between crosslinks will be indicated with M_c . The mesh size, ξ , is another measure of crosslinking density, and is directly related to the molecular weight of the molecule between crosslinks.¹⁰¹

Influence of crosslinking parameters on the molecular structure of the hydrogel

In terms of mesh size, the molecular structure of the hydrogel can be controlled by the crosslinking conditions, as follows:

In general, the concentration of reactive groups strongly influences the resulting mesh size; i. e., the crosslinking density. First, the greater the macromer length, the lower the crosslinking density.¹⁰¹ Secondly, an increase in macromer concentration leads to an increase in crosslinking density.¹⁰² The mesh size for hydrogels derived from a PEG-DA macromer with the molecular mass of 3,500, for example, has a range which is dependent up on the solvent concentration during crosslinking, from 140 to 40 Å.¹⁰² Thirdly, a high number of reactive groups per macromer increases the crosslinking density.⁷⁶ Apart from the reactive group concentration in the reaction solution, another parameter used to control the mesh size is the irradiation time necessary for

the photopolymerization to occur – the longer the time, the more crosslinking occurs.¹⁰¹

A high degree of crosslinking cannot be achieved when the reaction conditions favor chain ending reactions (Fig. 26); in particular, those leading to cyclization reactions. Intrachain cyclization reactions do not contribute to the overall polymer network, and can be minimized by avoiding highly diluted macromer solutions, thereby guaranteeing sufficient entanglement between the macromers.¹⁰³

Another parameter which greatly influences the crosslinking is the initiator concentration.¹⁰⁴ In a kinetic sense, high concentrations yield fast reactions, and thereby result in heterogeneous molecular structures within the hydrogel, in terms of molecular size and mesh size. Furthermore, in the case of high initiator concentrations, the initiator radicals themselves do not only initiate radical chain reactions, but also function as chain reaction blockers, by reacting with macromer radicals. Therefore, the initiator concentration chosen should be as low as possible, but as high as is necessary to ensure an efficient chain reaction.

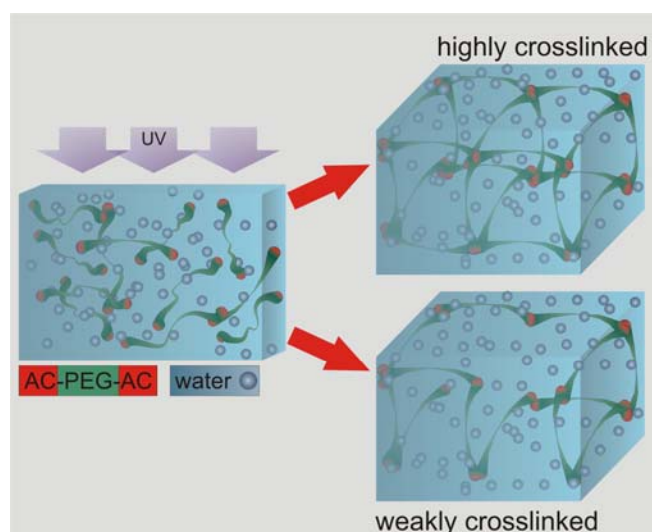


Fig. 27: Reaction of a PEG-DA/water mixture to a hydrogel. Variations in reaction conditions result in different crosslinking densities.

The influence of the crosslinking density on the mechanical properties of the hydrogel

The crosslinking density determines the following properties of the hydrogel:

Gel content: The gel content is defined as w_2/w_1 , the ratio of the weight of the resulting (dry) hydrogel, w_2 , and the macromer used for the crosslinking reaction, w_1 .¹⁰⁵ Obviously, the gel content is indirectly related to the crosslinking density, in that it is lower for incomplete crosslinking reactions. However, hydrogels with long macromers and a high degree of cyclization, display a low crosslinking density and a low gel content. The gel content for crosslinking systems with macromers with a

molecular weight of between 5,000 g/mol to 20,000 g/mol, and two crosslinkable groups per chain, ranges from 60-90%.

Swelling and water content: The swelling property of a hydrogel is defined as the ratio of the swollen and the dry gel, either referring to the volume $[V(\text{swollen})/V(\text{dry})]^{106}$ or the mass $[w(\text{swollen})/w(\text{dry})]$. Here, we are interested in the geometric properties of the nanostructure that has been transferred to the hydrogel: the swelling behavior is characterized by the change in distance between two arbitrarily-chosen points. Instead of relating the change to the completely dry gel, the change is related to the initial gel containing water after its crosslinking. Thus, the swelling behavior is defined in this context as $d(\text{wet})/d(\text{initial})$, or $d2/d1$. This second definition was used in this work to draw a relationship between the two different states of the hydrogel (Section IV.3.2). A low crosslinking density permits more uptake of water into the network, which typically displays a high water content, leading to a higher volume and mass of the gel in the swollen state. Increasing the solvent concentration during the polymerization increases the molecular weight between crosslinks by nearly a factor of three, and more than doubles the swelling ratio.¹⁰⁰

Elasticity: According to Hooke's law, the strain, ε , which is the change in the length of the hydrogel divided by its original length, is proportional to the stress, σ , the force applied on the surface of the material at the contact area. The ratio of the two is a constant commonly used to indicate the elasticity of a substrate.¹⁰⁷ This constant represents the Young's modulus E , with $E = \frac{\sigma}{\varepsilon}$. The elasticity decreases, concomitant with a decrease in crosslinking density. The Young's modulus of PEG-DA hydrogels with a molecular weight of 8k varies, depending on the solvent concentration during polymerization, which ranges from 50 to 180 kPa.¹⁰⁸

IV.2. Characterizing the mechanical properties of a hydrogel

IV.2.1. Determination of the mesh size, swelling and gel content

One of the major factors determining the swelling ratio and the water content in a hydrogel, as described in Section IV.1.2, is the mesh size. Thus, the average mesh size can be determined by measuring either the swelling behavior, or the gel content.

In experiments, the gel content is determined by washing and drying the gel repeatedly, until the dried gel does not show any further loss of weight. The ratio between the mass of the dry macromers and the mass of the washed and dried gel, yields the gel content (Section IV.1.2). Once the macromers, which are not covalently bound to the gel, are washed out, the ratio of the gel's weight in both the dry and the swollen state yields the swelling ratio of the gel. It has to be noted that in their

swelling behavior, most hydrogels show sensitivity to the ion concentration and pH of the solvent.

The mesh size, ξ has been related to the swelling behavior; more precisely, to the volume fraction of the polymer in the swollen state, f_v , by Canal and Peppas¹⁰⁹,

$$\xi = f_v^{-1/3} C_n^{1/2} n^{1/2} l, \quad (1)$$

where C_n is the characteristic ratio of the polymer, in this instance, for PEG 4.0¹¹⁰, and l is the average bond length. The average number of bonds between crosslinks, n , is given by

$$n = \frac{3M_w}{M_r}, \quad (2)$$

where M_w is the average molecular weight of the polymer, and M_r is the molecular weight of the repeat unit ($M_r = 44$ for PEG).

Similarly, the molecular weight between crosslinks, another way to measure the crosslinking density of the polymer, can be calculated from ν_2 , using the approach of Flory and Rehner.¹¹¹ Here, the calculation of the mesh size, as described above, was sufficient to gain insight into the network properties of the hydrogel.

IV.2.2. *Measuring elasticity at the nanoscale*

The elasticity of a polymer can be measured by various approaches. Most commonly, the methods are based on compression and elongation analysis as well as dynamic mechanical analysis on a macroscopic scale, thus yielding the macroscopic elasticity of the material.¹¹² Here, we are interested in the local elasticity of the hydrogel on a nanometer scale, because this is the molecular quantity sensed by the cell. Therefore, an alternative analytic approach was used, the indentation of the hydrogel with an atomic force microscope (AFM). In brief, the AFM consists of a tip positioned at a flexible linker, the cantilever, with a known spring constant which can be precisely adjusted relative to the surface to be analyzed. It is increasingly used to measure mechanical properties on a molecular scale.^{113,114}

Atomic force microscopic measurements are carried out as shown in Fig. 28. The cantilever is brought toward the surface (A), touches the surface and is deflected by a repulsive force of the hydrogel which is proportional to its elastic modulus (B). The force itself, in dependency of the cantilever position, is monitored. The cantilever is then retracted from the surface (C) so that the force decreases, until the tip is again detached from it (D). The overall force profile results from averaging values from a range of experiments. As schematically drawn in Fig. 28, the profile typically shows a

IV.3. Experiments, results and discussion

IV.3.1. Crosslinking of PEG

One of the steps involved in the modular design of artificial ECMs consists of the transfer of gold structures onto hydrogels. For high reproducibility and quantitative comparisons, the preparation of the hydrogels, including the crosslinking conditions and PEG mixtures used, were standardized. To this end, the reaction conditions as well as the concentrations of the involved chemicals were varied, to obtain hydrogels appropriate for the experiments involving the transfer of gold structures onto the gel, and their application to cell experiments (described in Chapters V - VIII). The reaction conditions were chosen, by addressing the following criteria:

- For a high gel content in the resulting hydrogels, the maximal concentration of PEG-DA in water near to saturation was chosen, as described in Section IV.1.2. The chemicals used for the crosslinking reaction (water and PEG) were degassed before usage, and all steps of the reaction were performed in a nitrogen atmosphere, in order to avoid non-specific reactions with oxygen radicals, which would result in a lower gel content.
- The elasticity of the different gels should cover a wide range of Young's moduli. This requirement was achieved by varying the chain length of the macromers (Section IV.1.2). However, using PEG-DA with chain lengths differing by a few orders of magnitude, does not permit routine application of a standard reaction protocol, but instead requires that reaction conditions be adapted, accordingly.
- Furthermore, the reaction process should be easily controllable. In general, photo- initiated crosslinking reactions are more defined and better controllable than thermal- initiated reactions, both of which is essential for the reproducibility of the mechanical properties.
- The hydrogel should not contain cytotoxic substances. The slightly water soluble and non-cytotoxic photo initiator 4-(2-hydroxyethoxy)phenyl-(2-hydroxy-2-propyl)ketone (Irgacure 2959) was therefore chosen for the reactions.⁹⁹
- To obtain homogeneous planar gel slices with a defined thickness, the crosslinking of the PEG-DA solution was performed between two glass slides, separated by two spacers (Fig. 29. a).

In order to clarify the proper reaction conditions, experiments were carried out using various concentrations of components and other reaction parameters. A special experimental set-up, consisting of a nitrogen-filled glass tube with a UV light source

placed at a defined distance to the reaction mixture, was constructed, in order to guarantee reproducible reaction conditions (Fig. 29. b). The parameters for the preparation of the gels used in all of the following experiments are given in the protocol described below. Table 1 details the corresponding ratios of the various components.

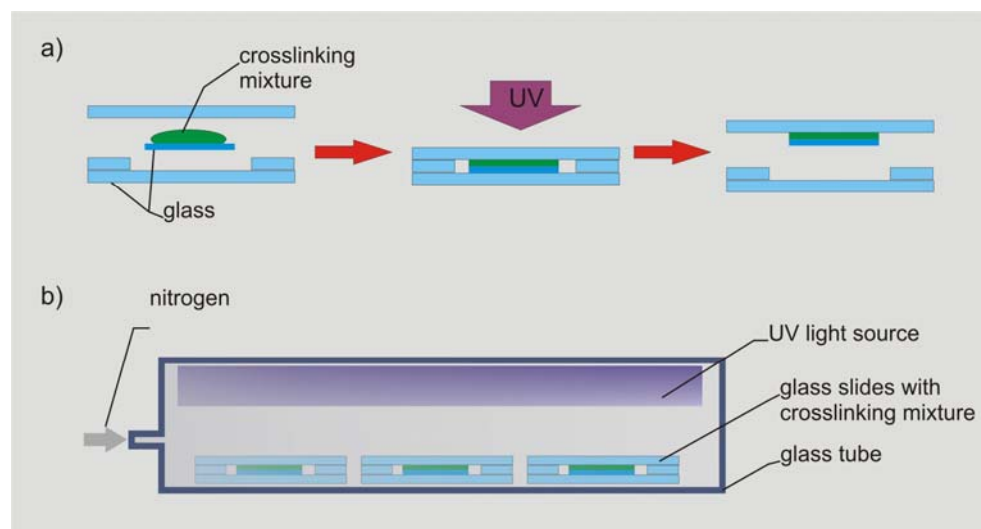


Fig. 29: Scheme for the crosslinking reaction set-up. a) A drop of the crosslinking mixture is flattened by two glass slides during the crosslinking procedure. b) A special reaction chamber with a UV light source at the top, the reaction chamber at the bottom, and a nitrogen supply, was designed to guarantee reproducible reaction conditions.

The PEG-DA crosslinking protocol

All hydrogels used in this work were prepared according to the following protocol:

The PEG-DA was degassed in a Schlenk flask under vacuum conditions, for 10 min. The water was degassed in a Schlenk flask by heating it to boiling (100°C) and bubbling nitrogen through the water for 10 min. Water was added to the PEG-DA, according to the volumes reported in Table 1. The mixture was kept under nitrogen in the dark, and was stirred until the solution was transparent. A tight vacuum was then used to remove bubbles from the solution. A spatula tip of initiator was added to the rest of the degassed water, which was also kept in the dark under nitrogen. The mixture was tempered at 25 °C and stirred for at least 30 min, to obtain a saturated initiator solution. The initiator solution (Table 1) was then filtered with a 0.2 μm syringe filter, and added to the polymer solution. A drop of the reaction mixture was put on a glass slide under nitrogen in the reaction chamber (Fig. 29. b) and covered with a glass cover slip (Fig. 29. a). Polymerization was carried out for about 30 minutes with 350 nm UV light. After crosslinking, the gels were peeled off of the glass slides.

Standard mixtures for the preparation of the hydrogels

The crosslinking mixtures of PEG-DA, water and initiator were chosen according to the criteria described above. We aimed at generating gels with a high gel content, covering a wide range of different Young's moduli. In some cases, an additional component, 2-carboxyethylacrylate (in the following termed as Carb AC), was copolymerised to the PEG chains to obtain chemically functional binding sites with a certain concentration in the crosslinked hydrogel (Fig. 62). The functionality and the further processing of the functionalized gels will be discussed in Chapter VII.

According to the literature,⁹⁹ the concentration of the initiator Irgacure 2959 was chosen to be between 0.05% and 0.1% w/w to PEG-DA. Its solubility in water is 7.6 mg/ml at 25 °C.⁹⁹

Table 1: The ratios of the various components used for the preparation of the PEG-based hydrogels.

PEG-DA	carboxyethylacrylate (Carb AC)	water	Irgacure
Mw 700 (2 ml)	-----	100 μ l	130 μ l
Mw 10K (0.2 g)	-----	120 μ l	30 μ l
Mw 20K (0.2 g)	-----	120 μ l	30 μ l
Mw 700 (2 ml)	100 μ l	100 μ l	130 μ l
Mw 10K (0.2 g)	50 μ l	120 μ l	30 μ l
Mw 20K (0.2 g)	50 μ l	140 μ l	30 μ l

IV.3.2. Gel content and swelling ratio

The hydrogels prepared by following the protocol in Section IV.3.1 were tested as to their mass, diameter and volume. As described in Section IV.1.2 and IV.2.1, these values can be used to calculate the gel content, swelling ratio and volume fraction of the polymer in the swollen state f_v , and to estimate the mesh size of the hydrogel. For the cell experiments in the Chapter VIII, the behavior of the gels in cell media was essential thus, the gels were swollen in media and not in water. To estimate in the following experiments the changes in the structures applied to the gel, or the distance of copolymerized ligands, it was necessary to measure the swelling ratio between the gels, directly after polymerization, and the completely swollen gels in cell media. Fig.

30 describes the different swelling states of a hydrogel. For some values, it was necessary to wash and dry the gel over several cycles, until the dried gel ceased to show any loss of weight after repeated washing. The measured values mass M , diameter D and volume V are shown in Fig. 30.

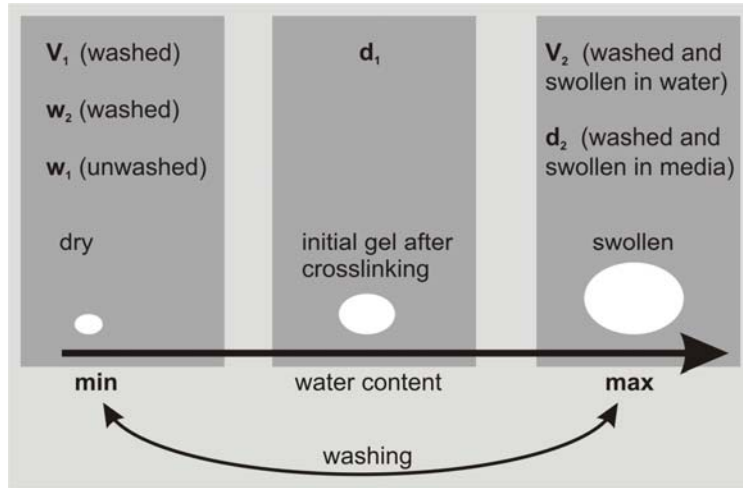


Fig. 30: Schematic of the different swelling states of a hydrogel.

These values were used to determine the swelling ratio $= \frac{d_2}{d_1}$, the gel content $= \frac{w_2}{w_1}$, the volume fraction $f_v = \frac{V_1}{V_2}$, and the resulting mesh size ξ as described in IV.1.2.

The results are compiled in Table 2.

Table 2: Experimental data characterizing the PEG hydrogels obtained by the crosslinking of PEG-DA of different molecular weights, following the protocols described in the previous section.

PEG-DA (Mw in g/mol)	Swelling ratio	Gel content	Volume fraction	Mesh size (nm)
Mw 700	1.19 ± 0.05	0.50 ± 0.09	0.79 ± 0.04	2.1 ± 0.18
Mw 10K	1.70 ± 0.05	0.86 ± 0.09	0.30 ± 0.04	11.0 ± 0.18
Mw 20K	2.36 ± 0.05	0.53 ± 0.09	0.29 ± 0.04	15.6 ± 0.18
Mw 700 (Carb)	1.15 ± 0.05	0.45 ± 0.09	0.86 ± 0.04	2.0 ± 0.18
Mw 10K (Carb)	1.75 ± 0.05	0.15 ± 0.09	0.92 ± 0.04	7.5 ± 0.18
Mw 20K (Carb)	2.61 ± 0.05	0.40 ± 0.09	0.67 ± 0.04	11.9 ± 0.18

As expected, the swelling ratio increases from PEG 700 hydrogels, to PEG 20,000 hydrogels. The same tendency was found for the swelling of the gels resulting from PEG / Carb mixtures. One example which illustrates the effect of the swelling behavior of the hydrogel with micrometer scale marks is shown in Fig. 31. The hydrogel was obtained from PEG 4,000, and the microstructure was added to the hydrogel during cross-linking, as described in further detail in Chapter V. Upon swelling, the scale of the micro-structure increased by a factor of roughly 1.4.

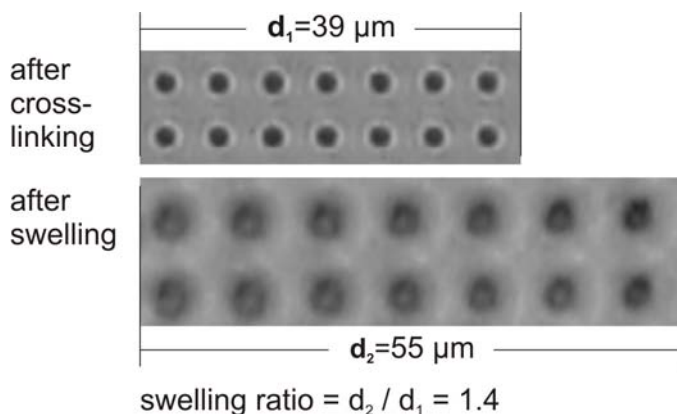


Fig. 31: Light microscope images of a PEG 4,000 hydrogel with microstructures after crosslinking with a size of d_1 and after swelling in water d_2 . The distance between the microdots increased by 40%.

The gel content did not show a simple dependency on its molecular weight. This inconsistency can be explained by the application of PEG-DAs which were not dried before usage. To obtain more meaningful data for the gel content, experiments would have to be repeated with dried PEG-DAs.

The mesh size is calculated from the volume fraction and the molecular weight as given in Equations (1) and (2). The expected increase in the mesh size, from a PEG 700 hydrogel to a PEG 20,000 hydrogel simply arises from the increase in the molecular weight of the macromer that determines the distance between crosslinking moieties. In hydrogels containing Carb, the values show the same tendency, but the mesh sizes are smaller than the respective values for hydrogels without Carb. As expected, the addition of Carb leads to a higher density of crosslinks by providing additional acryl groups for crosslinking reactions (Fig. 32).

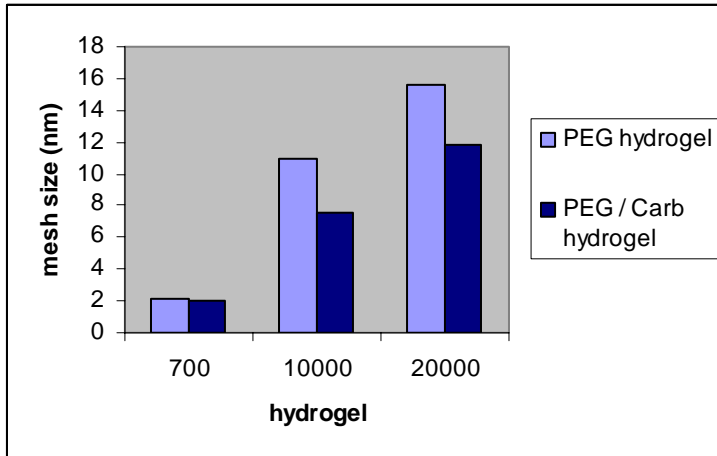


Fig. 32: Mesh sizes calculated from volume fractions for hydrogels of different molecular weights.

IV.3.3. AFM Indentation

The application of hydrogels as artificial ECMs renders their elastic properties as one of their most crucial characteristics. Therefore, a series of hydrogels with varying compositions of reaction mixture were prepared as described above, to establish their elasticities and associated properties in cell experiments.

The parameter used to assess the elasticity of the hydrogel is the Young's modulus (Section IV.1.2). It was measured by means of AFM indentation experiments, and derived from the indentation of the AFM tip into the gel at a given force (Section IV.2.2). This method has the advantage of yielding elastic moduli resolved on the nanometer scale, which is the quantity sensed by the cells which would be relevant to future biological applications.

The measurements were carried out in a liquid environment, to avoid drying effects on the gels. Instead of a conventional sharp tip, a cantilever with a spherical polystyrene bead with a diameter of $6\mu\text{m}$ was used. This enables the calculation of the Young's modulus as described in Section IV.2.2, as the contact area of the bead can be easily estimated from its diameter. The measurements were carried out with cantilevers with spring constants of 0.58 N/m .

For each hydrogel, the indentation was measured as the difference of the cantilever deflection at a given cantilever position between sapphire, as a solid non-elastic reference, and the hydrogel under investigation. The corresponding force was obtained from the deflection and the cantilever spring constant, and finally yielded the Young's modulus by fitting the data to Equation (3). The results are given in Table 3.

Table 3: Young's modulus for hydrogels of different mesh sizes, as determined by AFM indentation. The measurements were kindly carried out by Dr. Nicole Rauch.

Hydrogel type	PEG 700	PEG 10 000	PEG 20 000
Young's modulus (kPa)	7000 ± 3700	60 ± 12	1.2 ± 0.3

The measured Young's moduli covered a range of between 10^3 and 10^6 Pa. Thus, the series of synthesized hydrogels prepared in this thesis for the nano-lithography transfer method indeed encompasses the range of elasticities within which cell mechanics can be addressed. AFM indentation proved suitable to measure this range of Young's moduli at the nanoscale. It must be noted that the measurements are still incomplete (Carb-containing hydrogels remain to be characterized), and involve significant uncertainties up to a factor of 1.5 of the measured Young's moduli. However, the accuracy is sufficient for estimating the order of magnitude of elasticities, and for revealing the expected tendencies among the different hydrogels.

IV.4. Conclusion

The first module of the modular artificial ECM developed in this thesis, a hydrogel as the basic material, was prepared and characterized as described in this chapter. The PEG hydrogel was prepared under reaction conditions that enabled quantitative control over the properties of the resulting gel. For this purpose, the photo-initiated crosslinking reaction of PEG-DA macromers was developed and optimized. Parameters of interest such as mesh size, as given by the volume fraction and the swelling behavior, were determined. The crucial parameter for subsequent cell experiments, the nanoscale elasticity of the hydrogel, was measured by the AFM indentation method. Since the medium affects the swelling behavior and thus the elasticity of the hydrogel, measurements of the gels used for cell experiments must be carried out in the cell culture medium in future tests. A series of hydrogels with varying elasticities have been successfully prepared as the basic material for nanopatterned surfaces. After the description of the other two modules of the artificial ECM, used to determine its structural and chemical properties, cell experiments are described in Chapter VIII which illustrate, among other things, the influence of the hydrogel mechanics on the adhering cells.

V. Nanostructured polymeric supports

V.1. Nanostructures

Biological systems are regulated by arrangements and interactions of proteins on a molecular level. As described in Section III.1.2, fibronectin and collagen fibrils are characterized by periodically appearing units on the nanometer scale, which interact with cells.^{14,24} To gain insight into the biological mechanisms of cell-environment interactions at this molecular scale, investigations of the crosstalk between the cell and the artificial ECM designed herein must be carried out at the level of single proteins and their assemblies; in other words, at the nanoscale. An essential prerequisite of the artificial ECM, therefore, is the structuring of the materials at the nanometer scale. This chapter reviews nanostructuring approaches; in particular, block copolymer micelle nano-lithography, as well as the transfer lithography developed for this study, to structure hydrogels for cell experiments.

V.1.1. Different nano-structuring approaches

With the basic material of a hydrogel as the first module at hand, the second aim of this thesis was to nano-pattern these substrates, in order to provide a well-defined structure for cell adhesion at the artificial ECM.

Different methods exist to structure surfaces periodically at the micro- and nanometer scales, for technical applications in areas such as optics or electronics.^{116,117} Most of the conventional structuring techniques follow the so-called “top-down approach”.¹¹⁸ These techniques have in common a surface which reacts chemically to excitation by energetic waves, is partially irradiated. In turn, either the irradiated or the non-irradiated areas can be dissolved in a solvent, or are chemically activated for the binding of other molecules. These procedures lead to chemically⁶⁸ and/or topographically¹¹⁹ structured surfaces with the desired structure mapped onto it. Examples for commercialized variants of this lithography principle are photolithography and electron beam lithography (e-beam lithography). The photolithographic method is based on light waves shining through a mask with transparent and non-transparent regions, onto a surface coated with a photo resist. In the next step, either the exposed or the non-exposed regions can be washed away, and the structure of the mask is topographically reproduced on the surface.¹¹⁹ Alternatively, the exposed regions are chemically activated, and can then be used to immobilize other molecules, such as proteins or peptides, onto the activated regions.⁶⁸ The resolution limit of the photolithographic method is set by the physical refraction limit of light ($\sim \lambda/NA^2$). By means of resolution enhancement techniques, the photolithography reaches a resolution limit of 50 nm. The structuring area is restricted

to several square micrometers. Electron beam lithography, in contrast, has a resolution limit of 10 nm, and employs a focused electron beam to etch structures into a resist which is sensitive to an electron beam.¹²⁰ Another lithographic approach, which is not based on the irradiation of a surface, is known as dip-pen-lithography¹²¹ which makes use of an atomic force microscope (AFM) to write structures to a surface. All these lithographic techniques are highly time-consuming and costly.

Another class of techniques, the soft lithographies, includes micro-contact printing^{122,123} and micro-fluidic patterning.^{124,125} These techniques are faster and cheaper than the structuring procedures described above, but require pre-structured masks which, in turn, depend on other structuring techniques.

A new, very promising approach to nano structure surfaces is based on the self-organization of molecules or particles which, under the right conditions, form periodical structures. One example is block copolymer micelle nano-lithography⁹⁰ used in this thesis, which is described in the following section (Section V.1.2). This technique, however, is restricted to inorganic, solid surfaces. Subsequent section (Section V.3) will then focus on the transfer of block copolymer micelle nano-lithography to soft, organic materials such as PEG hydrogels.

V.1.2. Block copolymer micelle nanolithography

Block copolymers

Block copolymers are macromers consisting of at least two polymeric blocks with different chemical compositions (Fig. 33 a). The larger the chemical difference between the blocks in terms of polarity, the higher their tendency to undergo phase separation. Since the blocks are covalently bound to each other, the maximum separation distance is restricted to the molecular dimensions. Thus, the blocks undergo a micro-separation.^{126,127}

Fig. 33 b illustrates a diblock copolymer consisting of a non-polar polystyrene (PS) and a polar poly(2-vinylpyridine)-block (P2VP).

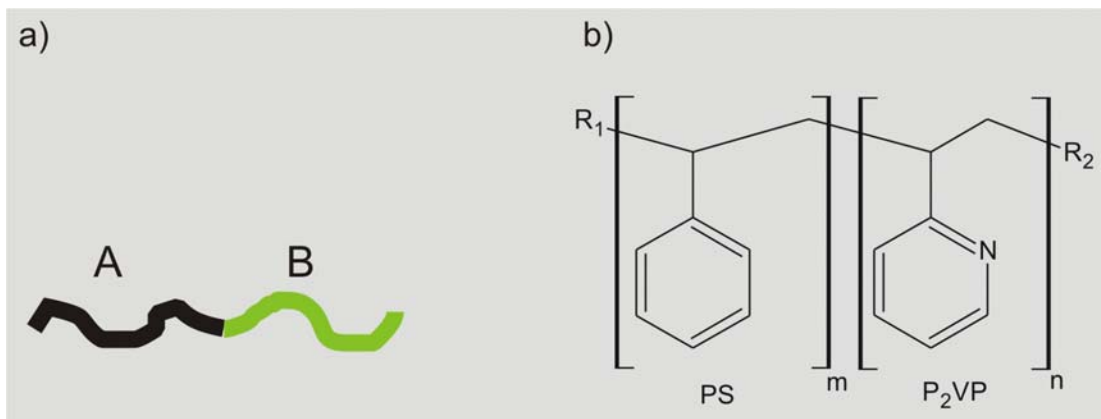


Fig. 33: a) Schematic drawing of a diblock copolymer consisting of block A and block B. b) A polystyrene (PS) - polar poly(2-vinylpyridine) (PVP) diblock copolymer.

Formation of micelles

Based on the micro-separation phenomenon, insoluble blocks of block copolymers can assemble in solution in supra-molecular structures called micelles.^{128,129,130} Two main factors influence the appearance and form of these assemblies. One is the concentration of macromers in the solvent. Above a critical concentration of monomers, known as the critical micellar concentration, association, which is based on the equilibrium between n -unimers and n -meres, sets in.¹³¹ The second factor influencing copolymer self-assembly is the relative concentration of the blocks in the macromere. Depending on the ratio between block A and block B of a diblock copolymer, the micelles can exhibit spherical (Fig. 34), rod-like or fibrillar structures. This behavior of the polymers is caused by the sterical hindrance of the blocks, which determines the number of aggregated macromers in a micelle and, thereby, the shape and size of the micelle.¹³² In this work, the diblock copolymer PS-P2VP is used to form spherical micelles in toluene, with the hydrophobic PS block as a peripheral shell, and the hydrophilic block, in a toluene-insoluble P2VP block, as the core (Fig. 34).

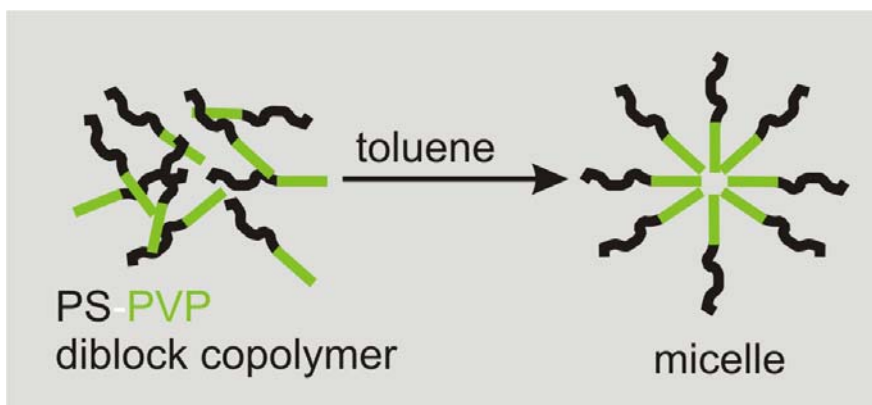


Fig. 34: Formation of spherical micelles of the diblock copolymer PS-P2VP in toluene

Block copolymer micelle nano-reactors

Once a micelle is formed, it provides a variety of well-segregated sections with defined chemical properties. This enables the performance of localized chemical reactions. In the case of the aforementioned spherical PS-P2VP micelles in toluene (Fig. 34), the hydrophilic vinylpyridine domains in the core of the micelle can be protonated, whereas the shell of the micelle is inert against acid-base reactions. Thus, metal salts such as HAuCl_4 , H_2PtCl_6 , ZnCl_2 , or AgOAc can be complexed specifically to the core of the micelles by protonating the vinylpyridine (Fig. 35). In thermodynamic equilibrium, the metal ions are distributed homogeneously over the micelles.

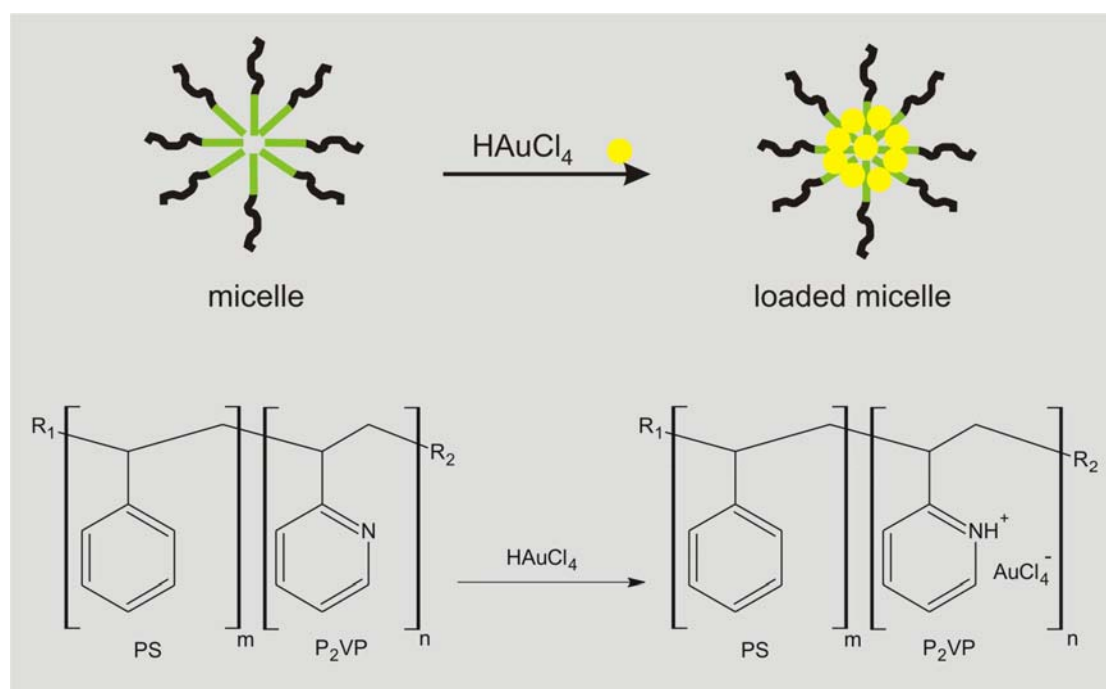


Fig. 35: Complexation of a metal salt in the core of a PS-P2VP micelle.

The degree of loading of the micelle with a metal salt can be defined as the ratio of the protonated number of vinylpyridine versus the total number of vinylpyridine units, thus:

$$L = n[\text{HVP}^+ \text{AuCl}_4^-] / n[\text{VP}]_{\text{tot}} \quad 3$$

In the next step, the metal salts can be reduced in the micelles to form metal nanoparticles of well-defined size, which is controlled by the degree of loading and the length of the P2VP block.^{133,134} The diblock copolymer micelle functions as a template for the arrangement of the metal salt, thus forming a nanostructure.

Periodical arrangement of nanoparticles

To obtain structured surfaces, the micellar nanotemplates have to be arranged on the surface in an organized manner. Even the smallest spherical particles can be arranged on a surface in an orderly fashion via self-organization processes.

To this end, a substrate must be coated with a thin layer of liquid containing the particles, either by simple drying of the solution,¹³³ by spincoating,¹³⁵ or through a dipping process (Fig. 36.a).¹³⁶ Under the right conditions, particles arrange in a closely-packed hexagonal monolayer during the evaporation of the solvent. The conditions required to form a monolayer comprise good wettability of the substrate with the used solvent, high mobility of the particles during evaporation, and a certain concentration of particles in the solvent. The self-organization can be described as a crystallization process of a two-dimensional crystal¹³⁷. It occurs in two steps, the nucleization event, and the subsequent crystal growth.¹³⁸ Both are driven by the attractive lateral capillary forces between particles partially immersed in a solvent film,¹³⁹ and the evaporation of the solvent of the previously-patterned area, which leads to a convective particle flux.

This self-organization process can be also achieved with spherical micelles. It allows the deposition of micelles on a surface in a hexagonal array (Fig. 36.b).¹⁴⁰ The main difference between micelles and solid spheres is their flexible shape, which allows variations in the packing density within a certain range. Due to the fact that the dragging of the substrate in Fig. 36.a influences the thickness of the solvent film, and thus the amount of micelles forming the monolayer, the pulling velocity has a strong impact on the density of the arranged micelles.

Besides the pulling speed necessary for the preparation of the hexagonal order, the chain length of the polymers in the micelle is responsible for the distance between the micelle cores in the hexagonal arrangement.

Once the micelles are deposited on the substrate, the polymeric template for the localization of the metal salt can be removed, while the metal salt is reduced with a gas plasma treatment, resulting in a periodical array of metal clusters. (Fig. 36 a,c,d).

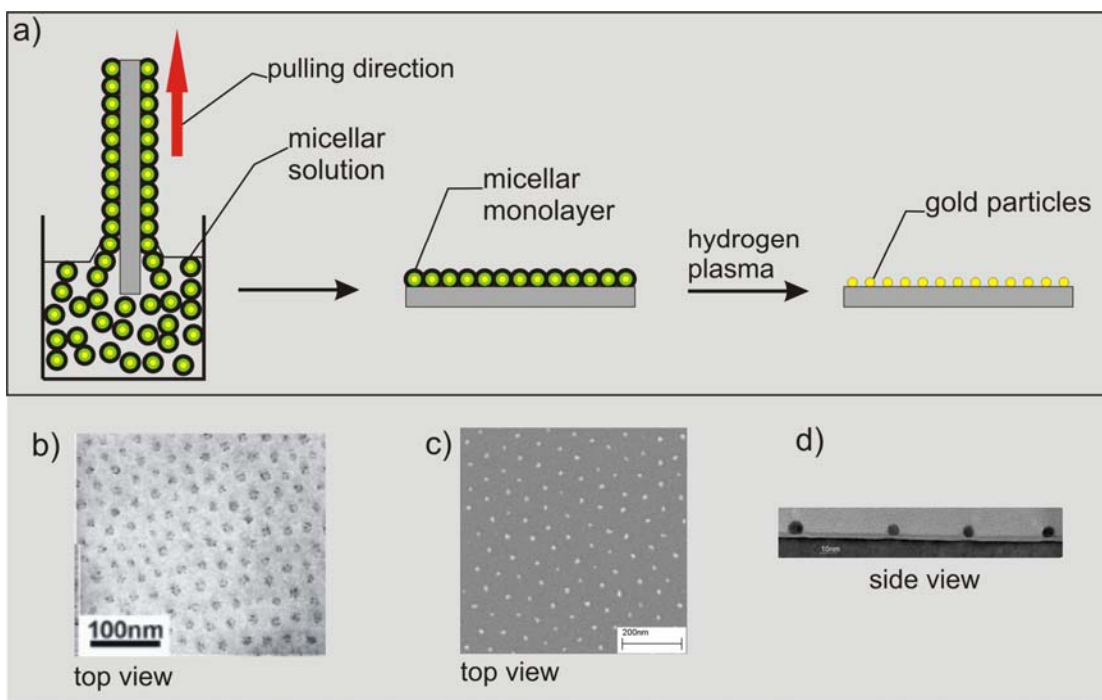


Fig. 36: (a) Formation of a micellar 2D crystal on a substrate surface via dip-coating, followed by a gas plasma treatment. (b) Transmission electron microscopy (TEM) image of loaded micelles in a hexagonal, closely-packed array. The contrast is caused by the metal ions, whereas the polymer core is not visible. (c) Scanning electron microscopy image of gold particles in a hexagonal array. (d) TEM side view of gold particles on a silicon surface. (The microscopic images were taken by Spatz *et al.*)

V.1.3. Preparation of gold nanopatterned substrates

The preparation of glass substrates decorated with gold nanoparticles of different sizes and separated by various distances, based on the principles described in Section V.1.2, is an established and standardized procedure.⁹⁰ If not otherwise mentioned, the nanopatterned substrates used in the following experiments have been prepared following these protocols. Three diblock copolymers with different block lengths were mainly employed in this study, in order to obtain three different standard distances of gold particles on glass substrate. The protocol for the preparation of hexagonally-arranged gold nanoparticles is described in the following paragraph. In Table 4 the specific parameters of the three used block copolymers are listed.

Protocol for the preparation of hexagonally-arranged gold nanoparticles

Polystyrene(x)-block-poly(2-vinylpyridine)(y), PS(x)-b-P2VP(y), was dissolved in toluene at room temperature, while stirring, for twenty-four hours. The molecular weights of the selected diblock copolymers are shown in Table 4. Hydrogen tetrachloroaurate(III) trihydrate was then added to the solution and stirred for twenty-four hours, resulting in a clear, precipitate-free solution.

Using a mixture of hydrogen peroxide and sulphuric acid (the so-called “piranha solution,”) the glass slides were cleaned by oxidation prior to usage. First, hydrogen peroxide and then sulphuric acid were added into the glass beaker at a ratio of 1:3. After the reaction proceeded for 30 min or more, slides were washed with MilliQ water and dried under nitrogen. The highly oxidative mixture removed all organic compounds from the surface, yielding a clean and highly hydrophilic glass slide, as required for the regular self-assembly of the micelles in the following steps.

A freshly-cleaned glass cover slip was then dipped into a solution with gold-loaded micelles derived from amphiphilic diblock copolymers [PS(x)-b-P2VP(y)]. Retraction at a constant speed yielded regular mono-layer films of micelles on the glass surface. The dipping procedure was performed with a voltage-adjustable power supply connected to a custom-made dipping device. The standard pulling speed was 12 mm/min. As soon as the samples were completely withdrawn from the solution, samples were removed from the solution beaker to avoid the influence of the toluene vapor upon the micellar film quality. After drying, the substrates covered with monomicellar films were exposed to a hydrogen plasma for 30 min, so that the desired hexagonally-ordered gold nanoparticle array was generated. A plasma cage was used to prevent the sputtering of silicon oxide from the chamber walls. The samples were then placed in a new designed alumina sample holder, to treat the glass coverslips from both sides with hydrogen plasma.

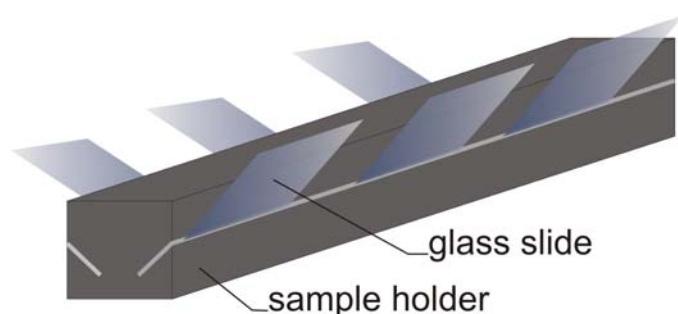


Fig. 37: Alumina sample holder. The sample holder was constructed to treat both the front and the back of the glass coverslips.

Table 4: Parameters for the three different PS-b-P2VP copolymers used in our experiments

Polymer	P3670-S2VP	P4707-S2VP	P4554-S2VP
Mw of PS-units (g/mol)	25500	52200	190000
Mw of PVP-units (g/mol)	23500	34,000	55000
Number of PS-units / polymer	245	501	1827
Number of VP-units / polymer	223	323	523
Concentration of the polymer	10mg/ml	5mg/ml	3mg/ml
Loading of the micelles (Eq. 3)	0.2	0.5	0.4
Particle distance	38nm	56nm	110nm

V.2. Transfer nanolithography

Block-copolymer micelle lithography and other lithographic techniques to nanopattern surfaces can only be applied to solid and mostly inorganic materials, typically silicon, quartz, or glass, due to the technical procedures involved.⁹⁰ Structuring soft materials has been achieved by means of contact printing procedures; however, with a limited resolution not lower than 50 nm,¹⁴¹ and only restricted possibilities as to the choice of the chemical composition of the support. This limits their application for the design of artificial ECMs, which requires the fast, simple and large-scale nanopatterning of elastic materials.

Generally speaking, the chemical and mechanical properties of the nanostructured material are strongly restricted by their preparation conditions. Hence, the broad application of a certain technique for the fabrication of a wide range of nanostructured materials, e.g. customized for their usage in cell experiments, presents a challenge.

For the second module of the artificial ECM, we describe a novel method to decorate polymeric surfaces with metallic nanopatterns, and the functionality of these new materials for cell experiments.¹⁴² We transfer metallic structures fabricated with an established nanolithography technique from the original surface to a polymeric surface of choice, with nanoscale precision. The so-called “transfer nanolithography” technique enables the flexible design of nano-structured systems, of which the properties of the basic material and the nano-structure can be adjusted independently, due to the transfer principle.

The principle method used for the transfer lithography is outlined in Fig. 38. A metal structure, e.g. gold nanoparticles, placed on an inorganic support such as glass or

silicon oxide, is functionalized by linker molecules binding selectively to the metal (Step 1). The function of the linker is to covalently connect the gold particle with the polymer to which the gold pattern is transferred. The structured surface is coated with a solution or melt of a polymer, which in turn is solidified. The metal structures are embedded in the polymer to which the linker molecules are connected by forming covalent or non-covalent interactions (Step 2). Separation of the original support from the polymer layer (Step 3) yields a polymeric material to which the metal structure has been transferred one-to-one.

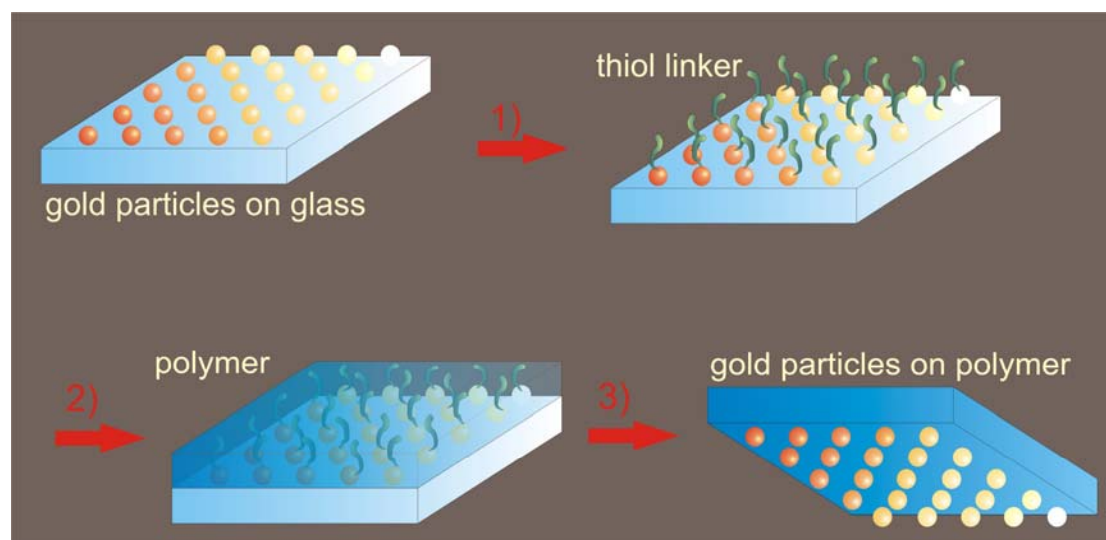


Fig. 38: Schematic of transfer nanolithography. 1) A metallic structure on a solid inorganic support is functionalized with linker molecules. 2) The inorganic support is coated with a polymer. The metal structures are embedded and connected via the linkers to the polymer. 3) The inorganic support and the polymer layer are separated, so that the metal structure is finally transferred from the first support to the polymer.

V.3. Transfer of gold clusters to different polymers

In principle, transfer lithography enables the passing of any initial metal micro- or nanostructure onto polymeric supports. Here, gold nano-patterns prepared by the block copolymer micelle nanolithography on glass as original nanostructures (Section V.1.3) were transferred. The target materials to be nanopatterned were hydrogels of different elasticities, prepared as described in Chapter IV. To test the transfer nanolithographic technique, and to extend its usage to other applications, the procedure was also applied to polymers other than PEG hydrogels. The resulting pattern transfer onto various different polymers was based on the same principle. The gold nanostructures were transferred from glass onto different polymeric systems, namely polystyrene (PS), poly(ethylene glycol) diacrylate (PEG-DA), epoxy resins and poly(dimethylsiloxane) (PDMS).

V.3.1. Linker system: Experiment and characterization

The artificial ECMs developed in this work are designed for probing the mechanical interactions of the cell with its environment. Therefore, the modular design must be such that the gold nano- and micropatterns are linked to the hydrogel surface. To form a link between gold and organic compounds, the thiol-gold bond proved not only to be a useful system, but also very versatile in organometallic synthesis. In this study, the bond between the hydrogel and the gold was established by incorporating a linker that was connected to the polymer at one end, and carried a thiol moiety to bind to gold, at the other end. The first step in Fig. 38 shows how this was achieved: The thiol linker was added to the glass surface, and those molecules in contact with the substrate self-assembled exclusively on the gold particles. The link to the polymer (second step in Fig. 38) could be established by either a covalent (e.g., PEG-DA or epoxy resin) bond, or a non-covalent (PS, PDMS) intermolecular interaction. In the case of PEG-DA, when the photo-polymerization reaction was initiated, the other end of the thiol linker, carrying a double bond, was incorporated into the polymer by reacting with a macromer double bond. Otherwise, the linker would form hydrophobic contacts with the polymer, and remain entangled within the polymer network upon evaporation (PS) or crosslinking (PDMS, epoxy resin).

The thiol-gold bond

The strong, covalent bond between thiol and gold has been intensively studied, and applied to surface chemistry. The spontaneous formation of monolayers of alkane thiols on polycrystalline gold can either be achieved by dipping the substrate into a solution with the corresponding molecules, or by vapor depositing the molecules in vacuum.¹⁴³ Within domains, the layers are ordered at the molecular level, and are therefore called self-aggregating mono-layers (SAM). Formation of Au(I)-thiolate during the chemisorption process of the thiol to the gold involves the oxidation of gold, and the reductive elimination of hydrogen. The detailed reaction mechanism, however, has not yet been clarified.¹⁴⁴



The exothermal recombination of hydrogen atoms occurs at the metal surface. The formation of thiolates when thiol is absorbed on gold could be shown by means of XPS measurements. However, both IR and Raman spectroscopy could not detect SH stretch vibrations.¹⁴⁵ The formation of thiol films is caused by the high affinity of sulphur for gold. The binding energy of the covalent bond between sulphur and gold is 120-180 kJ/mol.¹⁴³

The energy balance of the adsorption of alkane thiols to gold, according to the mechanism described above, and involving the following binding energies:

RS-H: 364 kJ/mol

H₂: 435 kJ/mol

RS-Au: 167 kJ/mol

yields an exothermic reaction energy of 21 kJ/mol. The hydrogen-hydrogen and gold-thiol bonds compensate for the loss of the sulphide bond. The physisorption of the alkane chain onto the gold has an additional favorable effect. The selective binding of thiol linkers exclusively to the gold particles, and not to the polymer surface itself, was tested by a number of control experiments. These included contact angle measurements and AFM measurements. In the example shown here, the linker used was PEG (Mw 40,000 g/mol) dithiol (Fig. 41 a). This linker was initially applied to the transfer lithography, but was substituted with the cysteamine-acryloyl chloride system, due to its inefficiency. However, the specific gold binding of thiols is exemplified here. The linker was incubated on the respective surfaces (glass, gold-patterned glass and homogeneously-coated gold surfaces) in 1 mmol/ml ethanol solution for 1 h. The substrate was then washed with MilliQ water, and dried with nitrogen.

In Fig. 39, the contact angles of a water droplet on three different surfaces - glass surfaces without gold particles, glass surfaces completely coated with gold - are compared. Each measurement was taken before and after the incubation of the linker with the PEG thiol, as described above. The contact angle, a measure for the surface hydrophobic properties, did not change on the glass surface upon incubation, but did change on the gold-patterned and gold-covered surfaces. When the PEG thiol bound to the gold, the hydrophobicity of the surface decreased, as reflected by a decrease in the contact angle. This effect was found to be even greater for the surface totally covered with gold.

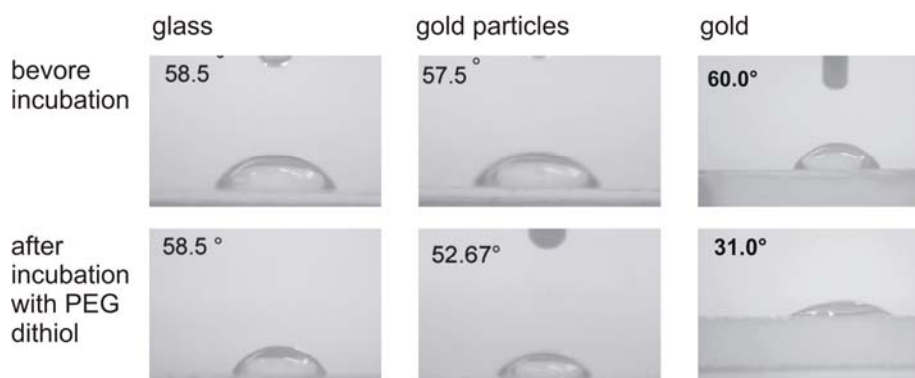


Fig. 39: Contact angle measurements used to test the specific binding of thiol to gold.

A second control experiment used to test the exclusive binding of the thiol linker to the gold particles, was performed by means of AFM phase contrast measurements. The phase contrast is a measure for the softness of the material, and can thus reflect the binding of thiol to glass or gold by an increase in the phase contrast. The comparison of the phase contrast diagrams in Fig. 40, a and b, shows that the intensity of the signal from the gold particles apparently increased after PEG thiol was added. A closer inspection of the profiles (Fig. 40 c) revealed that a significant change in signal intensity was observed for the gold particles (peaks). However, no such change was found for the surface in between the particles (baseline). We can therefore be certain that the linker system indeed enables their selective attachment to the gold particles and, as a consequence, builds up the link to the polymer, which then is nano-patterned by means of transfer nanolithography.

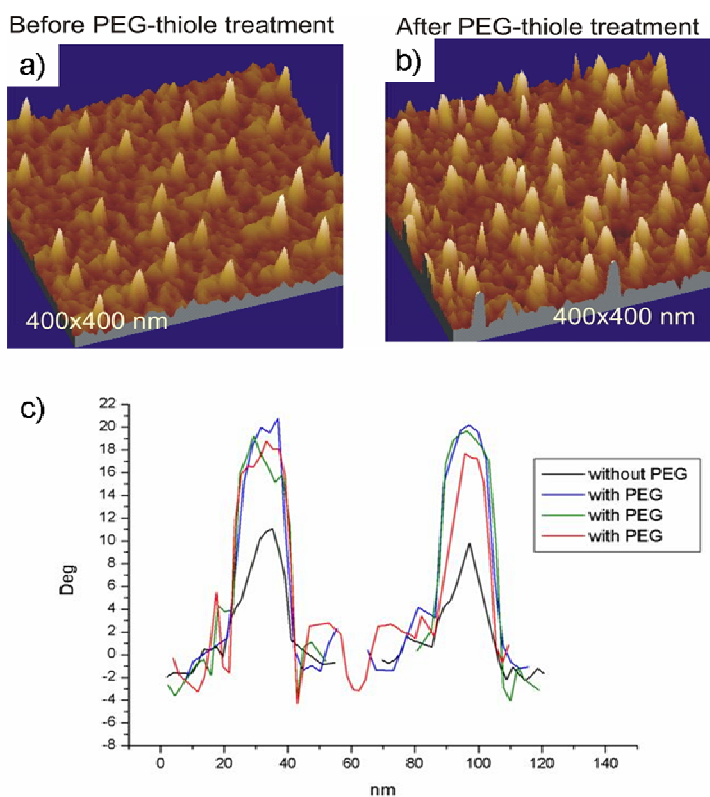


Fig. 40: AFM phase contrast measurements. Top: 3D diagram of two nanopatterned glass surfaces before (a) and after (b) incubation with PEG thiol. c) Sample profiles taken from the 3D diagrams, and aligned horizontally.

Linker systems

Due to the varying chemical characteristics of the polymers, different linker systems were tested in our study. The respective linkers are given in Table 5, and were chosen such that they match the polarity of the polymer, which in turn depends on the polymer type and its molecular weight. The choice of a suitable linker for the PEG-DA hydrogel system was not always straightforward, since this system requires a thiol

with a reactive head, but one that is simultaneously hydrophilic enough to be dissolved in the respective PEG-DA-water solution. Hydrophobic thiol molecules with the required reactive double bond head group are readily available. In the case of the PEG 700, propene thiol proved to be sufficiently soluble in the PEG-DA solution (Fig. 41). However, as the length of the PEG chain grew, the hydrophobicity of the PEG-DA decreased, and makes another solution for the linker necessary. Therefore, for the longer PEG-DA systems (PEG 4,000- PEG 20,000), the combination of cysteamine and acryloyl chloride was the thiol system of choice (Fig. 41).

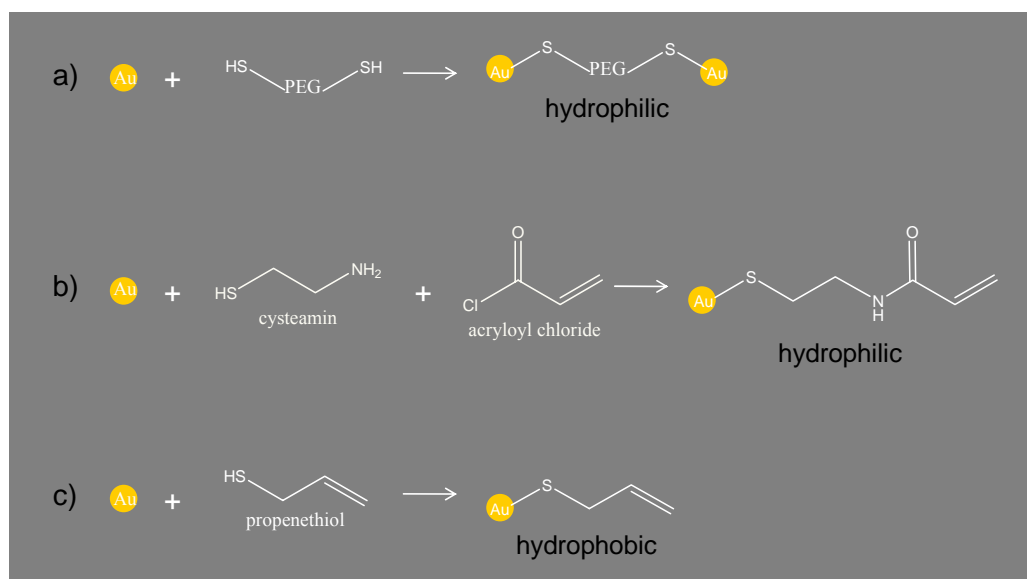


Fig. 41: Linker systems used to transfer metal nanostructures to polymer substrates.

The linker was bound via a terminal thiol group to the gold particle. The reaction conditions followed standard procedures for the formation of thiol monolayers on gold,¹⁴⁶ and were adjusted to the linkers. In the case of PEG-DA, we used a linker system consisting of two components. Cysteamine molecules immobilized on the gold particles were converted to methacrylates at their terminal amino groups, using acryloylchloride. For the other polymers described herein, propene thiol was found to be a sufficient linker.

Table 5: Examples of used polymer – linker combinations for the polymers poly(dimethylsiloxane) (PDMS), polystyrene (PS), epoxy resin, and PEG-DA with different molecular weights.

Polymer	Epoxy resin	PS	PDMS	PEG-DA (Mw 700)	PEG-DA (Mw 20,000, Mw 10,000)
Linker	Propene thiol	Propene thiol	Propene thiol	Propene thiol	Cysteamine + Acryloyl chloride

The gold clusters were 8-10 nm in size. With the size of a single propene thiol molecule on the order of 0.5 nm, more than one molecule most likely binds to a gold particle. Hence, even in the case of partially unreactive thiol linker molecules, crosslinking yielded a comprehensive linkage of the gold particles to the polymer, as also demonstrated in the experiments below.

The high efficiency of the linkers is demonstrated in Fig. 44. Gold particles were transferred to PS by using propene thiol as a linker. In the absence of propene thiol, the gold particles left imprints in the PS, but were not transferred to it, due to the lack of a favorable interaction provided by the linker.

In the following section, the standard protocols developed for the immobilization of the linkers are described:

Protocol for immobilization of the propene thiol linker

Nanopatterned glass coverslips were dried under vacuum in the desiccator. The evacuated dessicator was connected to a Schlenck flask containing propene thiol, and the glass substrates were vapor-deposited with the propene thiol for 1h. The samples were then removed from the dessicator, and the excess unreacted thiol on the glass was cleaned with nitrogen. Contaminated equipment could be washed with 30% H₂O₂.

Protocol for immobilization of the cysteamine / acryloyl chloride linker system

Nanopatterned glass coverslips were dried under vacuum in the desiccator. The evacuated dessicator was connected to a Schlenck flask containing cysteamine, and the glass substrates were vapor-deposited with the propene thiol for 1h. The samples were removed from the dessicator, washed with dichloro ethane to remove the excess of unreacted thiol on the glass, and dried with nitrogen.

In Step 2, a large Petri dish on ice was filled with dichloro ethane (30 ml). After addition of 171 μ l (1mol) N,N-Diisopropylethylamine (DIPEA) as a base, the mixture was stirred for 10 min at 0°C before 81 μ l (1mol) of acryloyl chloride were added. Finally, the samples were added to the mixture and left at 0°C for 2 h. The samples were then washed with a 1:1 mixture of water and dichloro ethane, and dried with nitrogen.

V.3.2. Transfer of the gold particles: Experiments and results

After the preparation of gold nanostructures on glass surfaces (Section V.1.3) and the immobilization of a linker system on the gold (Section V.3.1), the gold particles were transferred from the glass surface to a polymer surface, in order to obtain polymeric supports with metallic nanostructures (illustrated in Fig. 38, Steps 2 and 3).

The transfer of gold particles to the various polymers

Depending on the specific polymer used for the second support, the conditions for the transfer of the gold particles were adjusted accordingly. The individual types of linkers used to bind the gold particles to the polymer of choice, were already described in Table 5. In the transfer step, the nanostructures, pretreated with the linker, were covered with the polymer which, in turn, was solidified. The protocols for the different polymer systems are as follows:

The preparation conditions for **PEG** hydrogel supports were detailed above (Section IV.3.1). The glass slide carrying the nanostructures was placed on a support, between two spacers. The PEG/water/initiator mixtures were dropped on this glass slide and covered with a second glass slide, thus forming a “sandwich,” with the PEG mixture in between both slides (Fig. 29). After exposure with UV light, the glass slides could be mechanically removed. The resulting hydrogel disc was now nanopatterned.

For the preparation of **polystyrene** based nanopatterns, polystyrene with a molecular weight of 50,000 was dissolved in toluene at optional concentrations, and spincoated on the nanopatterned glass slide. After evaporation, the slide with the PS film was placed on a Petri dish containing 5% hydrofluoric acid (HF solution). After a few minutes, the PS film and the glass were separated, and the PS film was left floating on the surface of the water.

For the transfer of gold particles to **epoxy resin polymers**, commercially available standard imbedding media for transmission electron microscopy (e.g., epoxy resins) were used. These polymers were crosslinked for several hours in an oven heated to 70°C. The separation of the glass from the nano-structured resins was achieved with HF solution, as described for PS.

The **PDMS elastomer** was obtained from a 10:1 mixture of vinyl-terminated 250 siloxane unit pre-polymer (18500 g/mol), and a short hydrosilane crosslinker (684 g/mol) with a platinum catalyst. The mixture was dropped onto the nanostructured surface and crosslinked in an oven heated to 70°C for 12 hours. Peeling the elastomer off of the glass did not result in a transfer. Instead, the whole glass slide was etched away with an HF solution. To prevent the reaction of PDMS with HF, the glass slide was placed above the HF solution, such that only the bottom of the glass was in contact with the solution (Fig. 42).

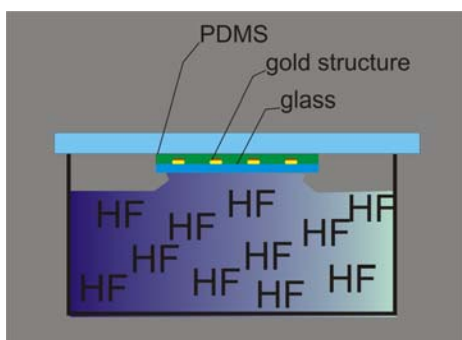


Fig. 42: Glass samples with the solidified polymer can be placed above a solution of hydrofluoric acid in such a way that the HF is only in contact with the HF solution.

Characterization of nanostructured polymers

The efficiency of the transfer of gold nanostructures to the various polymers was examined by both SEM and AFM. For the investigations using the SEM, polymeric materials such as PS, PDMS and epoxy resin were coated with a thin carbon layer prior to the measurements (Fig. 43, a-c). The resulting images show a pattern comparable to those on a glass slide (Fig. 36 c). The transfer of the structure to the polymer was found to be virtually complete, and without defects. To obtain SEM images of the nano-patterned hydrogels, the gels were frozen in liquid nitrogen and observed at $-130\text{ }^{\circ}\text{C}$ in the frozen state (Fig. 43 d). Also for the hydrogel systems, a regular pattern was obtained on the polymer by transfer of gold particles from the glass surface. Thus, independently of the polymer, the nanostructures were successfully transferred with nanoscale precision, and almost in their entirety, from the glass to the organic substrate. This technique demonstrates that the new nanostructuring concept can cope with polymers displaying widely varying chemical and physical properties, ranging from hydrophobic, stiff PS, to soft, water-containing PEG gels.

The versatility of the transfer lithography technique with respect to the scale of the gold pattern was demonstrated, by transferring micrometer-scaled structures obtained from photolithographic processes to soft surfaces as well. Fig. 43 e shows light microscopy images resulting from subjecting a microstructure to the transfer procedure, following the same protocol as that used for nanostructures.

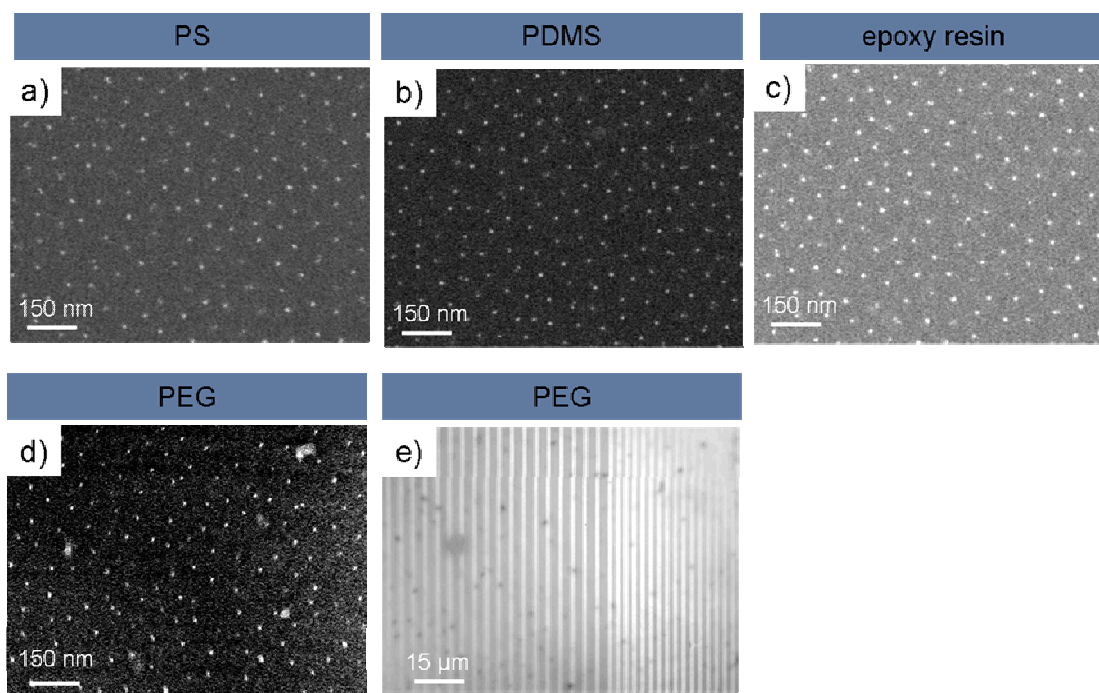


Fig. 43: Different polymers were patterned with gold structures by means of transfer lithography. (a-c) Images taken with an SEM after sputtering of carbon to the polymer surfaces. (d) Cryo-SEM image of a PEG hydrogel in a frozen state. (e) Light microscopy image of transferred microstructures.

The essential role played by the linker in connecting the polymer chains with the gold particles, was tested in a control experiment. In contrast to the efficient transfer of the nanostructure to poly styrene in the presence of propene thiol (Fig. 44 a), the gold particles were not connected to the PS, but rather retained simple imprints of the nanostructure in the surface, when no propene thiol was supplied. (Fig. 44 b).

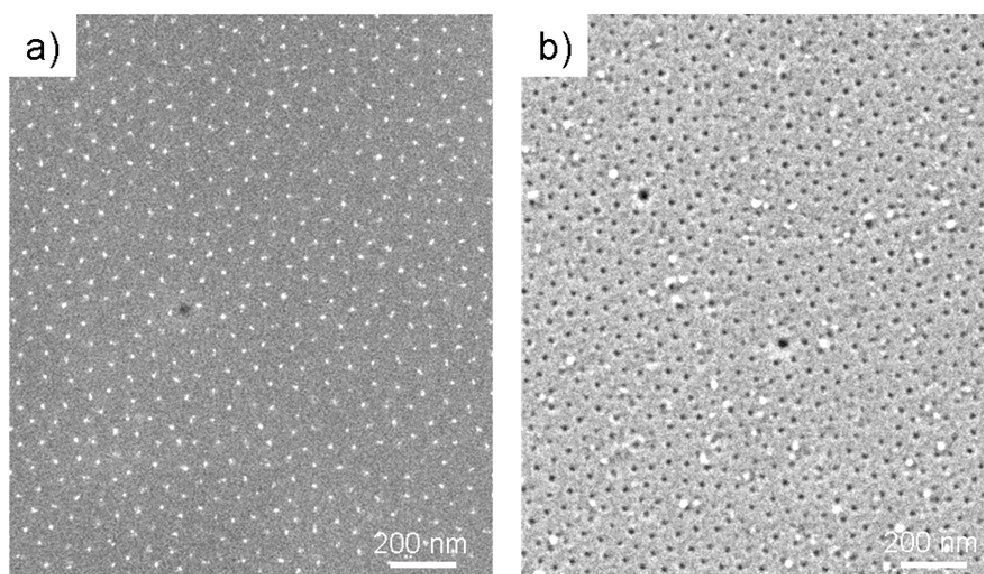


Fig. 44: SEM images of PS following the transfer experiment with (a) and without (b) propene thiol.

In addition to their characterization by means of SEM, nano-structured PEG 700 hydrogel surfaces were further characterized by means of atomic force microscopy (AFM) in a liquid environment, using the tapping mode. Phase contrast images (Fig. 45, a and b) reveal differences in the hardness of the material; the images depicted in Fig. 45, c and d, show the corresponding height profiles. The topographic images show that the gold particles were sticking into the gel, forming cavities. As shown in the periphery of Fig. 45, a layer of non-covalently bound polymer chains covered the gel surface, thereby hiding the gold particles. When scanning the sample with the AFM tip using high forces, the polymer layer could be swept away to reveal the gold particles, as can be seen in the central area of Fig. 45 a and c.

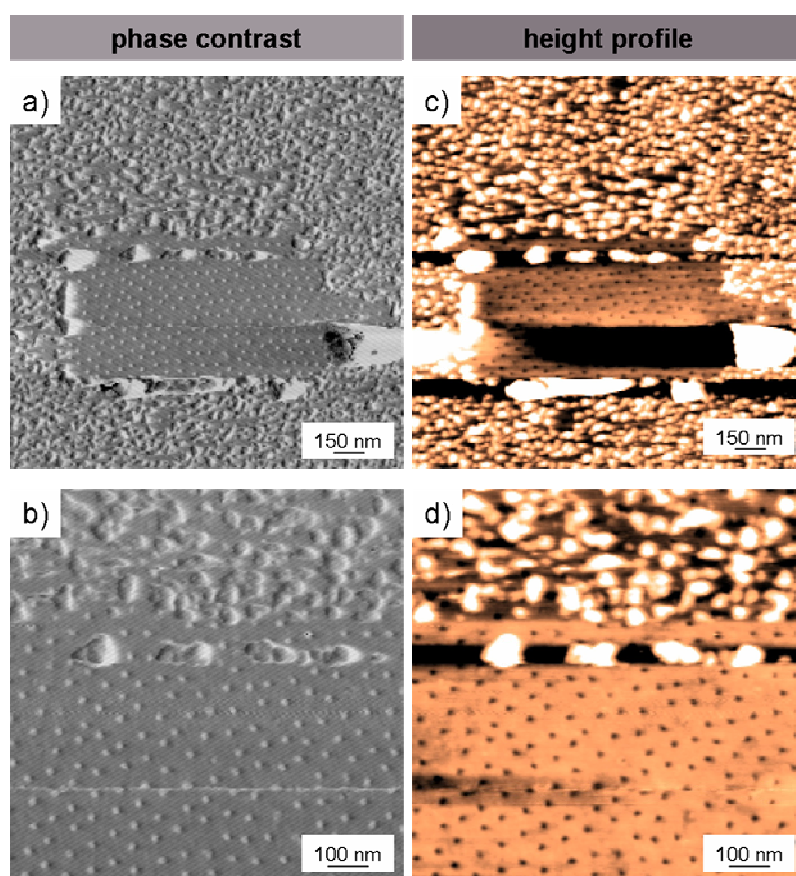


Fig. 45: Gold particles on a PEG 700 hydrogel. The AFM images were captured in an aqueous environment.

Attempts to carry out comparable measurements with softer hydrogels (PEG with molecular weights of 4,000 g/mol -20,000 g/mol) turned out to be hampered by the softness of the gels, and hence did not lead to conclusive AFM images. Instead, these softer hydrogels were visualized and characterized by cryo SEM. In contrast to the polymeric materials, coating of the samples with carbon was not necessary for cryo SEM measurements. Instead, the surface of the samples was dried for some minutes in air before freezing, in order to avoid the possible formation of a water layer on the top of the hydrogel. The samples were frozen in liquid nitrogen and kept at -130°C

during the measurements. The measurements were carried out with an acceleration voltage of 1 to 5 kV, and a chamber pressure that was less than 5×10^{-6} mbar.

Representative SEM images taken with different detectors and with varying number of scans for PEG 10,000 hydrogels are shown in (Fig. 46). Using the ESB detector, the first scan of the hydrogel reveals the gold nanostructure of the expected size and distance between the particles, in terms of the material contrast. Large parts of the hydrogel surface, however, did not show any patterning, which in principle could be due either to an incomplete transfer of the gold structure from the glass surface onto the hydrogel, or to the partial coverage of the structure, e. g. by spare polymer chains not crosslinked to the gel, as was also observed for other polymers imaged by AFM (compare Fig. 45). Indeed, by using the SE2 detector to visualize the topology of the material, regions for which no nanostructure could be revealed with the ESB detector were found to be covered with ice crystals or loose polymer chains. Drying the samples reduced, but could not completely prevent, the formation of ice crystals on the surface upon freezing. Uncovered regions were completely nanostructured. This coverage was partly removed when further scans were taken of the same part of the surface, as shown by an increasing ratio of nanopatterned regions revealed by the ESB detector. Repeated scans also caused the formation of pores in the polymer as shown with the SE2 detector, probably caused by damage to the gel from the electron beam. The gold nanopattern continued to remain stable, and was increasingly visible, after 10 scans. Taken together, the cryo SEM measurements clearly show that the transfer of the gold structure to soft hydrogels was as efficient and complete as for the other hydrogels and polymers discussed above.

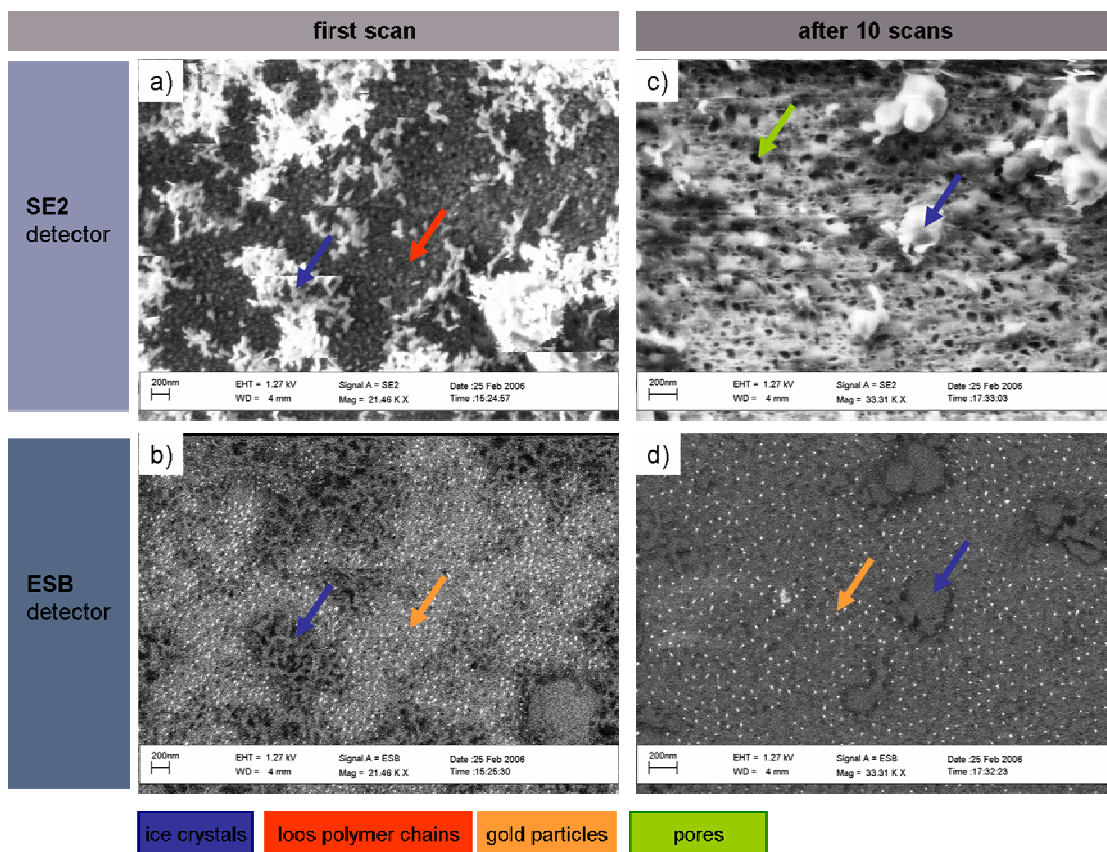


Fig. 46: SEM images of nanostructured hydrogels (PEG 10,000) obtained with the SE2 and ESB detectors, respectively, from both a first scan, and after several scans. Examples include hydrogel regions with ice crystals or non-crosslinked polymer chains hiding the gold particles, with exposed gold particles, and with pores caused by the scanning procedure, are indicated as colored shades.

Cell experiments require the use of nanopatterned hydrogels in the water-containing swollen state. To examine the stability of the gold particles on a swollen gel, and to characterize the changes in the nanostructure during swelling, gels before and after swelling were compared. Fig. 47 shows cryo SEM images of PEG 10,000 and PEG 20,000 hydrogels taken in the initial state, directly after the transfer process, and swollen after 24 hours in water. After swelling, the hydrogels show a pattern comparable to the one seen in the initial stage, but extended. Apparent defects in the pattern could be traced back to ice crystals covering the gold particles, and rendering them invisible to the SEM. The swelling ratio could be determined as the ratio of the distances after (d_2) and before (d_1) swelling, $\frac{d_2}{d_1}$ (described in Section IV.2.1). For PEG of 10,000 one obtains swelling by a factor of two; for PEG of 20,000 swelling by as much as a factor of 3.3 was obtained. Thus, as anticipated, the use of larger PEG-DA macromers results in a larger mesh size and, as a consequence, in a larger swelling ratio. The swelling process is to some extent heterogeneous, due to the distribution of mesh sizes within a gel. The increase in distance between the gold

particles is unexpectedly homogeneous. Here, the macroscopic swelling ratio, the average of the values for the increase in nanoscale distance, was determined. Alternatively, the microscopic swelling ratio of the distances between gold particles can be determined, resulting in a distribution and mean of swelling ratios as a measure for the heterogeneity of the swelling. The swelling ratios differ from those determined for standard gels (described in Section IV.3.2) because water instead of cell medium was used here.

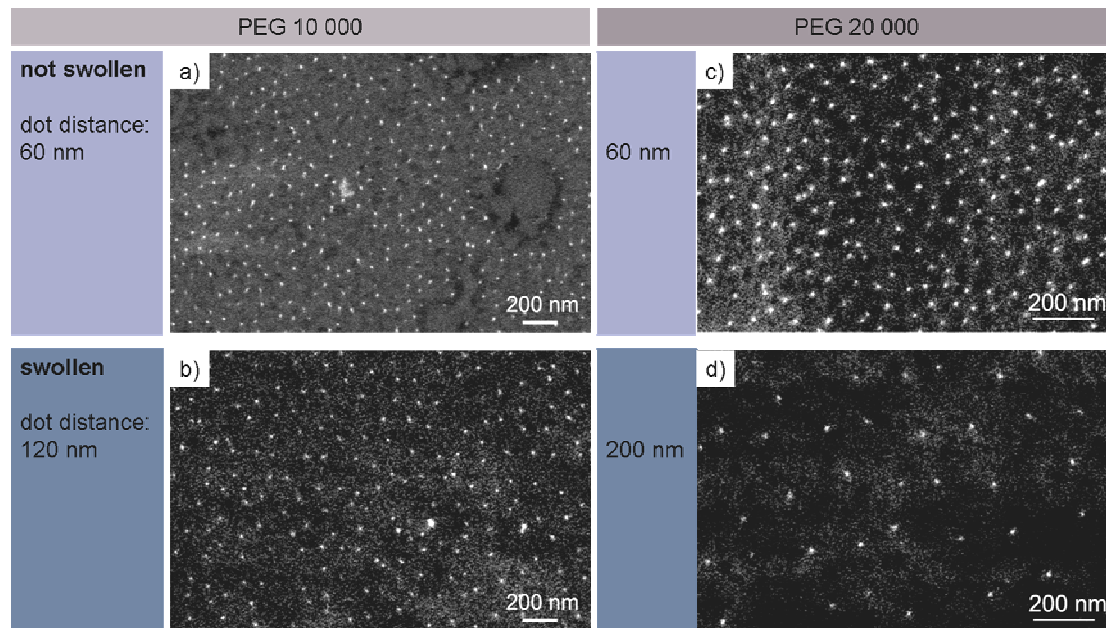


Fig. 47: Swelling behavior and swelling ratios examined by means of cryo SEM images of PEG 10,000 and PEG 20,000 hydrogels directly after transfer of the gold structure, in comparison to the same hydrogels after swelling in water. Swelling ratios of 2 and 3.3, respectively, were found.

V.4. Conclusion

A new transfer lithography technique was developed and described. Polymeric surfaces differing in both type and elastic properties were decorated with gold nanopatterns fabricated with an established nanolithography technique. The transfer of the pattern from the original surface to the polymeric surface of choice could be achieved virtually completely and with nanoscale precision, as shown by characterizing the nanopatterned polymers and gels obtained with AFM, SEM, and cryo SEM imaging.

For conventional nanolithographic methods, generally speaking, the chemical and mechanical properties of the nanostructured material are strongly constricted by their preparation conditions. Hence, the broad application of a given technique for the fabrication of a wide range of nanostructured materials; e.g., customized for use in cell experiments, is challenging. However, the transfer lithography method, based as it is on the transfer of nanostructures from an original substrate to another material of

choice, offers the possibility of nanostructuring soft and organic surfaces, as is required for biological applications. This stands in contrast to conventional lithographic methods that are restricted overall to solid inorganic materials such as silicon, quartz, or glass. Furthermore, the versatile transfer lithography technique can be applied easily, reproducibly, and on a large scale, to different patterns at both the nano- and micrometer scales, as demonstrated in this chapter.

The concept of transfer nanolithography paves the way toward the flexible design of novel nanostructured materials, including soft, organic, and non-planar surfaces. The design of non-planar surfaces; i.e., microtubes, will be described in Chapter VI. A wide range of applications for these nanopatterned surfaces can be envisaged, including artificial ECMs for cell experiments, as described in Chapter VIII, but also in the fields of electronics and optics.

A major feature of the newly-developed nanopatterned materials that are based on polymeric and hydrogel substrates, is their capability of being subsequently modified by chemical or biological compounds. Both the gold particles and the inter-particle surface can be modified as required in order to successfully apply the nanostructured material (described in detail in Chapter VII).

VI. Preparation of patterned hydrogel channels

The previous chapters addressed planar two-dimensional model systems which could be used to develop an artificial extracellular matrix. Indeed, most cells *in vivo* are embedded in and surrounded by the ECM in all three dimensions. In blood vessels and neuronal tissues in particular, cells assemble in channel-shaped formations, surrounded by a tube-like ECM. To investigate and modulate cellular behavior in such non-planar environments, the design of three-dimensional model systems is required. Tube-like structures, for example, enable adhered cells to be subjected to shear flow, thereby mimicking *in vivo* conditions in a blood vessel.

To our knowledge, no method has been described to date which enables the decoration of three-dimensional polymer structures with a regular pattern of metal nanoparticles. In this chapter, the components of the modular, artificial ECM (PEG and gold nanostructures) hitherto described, are applied to form three-dimensional systems. For this purpose, the block copolymer micelle nanolithographic technique, described in Sections V.1.2 and V.1.3, was modified to enable the decoration of three-dimensional glass tubes with gold particles. Transferring gold particles from these substrates to hydrogels yielded three-dimensional decorated tubes with variable diameters at the nanoscale.

VI.1. Decoration of non-planar glass structures

In principle, micellar block copolymer nanolithography (mentioned in the Sections V.1.2 and V.1.3) is not restricted to the planar substrates for which it was originally developed and has thus far been applied, but can also be applied in a similar manner to non-planar objects with bended and curved surfaces. Using this technique, the substrates, irrespective of their shape, can be decorated with a monolayer of hexagonally-arranged micelles with a metal salt in their core. This is achieved by dipping the substrates in a solution of diblock copolymers and dragging them out at a constant speed. Parameters influencing the formation of a monolayer of hexagonally-arranged micelles are the micelle concentration in the solution, the dragging speed, and the chemical surface properties. Experiments on planar surfaces have shown that overly high concentrations of micelles in solution lead to the formation of non-ordered multilayers; surfaces with inadequate chemical properties, or solutions with overly low concentrations of micelles lead to defects in the pattern due to de-wetting of the retaining nanostructures.

Depending on the extent of surface bending, and the surface tension of the solution, wetting and de-wetting effects change when swapping planar for non-planar surfaces. To obtain regular nanopatterns on non-planar surfaces at the level of precision achieved for planar surfaces, the parameters influencing the patterning (e.g., the

dipping and dragging process, and the micelle concentration) have to be re-optimized with respect to the properties of the non-planar surface.

De-wetting effects on non-planar substrates

Due to differences in the de-wetting properties of planar and non-planar surfaces, changes in the nanopattern can be expected when block copolymer micelle lithography is applied to curved substrates, using the parameters optimized for planar substrates. Fig. 48 illustrates the gold nanodecoration of a cylindrical glass fiber, obtained under standard lithography conditions for planar surfaces. As anticipated, the surface of the fiber is only partially decorated with a regular gold nanostructure. Areas carrying no gold particles were similarly observed on planar substrates dipped in micellar solutions containing micelle concentrations too low to guarantee formation of a complete monolayer.

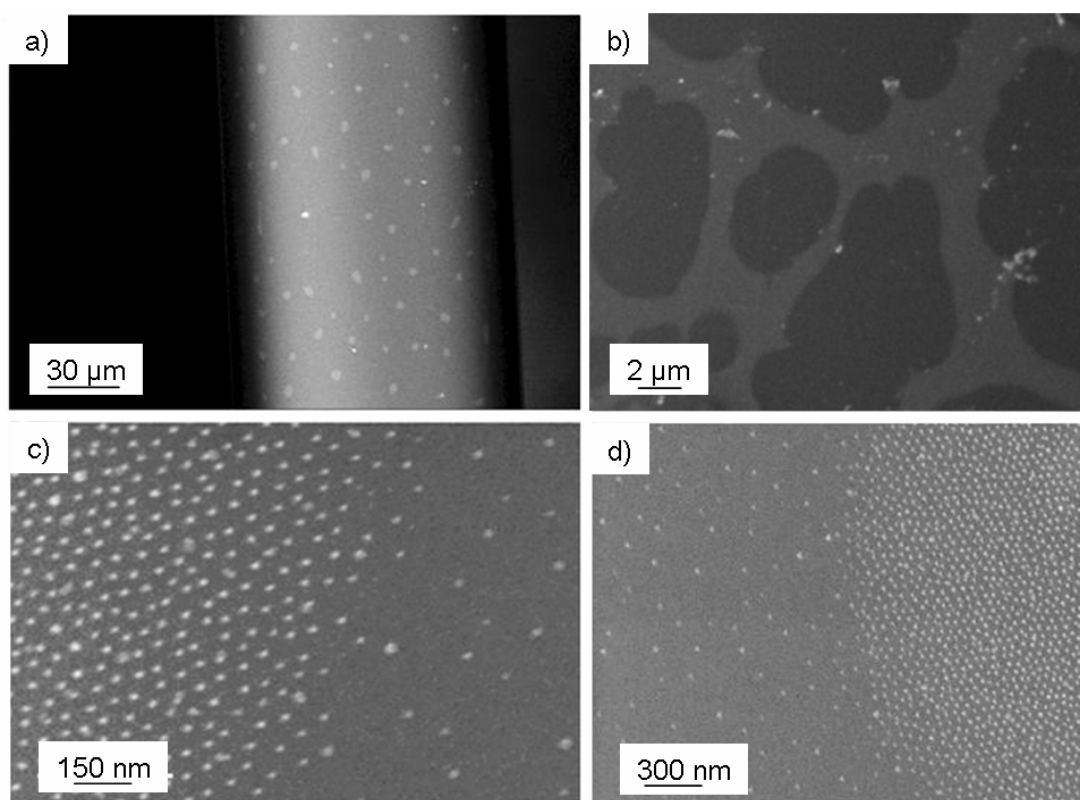


Fig. 48: SEM images of only partially nano-structured glass fibers with radii of 125 μm (a, c, d) and 500 μm (b), obtained using standard lithographic procedures for planar surfaces.

Fig. 48 also compares nanopatterns seen on glass fibers of different sizes, demonstrating the influence of the radius (i. e., the curvature) of the fiber on the monolayer assembly. Under the conditions by which a homogeneous nanostructure on planar surfaces is obtained, the defects caused by the different de-wetting behavior of curved surfaces increases with increasing curvature; i.e., with decreasing diameter of

the fiber (Fig. 48, a and b). The de-wetting effect can also be described as a premature rupture of the micellar film covering the surface, prior to drying. To exclude other potential reasons for the differences seen in the resulting nanopatterns, the surface treatment of the glass fibers prior to the coating was similar to that applied to the previously-used planar glass surfaces. This method excludes problems arising from other systematic differences in the preparation of nanostructured fibers, and enables the tracing of the observed differences in wettability exclusively to the surface curvature.

Modification of the standard protocol for block copolymer micelle lithography

The aforementioned de-wetting effects required modifications of the standard protocols (described in Section V.1.3) for the preparation of non-planar nanostructured substrates. Experiments were performed to test the influence of the parameters described, namely surface chemistry, micelle concentrations in solution, and dipping velocity.

Variations like oxidation, in the pre-treatment of the surface did not lead to improvements in the formation of nanopatterns on the fibers. Increasing the micelle concentration in the solution resulted in a decrease in the regularity of the patterns, and had no significant influence on de-wetting. Experiments involving variations in the dragging velocity or in evaporation conditions for the solvent, also did not yield homogeneously decorated surfaces.

To achieve homogeneous decoration of the total surface of the glass fiber and short drying periods, the glass fiber, pre-treated as described above (Section V.1.3) was hang up vertically for the coating procedure, as depicted in Fig. 49. A 10 μ l drop of standard micelle solution (Section V.1.3) was placed onto the top of the fiber, using an Eppendorf pipette. The drop comprised the total fiber diameter in size. Removing the contact to the Eppendorf pipette induced the solution to flow downwards along the fiber, forming a homogeneous coat. In contrast to the standard process of dipping and dragging the substrate into and out of the solution, the freely-hanging fiber could dry rapidly enough to ensure a sufficiently short period of contact with the micelle solution. This technique prevented the premature rupture of the micellar film covering the surface prior to drying, as observed in glass fibers nanopatterned according to the standard protocol. The short contact also guarantees homogeneous wetting and, as a consequence, the formation of a micelle monolayer along the entire length of the fiber.

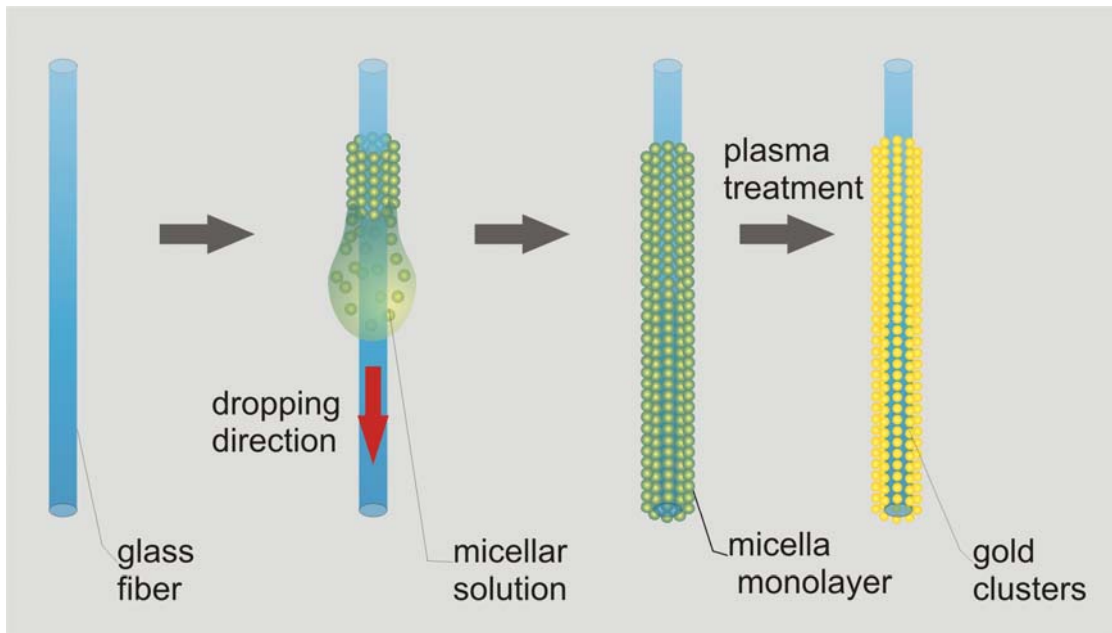


Fig. 49: Diblock copolymer micelle nanolithography modified for the patterning of a glass fiber. A drop of micelle solution is used to completely wet the fiber surface by flowing downwards along it. Other steps correspond to those used in the standard procedure.

SEM images (Fig. 50) show complete decoration of the glass fiber (125 μm diameter) with gold nanoparticles. A homogeneous pattern along the whole fiber was achieved. Examining the pattern along the glass fiber from top to bottom revealed a slight decrease in the distances between the gold particles on different segments of the fiber. This finding is most likely due to the accelerated rate at which the drop travels during wetting. However, the change in distance is only slight, and might be further reduced by optimizing the procedure

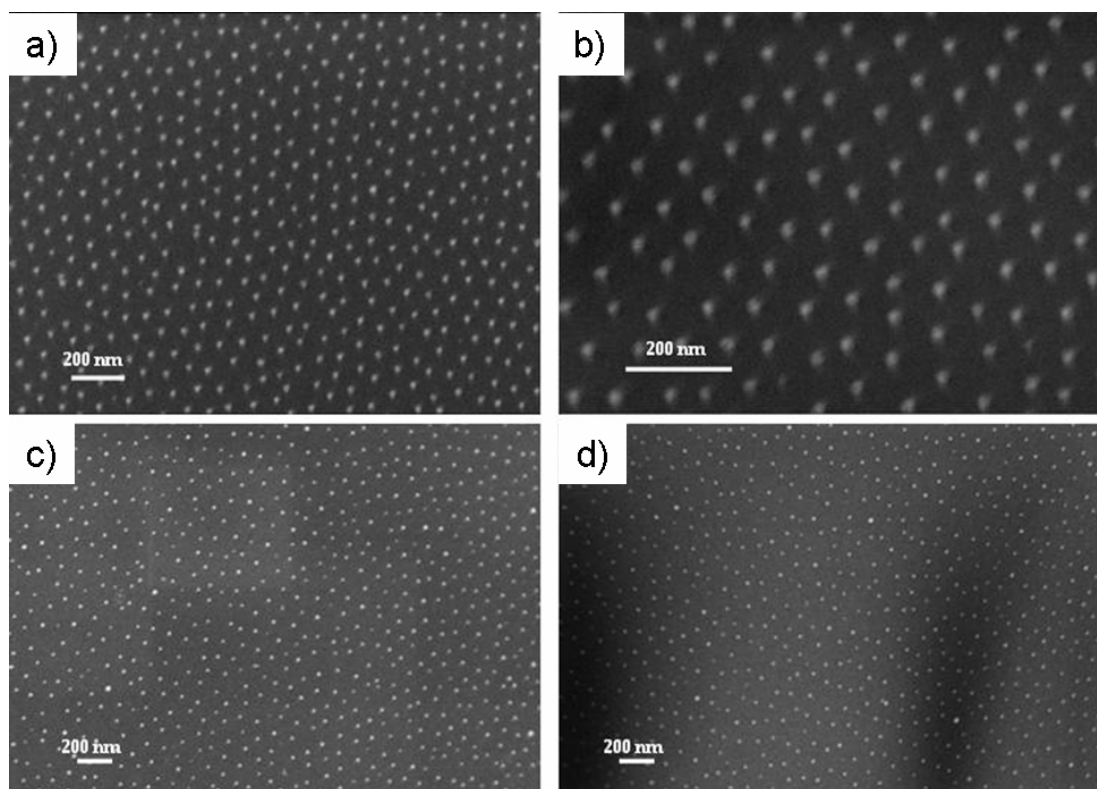


Fig. 50: SEM images of fibers with a diameter of 125 μ m decorated with gold nanoparticles, according to the block copolymer micelle lithography procedure modified for glass fibers.

VI.2. Transfer lithography for non-planar substrates

In accordance with the transfer process of particles on a planar substrate, gold particles from a glass fiber can be transferred to a polymeric substrate, yielding a nano-decorated microchannel.

Transfer of gold particles into hydrogel channels

The transfer of gold particles from a glass fiber to a hydrogel is illustrated in Fig. 51. In Fig. 51 a, the fibers decorated with gold nanoparticles, prepared as described in Section VI.1, were coated with a propene thiol linker, as described in the standard protocol (Section V.3.1). The fibers were mounted in a specially-designed holder, which enabled the fiber to be held in place, a certain distance from the ground surface. After embedding the fibers in PEG-DA 700 and crosslinking the PEGg the protocol from Section IV.3.1 above (Fig. 51 b), the glass fibers were removed with hydrofluoric acid (Fig. 51 c). This procedure yielded channel structures internally decorated with gold nanoparticles.

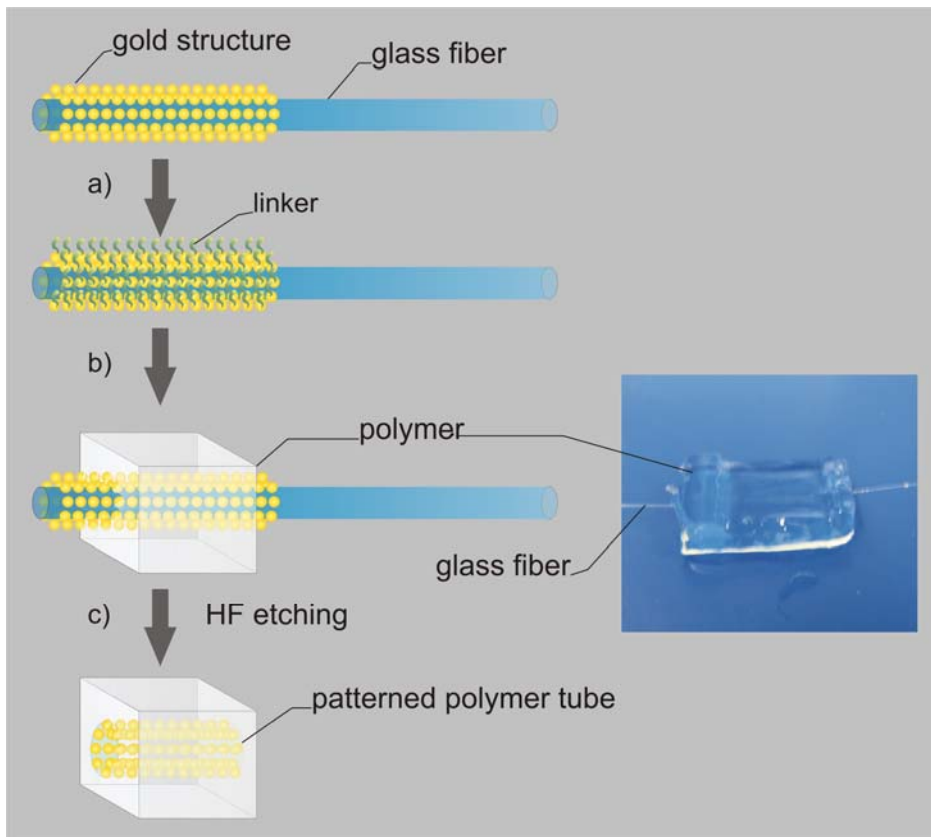


Fig. 51: Transfer lithography for tubular substrates: (a) Binding of the linker to the gold particles, (b) Embedding of the fiber into the hydrogel, (c) Etching the glass with HF solution. The photograph in the right panel shows the mounted glass fiber surrounded by hydrogel, prior to etching.

Characterization of nano-decorated PEG channels
 Light microscope images showed the formation of the channel and the complete removal of the glass fiber by etching. Fig. 52 a shows a PEG channel obtained from a glass fiber with a 125 μm diameter. The unhindered passage of an air bubble through the water-filled microchannel demonstrated the complete removal of the glass fiber (Fig. 52 b).

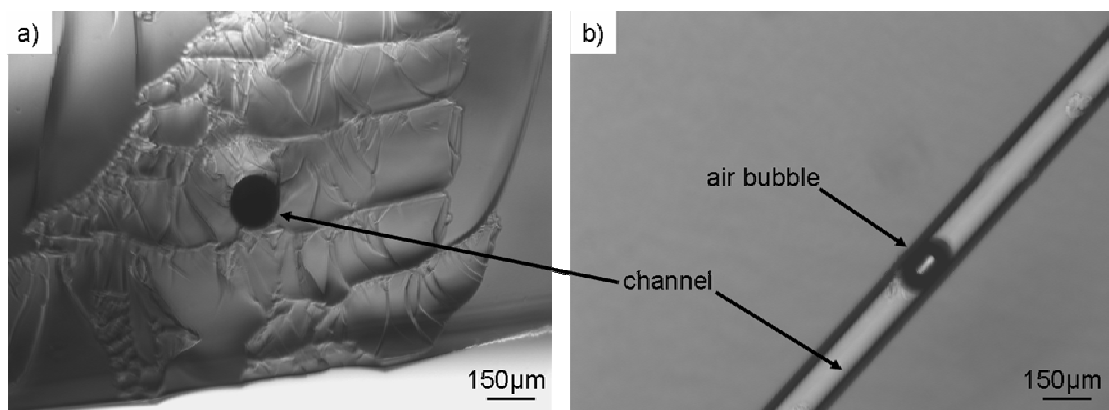


Fig. 52: Light microscope images of the microchannel in a hydrogel, obtained after etching of the glass fiber: (a) from the side of the hydrogel block showing the channel entrance, and (b) from the top of the hydrogel along the channel.

SEM experiments of surfaces from the inside of the channel were obtained by partially opening the channels with a scalpel. The resulting hydrogel blocks, with parts of the hydrogel removed in order to open the channel, were frozen in liquid nitrogen and observed with the SEM, as described in Section V.3.2. Fig. 53 shows representative images of a microchannel formed from a PEG 700 hydrogel, and gold-decorated as described. The gold nanostructure could be successfully transferred from the glass fiber onto the inside of the hydrogel channel. The resulting nanopattern is regular ordered and complete intact, without obvious defects.

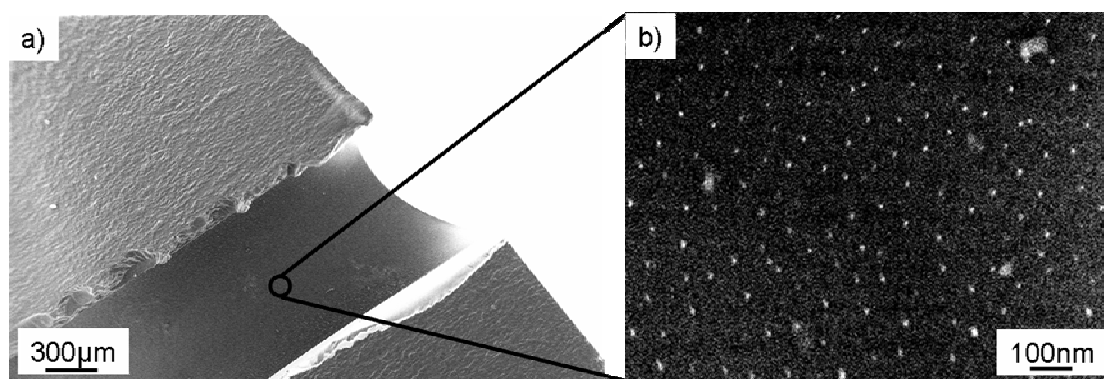


Fig. 53: SEM images of the inside of a gold-decorated microchannel obtained by means of transfer nanolithography. (a) A cross-section through the microchannel. (b) Enlarged image, revealing the regular ordered gold nanopattern on the inner surface of the channel.

VI.3. Conclusion

The transfer nanolithography technique developed herein to transfer gold nanopatterns from planar glass to planar soft and organic materials was modified and also successfully applied to curved surfaces. In a new experimental set-up, a glass fiber was decorated with gold nanoparticles by means of block copolymer micelle lithography, enabling the rapid and complete coverage of the fiber surface with micelle solution, thereby ensuring the formation of a regular and ordered nanopattern. Moreover, the pattern transfer was achieved without further principal modifications of the transfer lithography method described in Chapter V.

This is the first method described to date, which can routinely nanostructure three-dimensional surfaces. This feature of the transfer lithographic technique underscores its versatility. Since nanostructuring the surface using block copolymer micelle nanolithography is independent of the choice of substrate to be nanostructured, transfer lithography paves the way toward the flexible nanostructuring of surfaces composed of various materials, including polymers and gels (described in Chapters IV and V) and, beyond that, of different shapes, as shown in this chapter.

To demonstrate how transfer lithography may be applied to the patterning of non-planar surfaces, a microtube was nanostructured. In principle, however, this same procedure may be applied to any gold-decorated, three-dimensional glass substrate.

Gold-patterned microtubes made up of hydrogels are of particular interest, due to their potential application in cell biology experiments. They enable the mimicking of ECMs surrounding the cell, not only in terms of their elastic properties and possible anchor points for cell adhesion provided by the gold nanoparticles after appropriate modification, but also mimic the three-dimensional surroundings of the natural ECM, in contrast to the two-dimensional planar surfaces conventionally used when cell experiments are carried out *in vitro*.

The application of nanostructured hydrogel tubes can also be taken one step further, by directly mimicking the tubular arrangement of cells found in an *in vivo* environment; namely, in blood vessels and in tubular neuronal tissues. The diameter of the channel, its elastic properties, and the environment for cell adhesion are all parameters which may be adjusted, to mimic natural blood vessels. In addition, the mechanical forces exerted on cells flow in a blood vessel can be mimicked in shear flow experiments within the tube.

Before finally demonstrating, in Chapter VIII the application of both planar and non-planar nanostructured surfaces to cell experiments, the chemical modification of the nanostructured surfaces, another prerequisite for cell adhesion experiments and the third and last module of the artificial ECM designed in this study, will herein be described.

VII. Chemical modification of PEG hydrogels

Thus far, this thesis concerned itself with the design of the basic material and nanopatterning of the modular artificial ECM (Chapters IV, V and VI), defining its mechanical and structural properties, respectively. In order to apply the different modules to cell experiments, the surface of the ECM mimic - more specifically, the polymeric material, the gold nanoparticles, or both - must be activated. Accordingly, this chapter describes the third module of the artificial ECMs: the activation of the nanopatterned surfaces for specific interactions with cells, by means of chemical modification. Such modifications provide specifically-tailored anchor points for cell adhesion sites, in order to control the crosstalk between the cell and its environment.

PEG hydrogels are completely inert against protein adsorption; i. e., for biochemical interactions with cells. The gold particles, on the other hand, present cell interaction sites which, however, are unspecific enabling any kind of protein on the cell surface to adsorb. Thus, bioactivation of the nanomaterials is an essential third module in the development of artificial ECMs, in order to provide specific interaction sites for both the hydrogel surfaces and the gold nanoparticles.

In this study, the term “bioactivation” includes the chemical binding of biologically active molecules such as peptides or proteins to either the gold pattern or directly to the hydrogel, as previously mentioned (Section III.4.2). The selective immobilization of peptides or proteins on the gold particles (Chapter V) enables control not only of the density, but also of the spacing and positioning of the biomolecules. The type and spatial distribution of ECM interaction sites, in turn, can be chosen such that these parameters are preferable for a certain cell type and function. In combination with the modules defining the mechanical and structural properties of the artificial ECM (described in Chapters IV, VI), its bioactivation will enable the design of cell type- and cell function-specific ECMs.

The binding of bioactive molecules to diverse materials is a fundamental and well-established tool for biological experiments, in pharmaceutical and drug delivery systems. Various techniques to suit this purpose have been established. Each system and each application, however, requires the adjustment of one of the techniques to the special requirements, as described in Section III.4.1. For the chemical modification described in this thesis, the following criteria were the factors deemed critical for the choice and development of bioactivation systems:

- The preparation system should be applicable to various biomolecules such as peptides and proteins, and should be easily modifiable;
- The reaction conditions must be smooth, to avoid damaging both the sensitive biomolecules, and the nanostructure itself. Therefore, organic solvents, high temperature, and aggressive reaction agents were all excluded; e.g., the

copolymerization of peptides to hydrogels cannot be carried out in the presence of proteins, which will denaturize under polymerization conditions.

- Biomolecules are expensive. The copolymerization of peptides into the hydrogel, as suggested in literature (Section III.4.1), results in a distribution of the peptides throughout the gel, and thus is very costly. A more efficient use of peptide molecules is achieved herein by immobilizing peptides only on the substrate surface, thereby exposing the major part of the immobilized peptide molecule to the adhering cells for interaction.
- Once the bioactive molecule is immobilized, the chemicals used for the coupling reactions should be completely and easily removable, and should not stick to the hydrogel.

Different coupling schemes, via terminal thiol or amino groups, or via histidine tags, have been developed and applied to couple protein and peptides to gold particles and polymeric surfaces, as described in the following sections.

VII.1. Introduction

VII.1.1. *Chemical properties of PEG hydrogels*

Poly(ethylene glycol)s (PEG) are commonly used for biological experiments as for the cell experiments here, and as conventional ingredients in diverse cosmetics, pharmaceuticals, and even medical implants. Since they effectively resist protein adsorption, they are completely inert against biological systems. Their chemical properties are comparable to those of hyaluronic acid, the major component of the natural ECM. Thus, the PEG polymer renders itself suitable to take over the task of hyaluronic acid in a synthetic ECM, as designed for this study. The structural formula of PEG is shown in Fig. 54. The basic building block of the linear chain is ethylene oxide (Mw 44 g/mol) characterized by medium polarity and low chemical reactivity, in terms of acid-base reactions. Consequently, PEG is a water soluble, biologically inert, unreactive and non-toxic polymer.

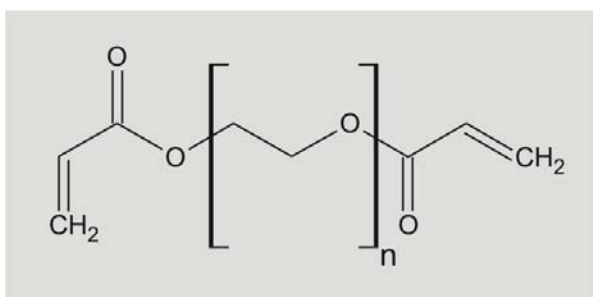


Fig. 54: Structural formula of poly(ethylene) glycol (PEG).

PEG polymers are typically obtained through polymerization of ethylene oxide, by means of basic catalysis. Water, mono- or diethylene glycol can be used as reactants. The reactions can be terminated when the desired average molecular weight of the chains is reached by the addition of acid. The average molecular weight is conventionally added to the nomenclature of PEG, e.g. PEG 700 denotes PEG with an average molecular weight of 700 g/mol. Increasing chain lengths are associated with increasing stiffness and a rise in the melting point of the polymer. PEG can be liquid or solid, depending on the chain length. Liquid PEGs are hygroscopic, with a decreasing capacity of the polymer to absorb water, as its molecular weight increases.

Applications of PEG coatings in medicine and cell biology are of particular interest, because of the potential of PEG to inhibit non-specific adsorption of proteins to the material. For this reason, PEG is used in this study as the basic material of the modular artificial ECM. Its natural resistance to protein adsorption can, among other reasons, be traced back to the helical structure of the PEG chains. In solution, the fluctuating long chains cause proteins to be repulsed from the material, a behavior described in terms of the steric repulsion theory.¹⁴⁷

Other instructive explanations are based on the theory of volume reduction and volume exclusion developed for the PEG-DA polymers, as used in this thesis.¹⁴⁸ The former, the theory of volume reduction, considers the volume shrinkage upon compression of the polymer layer due to the relative approach of the non-diffusing proteins. The volume shrinkage is associated with a decrease in entropy of the macromolecules, since the conformational space of each segment is narrowed in the more dense state. The latter theory of volume exclusion, in contrast, takes into account the changes upon intrusion of the polymer. Intrusion of the hygroscopic surface by adsorbing proteins expels water molecules from the polymer network. As a result, the polymer is compressed, the entropy decreases, and, in addition, the enthalpy increases. The inertness toward protein adsorption can thus be explained by an increase in free energy, in the case of protein molecules binding to PEG.¹⁴⁸

VII.1.2. Bio-molecules for surface activation

To biofunctionalize the gold nanostructure and the PEG hydrogel, representatives of various biologically active molecules were chosen to test the general applicability of the linking systems to these substrates. The adhesion peptide RGD as well as the proteins L1 and Green Fluorescent Protein (GFP) were accordingly immobilized, either on the gold particles or directly onto the hydrogel itself.

Cyclic RGD

The adhesion peptide RGD, which consists of the amino acids arginine (R), glycine (G), and aspartate (D), was bound either to the gold particles or directly onto the

hydrogel surface. Its presence and stability on the surface was tested by means of cell culture experiments.

As one of the most commonly-used cell adhesion-mediating peptides in tissue engineering, RGD was chosen as a first example to biofunctionalize and test the novel artificial ECM system. RGD adhesion sites are present in on the surfaces of many extracellular matrix proteins, including vitronectin, fibrinogen, von Willebrand factor, collagen, laminin, osteopontin, tenascin, and bone sialoprotein, as well as in membrane proteins, in viruses and bacteria, and in snake venoms (neurotoxins and disintegrins).¹⁴⁹ About half of the twenty-four integrins (Section III.2.2) have thus far been shown to bind to ECM molecules in an RGD- dependent manner.¹⁴⁹

Synthetic peptides which are solely made up of an RGD sequence have no selectivity and specificity. These features can, however, be retained, either by blocking the C-terminal carboxyl group, or by adding flanking amino acids in accordance with its natural sequence: RGD(inactive)<RGD-NH₂<RGDS<GRGDSP.¹⁵⁰ Through the use of cyclopeptides with varying spatial orientations of constitutionally identical amino acids of differing stereochemistries,¹⁵¹ the strong impact of the RGD sequence conformation on selectivity was proven.¹⁵² A more kinked conformation of the RGD sequence furthers its ability to bind to the integrin $\alpha_v\beta_3$, while a more linear arrangement encourages preferential binding with the $\alpha_{IIb}\beta_3$ integrin.¹⁵³ As an example, the RGD peptide c(RGDfK), where *c* stands for *cyclo*, *f* for *phenyl alanine* and *K* for *glutamic acid*, with strong selectivity for $\alpha_v\beta_3$, was successfully used to promote the adhesion of bone-related cells, such as osteoblasts¹⁵⁴ and chondrocytes¹⁵⁵ employing the $\alpha_v\beta_3$ and the $\alpha_v\beta_5$ integrins.

Cyclic RGDfK was used in this work to bind to the gold particles, as well as directly to the PEG hydrogel. Therefore, the RGDfK molecules were provided with 2 nm-long linkers containing either a terminal thiol or amino group (Fig. 55). The linkers themselves consist of a 6-aminohexanoic acid (Ahx) residue and a 3-mercaptopropionic acid (Mpa) (Fig. 55 a; the related 3-aminopropionic acid (Apa) is shown in Fig. 55 b). The synthesis of c[RGDfK(Ahx-Mpa)] has been previously described in the literature.⁵⁴ The molecules were a kind gift of Prof. Horst Kessler, TU Munich.

The linkers guarantee defined orientations of the peptides relative to the surface. The distance between the peptide and the surface to which it is bound, provides the required accessibility of the RGD to the integrins.

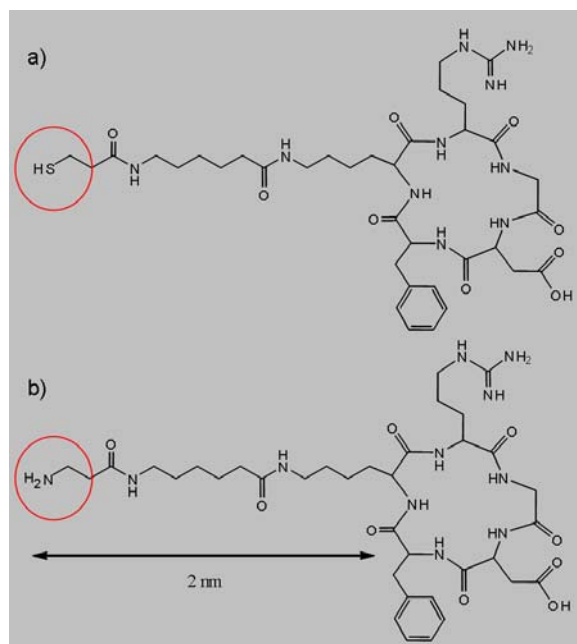


Fig. 55: Structural formula of a c[RGDfK(Ahx-Mpa)] (a) and a c[RGDfK(Ahx-Apa)] (b).

RGDfK molecules with a thiol spacer as shown in Fig. 55 (a) were previously immobilized and tested on glass surfaces decorated with gold nanoparticles, as described in Sections III.2.2, III.3.3 and III.4.1.

Neuronal cell adhesion molecule L1 (NCAM-L1)

The L1 protein was already introduced in Section III.2.3. L1 is a transmembrane protein that is known to play a role in axonal adhesion. L1 proteins form cell-cell contacts by clustering at contact sites. In this study, L1 with terminal bound histidine units (his-tag) was immobilized on gold particles via nickel-NTA complexes, in order to test the functionality and effectiveness of the applied binding reaction. Since L1 serves as a transmembrane protein in neuronal cells, the immobilization of L1 on surfaces of artificial ECMs enables mimicking of the presence of neurons.

In this study, a commercially available L1 protein with 6 N-terminal bound histidine units (L1 his-tag) was used for the immobilization. The histidine does not influence the biological activity of the protein. Fig. 56 shows a model of the L1 his-tag

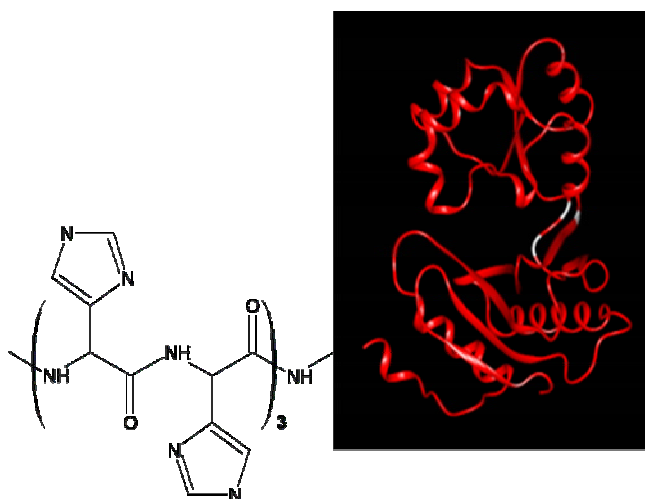


Fig. 56: The protein L1 with N-terminal bound histidines.

Green fluorescent protein

Fluorescent proteins are found in various deep-sea species, and have proven useful in biotechnology as markers in living cells. A well-studied representative is the green fluorescent protein (GFP) found in jellyfish.^{156, 157} GFP and its homologues feature a beta-barrel fold, the center of which is occupied by the chromophore, the light-absorbing and -emitting moiety (Fig. 57). The bright green fluorescence emission from GFP, with a wavelength of 508–515 nm, is readily induced by illumination of the molecule with blue light, with a wavelength of 470 nm. GFP-like proteins are widely used in cell biology as photolabels to track protein expression, protein trafficking, and protein-protein interactions *in vivo*. In this study, GFP was used to prove the efficiency of the coupling reaction of histidine-terminated proteins to the surfaces of chemically-modified PEG hydrogels. GFP containing 10 histidine units on its N-terminus (GFP his-tag) was kindly provided by Dr. T. Surrey.

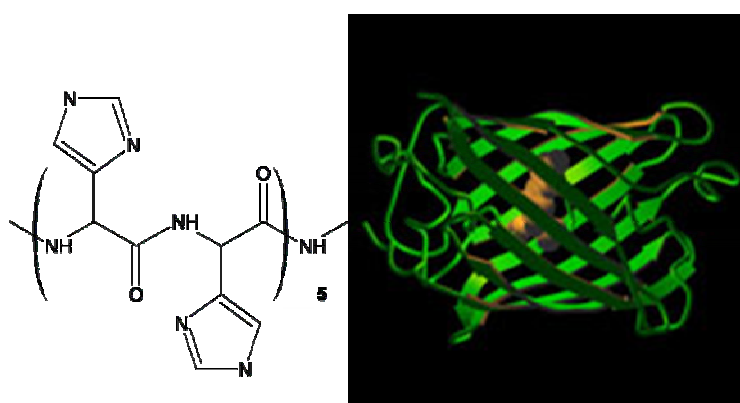


Fig. 57: GFP with terminally-bound histidine units.

VII.2. Bio-functionalization of gold particles on hydrogels

To use the gold particle-decorated hydrogels developed in Chapter V as a module for an artificial ECM, the gold particles themselves have to be activated by selectively binding selectively biologically active molecules to the gold. The immobilization of peptides or proteins on the gold particles leads to surfaces with a defined order and density of the biologically active sites at the molecular level, similar to conditions found in the natural ECM (Section III.1.)

The immobilization of molecules on gold surfaces is a well-established method used in cell biology to modify surfaces for cell experiments. As described in Section V.3.1, molecules can be bound to gold surfaces via thiol groups. This simple and highly selective reaction was described in connection with the transfer of gold particles to polymeric substrates. Via thiol groups, biologically active molecules can also be selectively bound to the gold nanoparticles. Peptides containing no thiol group can be endowed with thiol-terminated spacers (Fig. 55 a), leading to the immobilization of peptides with a controlled orientation and distance from the surface. Typically, proteins contain more than one thiol group. Thus, immobilizing the peptides directly on the gold particles will lead to non-ordered and uncontrolled protein orientations. The direct contact of proteins or peptides with a surface, results in limited biological accessibility within interactions with cells. A variety of different approaches for the immobilization of proteins on surfaces via a spacer molecule exist, as described in Section III.4.1.

In the present study, our task was to find the proper route for immobilizing peptides and proteins to gold particles, thereby enabling the binding of the molecules to gold particles on hydrogels. Even though the immobilization methods themselves are well-established, it is necessary to adapt them to the properties of the artificial ECM. To this aim, the influence of the reaction conditions on the sensitive gold pattern, and the reaction of the hydrogel upon exposure to solvents of varying polarities, was elucidated. Moreover, immobilization conditions had to be chosen such that used chemicals did not penetrate into and remaining in the hydrogel.

The following sections describe the chemical modification of planar gold-patterned hydrogels. The same principles and protocols apply in a similar manner to non-planar substrates such as the microchannels described in Chapter VI. In the following protocols, the sole modification concerned the incubation of the channel with the reactant mixtures and washing solutions, which had to be carried out by sucking the solutions into the channel using a micropipette.

VII.2.1. Binding of RGD peptides to the gold particles

The simple and straightforward immobilization of thiols on gold surfaces was used in this work to bind peptides to the gold particles via a thiol-terminated linker (Fig. 22 A, Section III.4.1). The RGD peptide contains only one cysteine residue which insures a well defined orientation of the molecule with respect to the surface. As described in Section VII.1.2 (Fig. 55 a), the c[RGDfK(Ahx-Mpa)] was directly bound to the gold particles on the PEG hydrogels, prepared as described in Section V.3, by following reaction conditions on gold-decorated glass surfaces described in comparable experiments.⁷⁴ The principal route is depicted in Fig. 58.

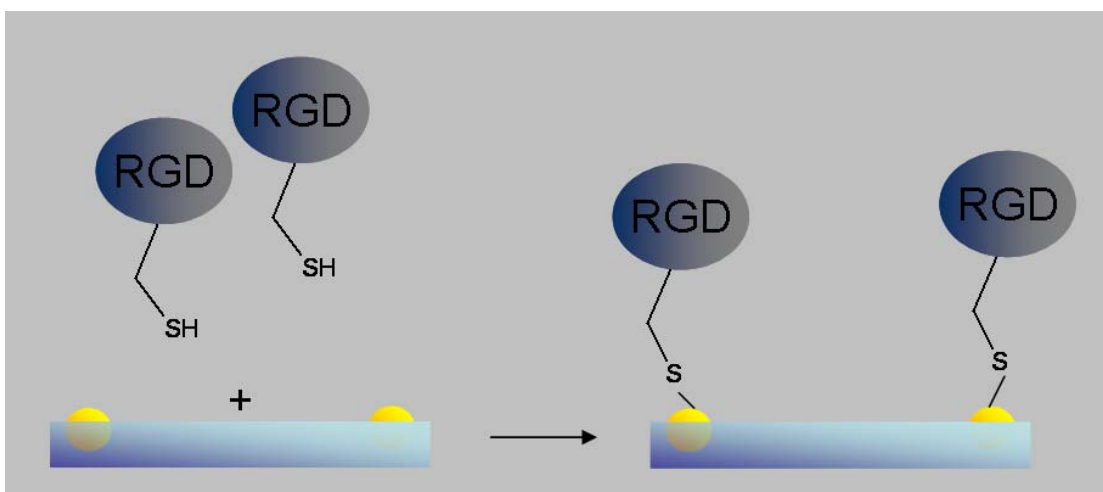


Fig. 58: Immobilization of c[RGDfK(Ahx-Mpa)] on gold particle-decorated hydrogels

Protocol for the peptide-thiol immobilization on gold

Hydrogels swollen in MilliQ water prepared according to the protocol described in Section V.3, were placed upside-down in a Petri dish on a 50 μ l drop of a 25 μ M c(RGDfK)-thiol solution in MilliQ water. A drop of MilliQ water was placed on the top of the samples to keep them humid. The Petri dish was sealed with parafilm. After 4 h, the samples were taken out and washed twice with MilliQ water. Before the samples were used in cell experiments, they were sterilized by storage in ethanol for 1 h. To remove the ethanol and RGD molecules which were not covalently bound to the gold but rather penetrated into the gels, the gels were stored overnight in sterile MilliQ water.

Results

To test for the presence of RGD and its specific immobilization on the gold particles, simple cell experiments were performed. The conditions for the cell experiments and the principal procedures used are described in the Chapter VIII. Here, the cells were simply used as an indicator of successful immobilization. Fig. 59 shows four types of hydrogel surfaces. Hydrogels were prepared such that an area decorated with gold

particles was directly adjacent to an area without gold particles. On one of these hydrogels, c(RGDfK)-thiol was immobilized as described above. The second sample was used without having been treated with c(RGDfK)-thiol. Fibroblasts were then seeded on these surfaces, according to the protocol in Section VIII.1.

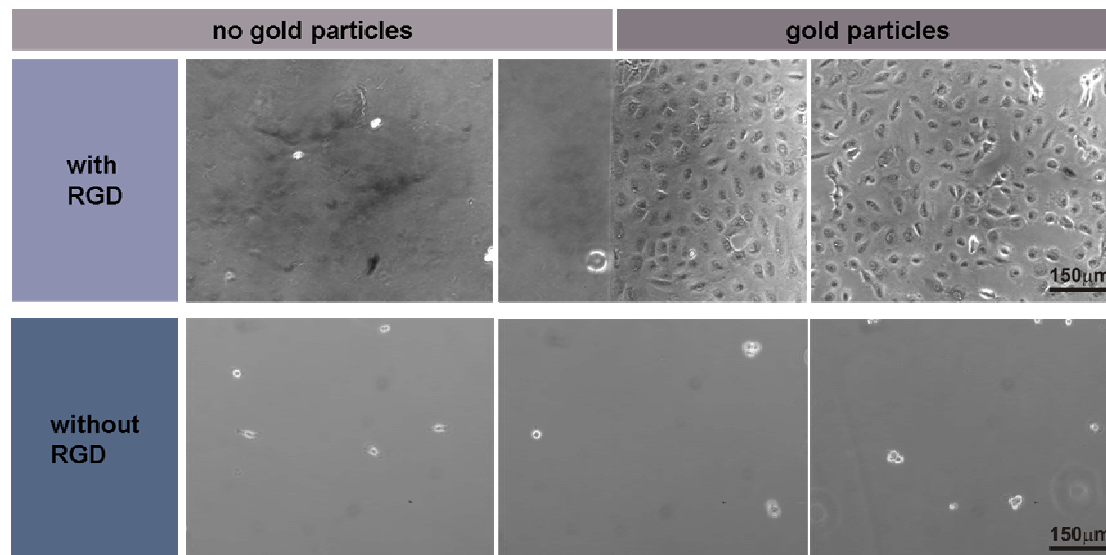


Fig. 59: The successful binding of RGD to gold particles was proven by cell experiments. The cells only adhered in the region of the PEG hydrogel, whereas RGD was immobilized on gold nanoparticles. In the other three regions, no cell adhesion was observed.

The experimental results, summarized in Fig. 59, show that cells only adhere to that region of the PEG hydrogel in which gold particles have been functionalized with RGD peptides. In those regions without gold particles on the gel or without RGD functionalization, no cells were found to adhere. Thus, it appears that:

- The cells, as expected, do not adhere to the plain hydrogel;
- The c(RGDfK)-thiol molecules do not stick non-specifically to the hydrogel;
- The c(RGDfK)-thiol can be selectively bound on the gold particles; and
- The cells require the presence of the c(RGDfK) peptide in order to properly attach to the hydrogels.

Further experiments carried out on PEG hydrogel surfaces decorated with functionalized gold particles are described in Chapter VIII.

VII.2.2. *Binding of proteins to the gold particles via a nickel-NTA complex*

The coupling of proteins to the gold particles via thiol groups of cysteine residues in the protein, as carried out for simple peptides described in the previous Chapter is not

feasible, for the following reasons: The binding of more than one reactive group - in this case, more than one cysteine residue in the protein - and direct binding without the presence of a linker, would make the coupling unspecific and denaturation more likely to occur.

For the immobilization of proteins to gold particles on hydrogels, an alternate route was chosen which based on nickel-histidine tags, according to the principles discussed in Section III.4.1, and described in Fig. 20. Here, the protein L1 with terminally bound histidine units as the coupling agent (Section VII.1.2), was coupled to the gold particles via a nickel-NTA (nickel-Nitrilotriacetic acid) complex. Fig. 60 shows the reaction steps involved in the immobilization of histidine-tagged L1 to gold particles. First, the samples were incubated in a solution of dithiobis(succinimidyl)propionate (DTSP) in methanol. The disulphide bonds were thereby broken, and the sulphur is coordinating to the gold particle. The immobilized molecule carries an N-hydroxysuccinimide ester (NHS ester) group, which in turn can be modified by means of nucleophilic substitution with the primary amino group of the $N\alpha,N\alpha$ -bis(carboxymethyl)-L-lysine (ANTA). Finally, the resulting NTA groups on the surface can be complexed with nickel chloride and with the histidine peptides bound to the L1.

This technique was developed on glass substrates decorated with gold nanoparticles, and found to be suitable for the immobilization of proteins in such systems. Here, we tested whether the same immobilization method could also be used for the binding of proteins to gold nanoparticles on hydrogels. These experiments were done with the help of Dr. F. Corbellini.

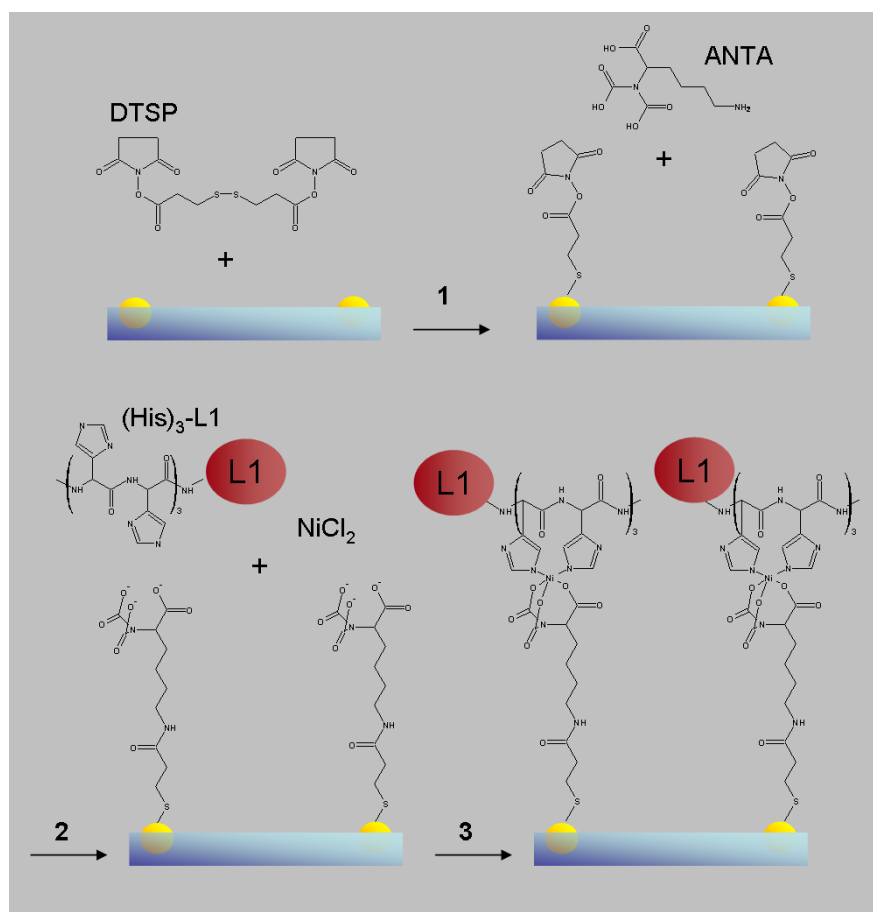


Fig. 60: Schematic of the technique used to immobilize L1 on gold particles.

Protocol for protein immobilization on gold particles

PEG hydrogels decorated with gold nanoparticles, prepared according to the procedure described in Section V.3.2. In order to completely replace the water in the gel with methanol, the methanol was changed twice. Samples were incubated for 15 min in a mixture of 1 mg/ml DTSP in methanol. After first rinsing the samples rinsed 4 times, for 15 minutes each with a 1:1 mixture of methanol and water, and then twice for 15 min with a 0.5 M K₂CO₃ buffer of pH 9.3, the samples were incubated for 1 h in a 150 mM solution of ANTA in a 0.5 M K₂CO₃ buffer. After this reaction, the samples were transferred into a 2 mM HBS buffer for 15 min. After equilibration, the samples were incubated in a 10 mM NiCl₂ solution for 15 min, and washed twice for 15 min in a 2 mM HBS buffer. The histidine-tagged protein was incubated for 4 h. Following incubation, samples were washed in HBS buffer.

Before using samples for cell experiments, samples were sterilized by storage in ethanol for 1 h. To remove ethanol and RGD molecules which were not covalently bound to the gold but rather penetrated into the gels, gels were stored overnight in sterile MilliQ water.

Results

To demonstrate the presence of the cell adhesion-mediating protein L1 and its specific binding exclusively to the gold particles, PC12 cells were plated onto the substrates. These cells are known to form cell-cell adhesion sites mediated by L1, so that cell adhesion to the substrate indicates the presence of L1. The culture conditions are described in detail in Chapter VIII. The substrates used for the experiments were decorated on one side only with gold particles. The cells were seeded on two types of nanopatterned hydrogels, one with immobilized L1 protein using the aforementioned procedure, and the other one without.

Fig. 61 summarizes the results. The cells only adhered the surface which was coated with L1. There appeared to be no adhesion on the gels not coated just with plain gold particles without L1. As described in Section VII.2.1 for RGD peptides bound to the gold particles, it can therefore be concluded that the immobilization of the L1 was specific for gold. Furthermore, cells do not adhere to the plain gold particles or the PEG. We also note that after careful washing, no cytotoxic substances remained in the gel.

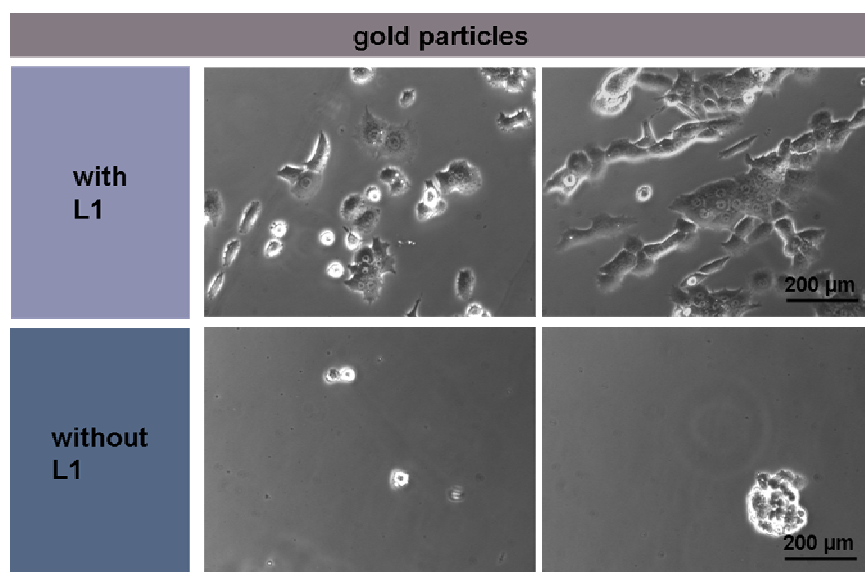


Fig. 61: PC12 cells on PEG hydrogels decorated with gold particles, with and without the addition of L1.

VII.3. Biofunctionalization of PEG hydrogels

After the immobilization of peptides and proteins on gold nanoparticles on PEG hydrogels, as described above (Section VII.2), the next step was to immobilize peptides or proteins directly onto the hydrogel. The intention is, the immobilization of molecules on both the gold particles and the hydrogel in between can be combined, enabling the combination of various bioactive molecules at these two different regions. For example, two types of proteins or peptides with different biological

functions could thereby be bound next to each other; the one in a defined pattern and spatial distribution determined by the gold nanopattern, and the other filling the areas in between.

As mentioned in Section III.4, the literature describes several approaches which may be used to bio-functionalize PEG hydrogels. All these approaches are based on the copolymerization of PEG macromers with adhesion-mediating peptides such as RGD, via a terminal reactive group.⁵¹ This method is a simple, but costly and highly inflexible way to perform bio-functionalization. First, cells in general only interact with the materials on the surface. Peptides embedded in the three-dimensional networks are not available to the cells. Secondly, the method can only be used for the immobilization of chemically stable molecules. The crosslinking reactions for the formation of PEG hydrogels tend to destroy sensitive molecules such as proteins. Therefore, it was necessary to develop a method which enabled the immobilization of peptides and proteins in a non-destructive manner.

The basic strategy used was to copolymerize simple molecules with the PEG macromers, in order to obtain functional groups in the resulting hydrogel. These functional groups enable the binding of biomolecules in the reactions which take place on the surface of the gels. The reaction steps for coupling the bioactive molecules to the functional groups had to be chosen such that the functional groups resist the crosslinking reaction with UV irradiation. In addition, the chemical reactivity had to be different than that commonly found in peptides and proteins (e.g., the nucleophilic behavior of amino groups) to avoid non-specific reactions with other residues of the peptide or protein. The molecule of choice is the carboxyethylacrylate (Carb AC). In Section IV.3, Carb AC was already introduced as an additive in the crosslinking reaction. The following sections will describe the copolymerization of Carb AC with PEG-DA, and the usage of the resulting hydrogels for the immobilization of peptides and proteins on the gel surface.

VII.3.1. Copolymerization of carboxyethylacrylate to the PEG-DA

The syntheses route to prepare biofunctionalized PEG hydrogels is outlined in Fig. 62. The fundamental idea behind this new approach to the biofunctionalization of PEG hydrogels is the copolymerization of carboxyethylacrylate (Carb AC) with PEG-DA. We assume, that the resulting hydrogel contains carboxylic acid groups in the concentration of the Carb AC initially utilized. These carboxylic acid groups can be modified with N-hydroxysuccinimide (NHS) to NHS ester groups. The NHS esters react selectively with all kinds of primary amines, as described in Section VII.2.2. Fig. 62 shows the general reaction pathway for these steps.

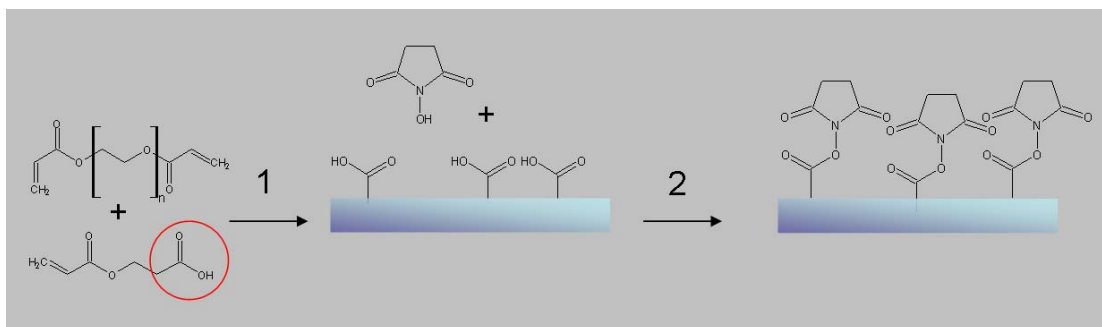


Fig. 62: The copolymerization of carboxyethylacrylate (Carb AC) with PEG-DA, and the modification of the carboxylic acid groups in the gel by N-hydroxysuccinimide ester (NHS ester) groups.

Protocol for the chemical modification of PEG hydrogels

The PEG-DA and the Carb AC were mixed with water in various ratios (Table 1 in Chapter IV) and crosslinked as described for the standard protocol (Section IV.3.1) for the preparation of hydrogels with different PEG macromers. To remove the Carb AC which was not covalently bound to the polymer meshwork, the gels were swollen in ethanol for 30 minutes, and stored in MilliQ water overnight. The gels were incubated for 30 min in a mixture of NHS (0.1M) and N-(3-Dimethylaminopropyl)-N'-ethylcarbodiimide hydrochloride (EDAC) (0.4M) in water. After the reaction, the samples were rinsed with PBS buffer and directly used for reactions with primary amines, to couple peptides or proteins to the NHS esters. The following reactions are described in detail in Sections VII.3.3 and VII.3.2.

Results

The presence of the carboxylic acid group in the gel was tested with a simple soluble indicator. Methyl red was used to indicate the difference in the pH of a normal PEG hydrogel, and a PEG hydrogel containing copolymerized Carb AC. To this end, the gels were washed for several days with water to remove all Carb AC molecules which were not covalently linked to the gels. They were then placed in a Petri dish containing methyl red dissolved in water. After 2 hours, the entire gel was penetrated by the indicator. Fig. 63 shows the color difference between a gel without Carb AC (a) and a gel containing carboxylic acid groups (b).

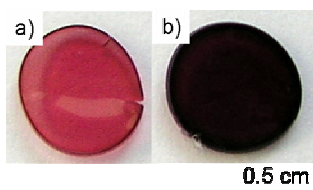


Fig. 63: Hydrogels incubated with methyl red. The indicator methyl red was used to test the presence of carboxylic acid groups in the gels in comparison to a gel without (a) and with (b) the addition of Carb AC.

Successful esterification with NHS was demonstrated by means of additional reactions, as described in the following two sections.

VII.3.2. *Binding of peptides to the hydrogel*

The immobilization of peptides directly onto the PEG hydrogel was tested by a simple coupling reaction of NHS esters and primary amines. Section VII.3.1 described how the surface of PEG gels could be activated for further reactions with NHS esters. Gels prepared in that manner are capable of reacting with primary amines in a highly specific manner. The c[RGDfK(Ahx-Apa)], a cyclic RGD with a spacer carrying a primary amino group (described in Section VII.1.2) was used for the reaction with the NHS on the surface of the hydrogels. The amino group on the spacer of the RGD reacts in one step with the NHS ester groups on the surface of the gels. The reaction is schematically illustrated in Fig. 64.

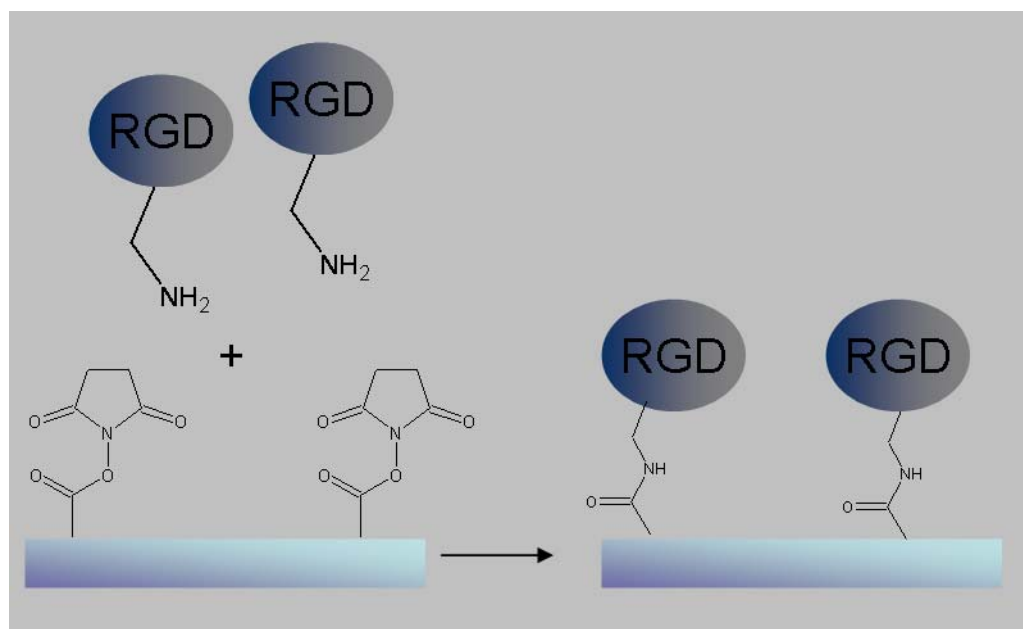


Fig. 64: Immobilization of the c[RGDfK(Ahx-Apa)] on the NHS ester-activated PEG hydrogel.

Protocol for the binding of RGD to PEG hydrogels

After preparing hydrogels according to the protocol described in Section VII.3.1, the samples were rinsed twice for 15 min with PBS buffer. They were then placed upside down in a Petri dish on a 50 μ l drop of a 25 μ M c(RGDfK)-amine solution in 0.5 M K₂CO₃ buffer, with a pH of 9.6. A drop of MilliQ water was placed on the top of the samples to keep them humid. The Petri dish was then sealed with parafilm. Before usage of the samples for cell experiments, the samples were sterilized by storage in ethanol for 1 h. To remove ethanol and RGD molecules which were not covalently

bound to the gel but penetrated into the gels, the gels were stored overnight in sterile MilliQ water.

Results

To test the specific binding of the c(RGDfK)-amine to NHS esters on the PEG hydrogel, fibroblasts were plated on the substrates according to the protocol described in Section VIII.1. Cells were cultured for 24h on three different surfaces as described in the following (shown in Fig. 65). On the first surface, cells were seeded directly after the crosslinking reaction; in this case, cells only adhere to the PEG with carboxylic acid groups (Fig. 65 a). The second surface was activated by esterification before the cells were plated (Fig. 65 b), and the third was incubated in the c(RGDfK)-amine solution (Fig. 65 c).

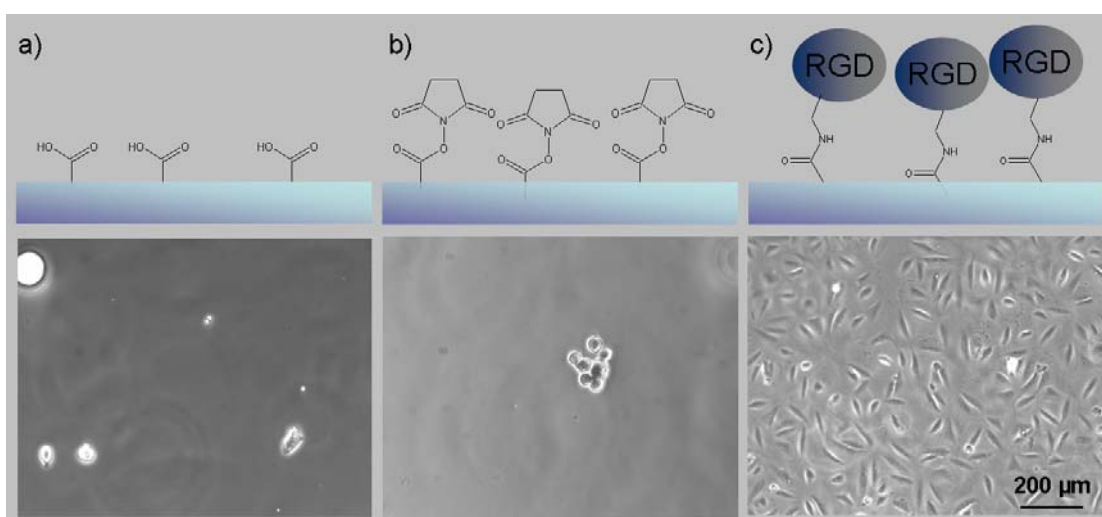


Fig. 65: Fibroblasts cultured for 24h on three different PEG hydrogel samples, to test the binding of RGD to the hydrogel. Chemical modification of the hydrogel by introduction of carboxylate groups (a), and esterification (b) did not result in the loss of the hydrogel's biological inertness, since only the additional presence of RGD (c) enabled cell adhesion.

As expected, the cells only grew on the biofunctionalized surface. This experiment demonstrates the efficient binding of RGD to the hydrogel surfaces. Secondly, it shows that chemical pre-treatment has no influence on the passivating effect of the hydrogel against cell adhesion.

VII.3.3. *Binding of proteins to the hydrogel via a Nickel-NTA complex*

Similar to the two alternative functionalization routes for gold with peptides and proteins, via thiol and nickel-NTA complexes, respectively, the functionalization of

the hydrogel was achieved again both for peptides, as described in the previous section, and for proteins, the subject of this section. PEG hydrogels prepared according to the protocol described in Section VII.3.1 were used to immobilize proteins on the surfaces.

Since NHS ester groups were introduced into the hydrogels (Section VII.3.1), immobilization of a protein on a hydrogel can follow the same route described for the L1 protein immobilized on gold particles via a linker system, which is also based on the property of NHS esters to react specifically with primary amines (described in Section VII.2.2). As in the case of L1, the NHS ester group was reacted with an $N\alpha,N\alpha$ -bis(carboxymethyl)-L-lysine (ANTA) to obtain NTA groups on the hydrogel. These groups are complexed with nickel chloride- and histidine-tagged proteins. In the present case, the protein used was histidine-terminated GFP, introduced in Section VII.1.2. and shown in Fig. 57. The principal immobilization procedure for the histidine-tagged GFP is illustrated in Fig. 66. These experiments were done with the help of Dr F. Corbellini.

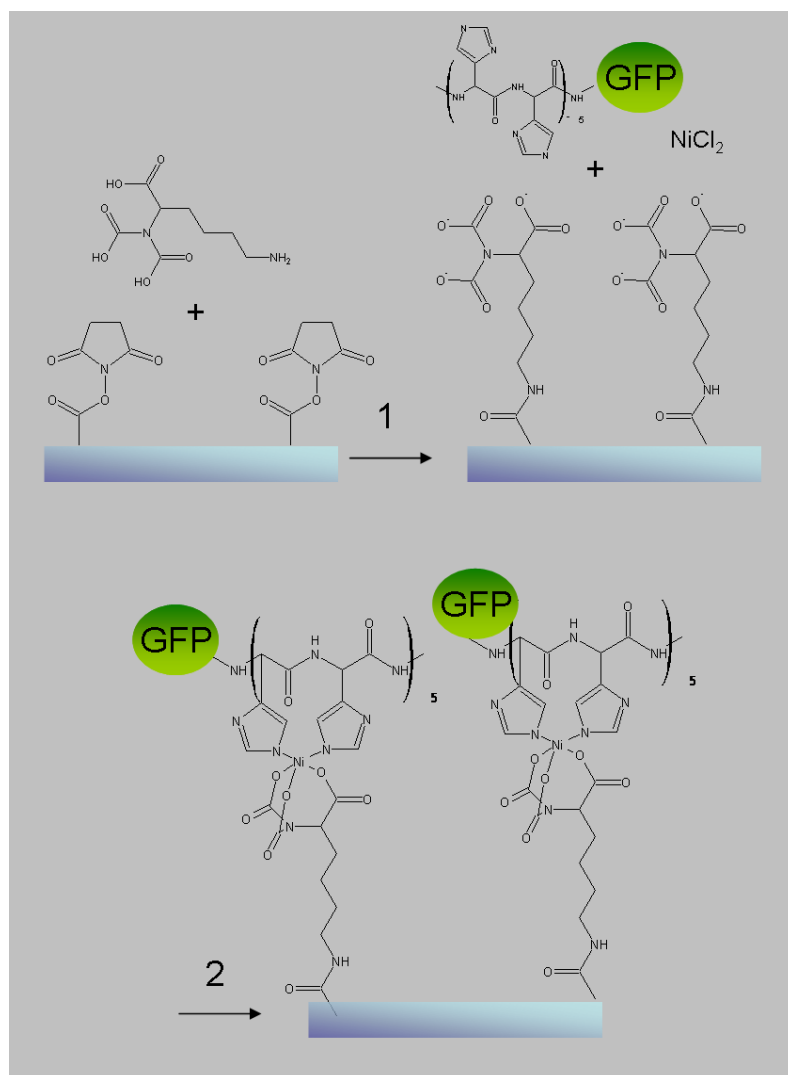


Fig. 66: Immobilization route of histidine-tagged GFP to a modified PEG hydrogel surface.

Protocol for the immobilization of GFP to PEG hydrogels

PEG hydrogels containing carboxylic acid groups were prepared according to the protocol described in Section VII.3.1. The same protocol describes how the carboxylic acid can be esterificated with NHS. After rinsing the samples two times for 15 min with PBS buffer with a pH of 9.3, the samples were incubated for 1 h in a 150 mM solution of ANTA in the 0.5 M K_2CO_3 buffer. Following this reaction, the samples were transferred into a 2 mM HBS buffer for 15 min. After equilibration, the samples were incubated in a 10 mM $NiCl_2$ solution for 15 min, and washed twice for 15 min each time in the 2 mM HBS buffer. The histidine-tagged protein was incubated for 4 h. After the incubation, samples were washed in HBS buffer.

Results

The efficiency of the GFP immobilization via the NTA nickel histidine complex was tested by fluorescent light microscopy. The green fluorescent color of GFP with a wavelength of ~ 510 nm was detected with a high intensity on the hydrogel onto which the GFP was bound via the nickel complex. In this experiment, shown in Fig. 67, samples were treated with the histidine-tagged GFP at three different stages of the procedure, and were then washed intensively with water. The fluorescent microscopy images show that when the sample is treated at the final stage, where the GFP is bound via the nickel complex (Fig. 67 c), the intensity of the detected light (wavelength of ~ 510 nm) increased rapidly. Low fluorescence intensity, instead, is found for the samples treated at the intermediate stages of the modification procedure, where the GFP was not able to form a chemical bond (Fig. 67 a, b).

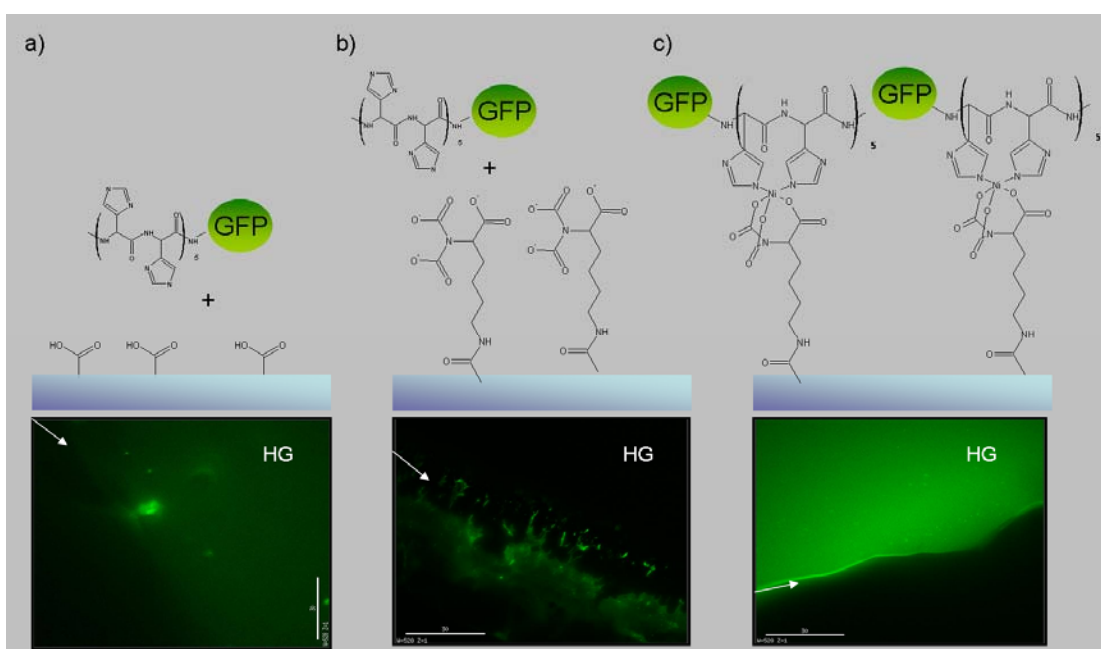


Fig. 67: Fluorescence images of hydrogels at three different stages of surface modification treated with histidine-tagged GFP.

The findings presented in Fig. 67 illustrate that the esterification with the NHS, the subsequent coupling of the ANTA, and the complexation of the NTA and the histidine units, were successful and specific.

VII.4. Conclusion

The third module of the artificial ECMs entails the activation of the nanopatterned surfaces for specific interactions with cells, by means of chemical modification. Peptides and proteins can be specifically bound to the gold particles or the PEG hydrogel surface in between, as described in this chapter. While the mechanical and structural properties of the ECM mimic are determined by the basic polymer material and the gold nanopattern itself, the chemical properties are defined by the subsequent modification of the surface with the active biomolecules. The chemical modification enables the biofunctionalization of the nanopatterned substrate, such that the artificial ECM is tailored for certain cell types.

In order to functionalize gold particles and PEG hydrogels, different basic modification routes are required, due to their differing chemistries. Coupling of bioactive molecules to gold was achieved via conventional thiol groups; i.e., coupling the hydrogel by copolymerization with a linker molecule, yielding PEG with carboxylate moieties. The two modification routes were again modified with respect to the biomolecule to be coupled, either peptides or proteins. Peptides, which are comprised of only a small number of amino acids, and thus a small number of reactive groups, can be simply coupled to the gold via a terminal thiol group, or to the carboxylate via a terminal amino group. For proteins, a more selective approach, coupling via NTA-nickel complexes, was chosen, requiring the introduction of histidine tags at the protein termini.

As a proof of concept, substrates were chemically modified on the gold particles or hydrogel surfaces with sample peptides, namely RGD sequences, and proteins, namely L1 and GFP. Their specific bioactivation was tested by cell experiments and in case of the GFP by fluorescence measurements. Efficient and selective bioactivation was achieved via all four modification routes.

Chemical modification of the surfaces involves the use of chemical compounds that are partly cytotoxic. Cell death was, indeed, observed in cell experiments using the chemically-modified artificial ECMs, due to chemical substances remaining after the bioactivation. Extraordinarily extensive washing of the substrates was thus essential, in order to minimize cell death.

The gold particles and the hydrogel surface can be functionalized independently from one another, enabling a combination of two different functional molecules, each of which is restricted to one of two areas, either the gold particles or the hydrogel surface. Such combined and complementary bioactivation will be the subject of

further studies. In this study, the chemical modification was shown for RGD, L1, and GFP, but in principle, peptides and proteins of any kind could be coupled in this manner. An interesting next step would be to combine the functionalization of the gold particles and the hydrogel, with RGD and epidermal growth factors (EGFs). Cells on this kind of artificial ECM could form integrin-RGD adhesion sites clustered on the gold particles, at distances dictated by the nanopattern. In addition, the cell-hydrogel interaction is known to be mediated via EGF, thereby stimulating cell growth. Within the framework of a specifically-tailored artificial ECM, the crosstalk between the two biological functions of the ECM, growth factors and adhesion sites, can be studied quantitatively for different cell types.

Thus far, we were able to qualitatively test the chemical modification of the substrates, via cell experiments and protein fluorescence. Other techniques for measuring the efficiency of peptide and protein coupling are required to determine the actual average density of the biomolecules; e. g., by means of solid-state NMR. Bioactivated hydrogels can be also characterized in terms of the ligand density, by quantifying the ability of the ligands to bind gold particles. In such an assay, gold particles could be decorated with cysteamine, and then incubated with the PEG hydrogel containing crosslinked carboxylate groups, thus coupling to the hydrogel by forming amide bonds. Furthermore, gold particle density, which could be used as a measure for the ligand density could be observed by means of cryo SEM. A related question, the number of ligands that can bind to a gold particle of a given diameter, also remains to be answered.

In summary, this chapter was concerned with the third module of the artificial ECMs, its chemical properties, as defined by bioactivation of the gold-patterned hydrogels. Taken together, we now are able to fully design artificial ECMs according to their desired structure, mechanics, and biological function. The first applications of the resulting ECM-mimicking systems are described in Chapter VIII.

VIII. Cell response to various hydrogel modules

The design of the three building blocks of the artificial ECM, the basic material, the gold nanopattern, and bioactive molecules, all of which define the mechanical, structural and chemical properties of the ECM, was already established (Chapters IV, V and VII). Our aim in designing an artificial ECM is its application to cell experiments, in order to study the crosstalk between cells and their environment in a well-defined and quantitative way. We began by carrying out cell experiments which could test the applicability of the artificial ECM to the following issues:

- the functionality of each of the three modules;
- the use of the gel-like substrates for cell culture experiments (sterilization, handling);
- microscopic methods for observation of cell behavior on the new substrates
- the use of microchannels for cell experiments

Overall, the cell experiments performed in this study were aimed at demonstrating the general functionality of the artificial ECMs. Future experiments will focus on specific biological applications, but are beyond the scope of this thesis.

VIII.1. Cell culture protocols

VIII.1.1. *Standard culture conditions*

To avoid contamination, all the steps involving eukaryotic cells were performed in a sterile hood, using sterile techniques and materials. The cells employed in this study were maintained in the suitable media as indicated in Table 2.2. Cells were cultured in an incubator kept at 37°C, and with a 5% CO₂ atmosphere. The media was changed every 2 days. Cells used for the experiments were REF WT-52 fibroblasts (also termed simply, “fibroblasts”), HeLa cells, and PC 12-27 cells.

Cell culture protocol

After the cells reached confluence, they were first rinsed with sterile PBS and then rinsing with a 2.5% trypsin-EDTA solution for 3-5 min at 37°C. After dilution of the cells in 5-10 ml of Dulbecco’s Modified Essential Medium (DMEM) and centrifugation at 1200 rpm for 5 min, the cell pellet was suspended in DMEM supplemented with 10% fetal bovine serum (FBS) and 1% L-glutamine (L-glut). Cells were then replated in tissue culture flasks, or in wells containing the substrates prepared for the adhesion studies.

In order to avoid differentiation, the PC 12-27 cells were not cultured until confluence. Every 5 days, the cells were split, and plated in new flasks. This procedure is therefore similar to the culturing of REF WT-52 cells. The culture medium for PC 12 cells consists of DMEM containing 10% FBS, 1% L-glut, 0.5% Pen-Strep and 10% of horse serum (HS).

Cell counting

In order to determine the total cell number, as well as the number of vital cells in the culture, the cell suspension in DMEM was diluted 1:10 in a 0.05% trypan blue solution in MilliQ water. This colored substance only enters and stains dead cells. The cell suspension in trypan blue was then transferred into two hemocytometer chambers. Each chamber was divided into eight fields. By using a 10x objective and light microscopy, it was possible to visualize the grid lines in the chamber, with each field consisting of a 1 mm² area. The number of cells per field was counted and averaged, in order to obtain the number of cells per given volume (ml) (excluding the dead cells stained in blue).

VIII.1.2. Cell experiments on hydrogels

Preparation of the hydrogels

Hydrogels were prepared as described in the previous chapters. Gels utilized in the following cell experiments were obtained from PEG-DA of varying molecular weights, as indicated in the respective experimental sections. Gels chemically modified in different ways were also used in our experiments, as indicated below. The gels were sterilized for 1 h in ethanol, washed twice with MilliQ water for 1 h, and incubated for 1 h with the same cell medium used for the subsequent cell experiments.

Cell plating on the hydrogels

The REF WT-52 and HeLa cells in the culture were trypsinized and plated on the hydrogel surfaces in DMEM containing 1% FBS (to minimize the effect of extracellular matrix molecules contained in FBS on cell adhesion and spreading) and 1% L-glut. For microscopy and imaging experiments, the cell plating density was 10–100 cells/mm².

The culture medium for experiments with PC 12-27 cells consisted of DMEM containing 1% FBS, 1% L-glut, 0.5% Pen-Strep and 1% HS.

VIII.2. Cells on biofunctionalized hydrogels

In this section, the results of cell experiments which illustrate both the general applicability of the artificial ECMs, and the roles played by each of the different modules, are described. Apart from the last experiment of this section, which focuses on soft hydrogels, all experiments were performed using a stiff PEG 700 hydrogel. This approach excludes the influence of elastic effects on cell adhesion behavior.

Previously-described cell experiments (Chapter VII) tested the functionality of the bioactivated substrate surfaces with RGD peptides. As described in Section VII.2.1, fibroblasts were cultured on PEG gels with and without gold particles under standard cell culture conditions, before and after immobilization of c(RGDfK)-thiols. Cell adhesion was only observed on PEG hydrogel surfaces with RGD functionalized gold nanostructures, but not on surfaces without gold particles or RGD, respectively. This finding demonstrated (i) specific binding of RGD molecules to the gold particles but not to the gel, (ii) cell adhesion specifically to RGD functionalized spots, and (iii) the passivating properties of the hydrogel.

The second test experiment, described in Section VII.3.2 correspondingly showed the functionality of the bioactivated hydrogel surfaces directly with RGD. Fibroblasts were seeded on hydrogels without nanopatterns, both before and after c(RGDfK)-amines were immobilized on the gels carrying carboxylate moieties. The coupling reactions performed to bind RGD to the gels were efficient; moreover, the reaction steps did not lead to reduced passivity for cell adsorption, or to any cytotoxic side effects.

From these two experiments, we conclude that biofunctionalization enables direct control of the interactions of the cultured cells with the ECM-mimicking material.

The use of Cryo SEM to observe the interactions of cells with the nanostructure

To investigate and influence the crosstalk between the cell and the microscopic environment on a nanoscale level using the artificial ECMs, high-resolution microscopes are essential. Such tools enable the direct observation of interactions between cells, and the nanostructures on the gel surface. Cryoscanning electron microscopy (cryo-SEM) permits the visualization of cells on surfaces in the frozen state, at resolutions down to the nanometer scale. Cryo-SEM experiments were performed by plating fibroblasts for 24h on a c(RGDfK)-thiol functionalized nanopatterned PEG 700 hydrogel. The samples were frozen immediately after careful rinsing with PBS. The SEM images in Fig. 68 show that the cells selectively form adhesive interactions with single gold particles. Hence, the interplay of the different modules enables the artificial ECM to function as an adequate cell environment, within which the properties of the adhesion sites may be adjusted. For example, the distances between adhesion receptors on the surfaces of the cells may be determined

by targeting the single receptors by means of RGD-functionalized gold particles. Thus, the gold nanoparticles, which serve as binding sites for the RGD sequences, function as a “nano-ruler”, enabling the visualization and measurement of the distances between the adhesion sites at the molecular level. Furthermore, cryo-SEM proved suitable for visualizing discrete cell-surface interactions (also shown below for soft hydrogels), and will therefore be used as the standard microscopic method in our future cell experiments.

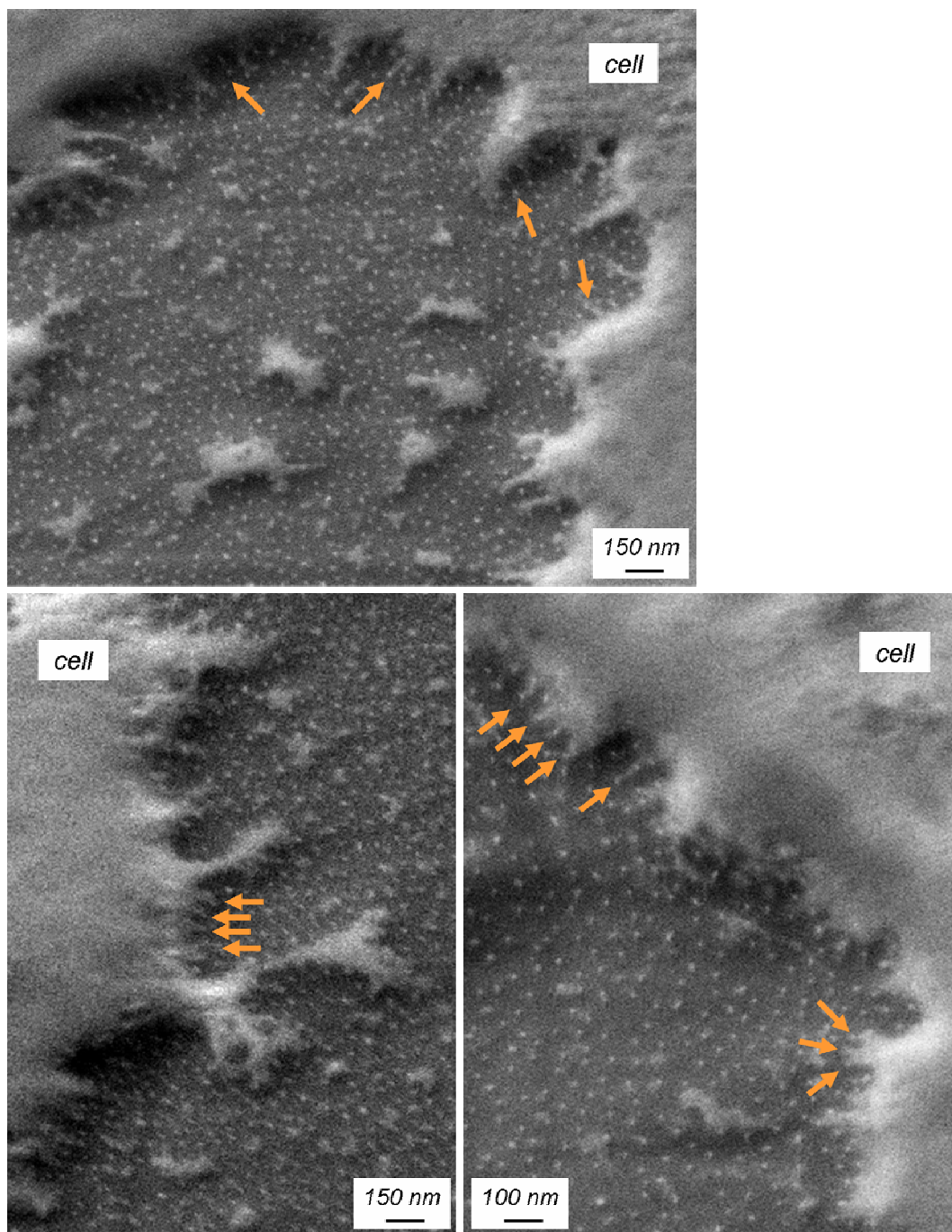


Fig. 68: Cryo-SEM images of fibroblasts plated on RGD-functionalized, nanopatterned PEG 700 hydrogel surfaces, revealing the cells’ adhesive interactions with the nanoparticles. The yellow arrows mark some of the most significant binding sites between the cell and the gold particles.

Long-term stability of the patterned hydrogels

The biological activity of the gold-decorated hydrogels, including the passivity of PEG and the mechanical stability of the gold pattern, might change over time, due to the deposition of ECM proteins expressed by the cells, as well as to mechanical stress during culturing. The long-term stability and biological activity of gold-decorated hydrogels was investigated by culturing fibroblasts for more than 14 days on a PEG 2000 hydrogel decorated with c(RGDfK)-thiol functionalized gold particles. Cells only grew on regions with gold structures (Fig. 69). The resistance of the hydrogel to protein adsorption, as well as the adhesion activity of the functionalized gold structure, endured over this period, demonstrating the long-term applicability of the materials to cell experiments. This finding demonstrates a major advantage of the hydrogel-based artificial ECMs, as compared to glass substrates. The latter type of substrate demonstrates loss of biological inertness after a few days, rendering itself inadequate for long-term cell culture studies.

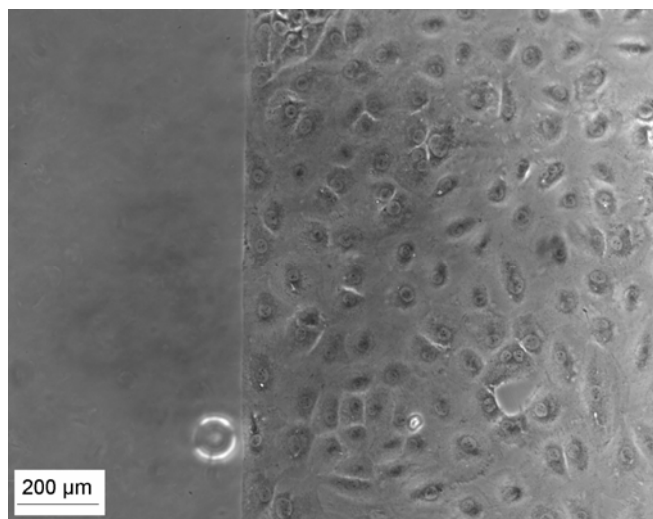


Fig. 69: Cells seen after 14 days on a surface partially coated with RGD-functionalized gold particles. The hydrogel stays resistant towards protein adsorption.

Influence of interdot spacing

The structural properties of the artificial ECM, primarily the average distance between the gold particles, are a critical parameter influencing cell adhesion, by determining the inter-receptor distances. The influence of the inter-particle distance onto the adhesion behavior has been previously shown for gold nanopatterned glass substrates, as described in Sections III.3.3 and III.4.1.⁵⁴ Our results were in agreement with data from studies of nanopatterned glass surfaces, in that the adhesion behavior of the cells differed, depending on the nanopattern on coupled the gel surfaces (Fig. 70). If the distance between the adhesive RGD ligands was less than 58 nm, cells showed typical spreading behavior, and were thus able to adhere to the substrate (Fig. 70, top). Distances larger than 58 nm enabled the attachment, but not the spreading, of the cells

(Fig. 70, center and bottom). We can therefore conclude that we have designed a versatile hydrogel system as our artificial ECM, displaying the same favorable properties as previously-used glass substrates, and with the additional advantage of tunable elastic properties. In contrast to glass substrates, the swelling behavior of hydrogels changes, depending on the mesh size; i.e., different molecular weights (Section IV.3), so that the interdot distance changes with the type of hydrogel used (Section V.3.2). When designing an artificial ECM suitable for a certain cell type, the effect of hydrogel-specific changes in the spacing has to be taken into account.

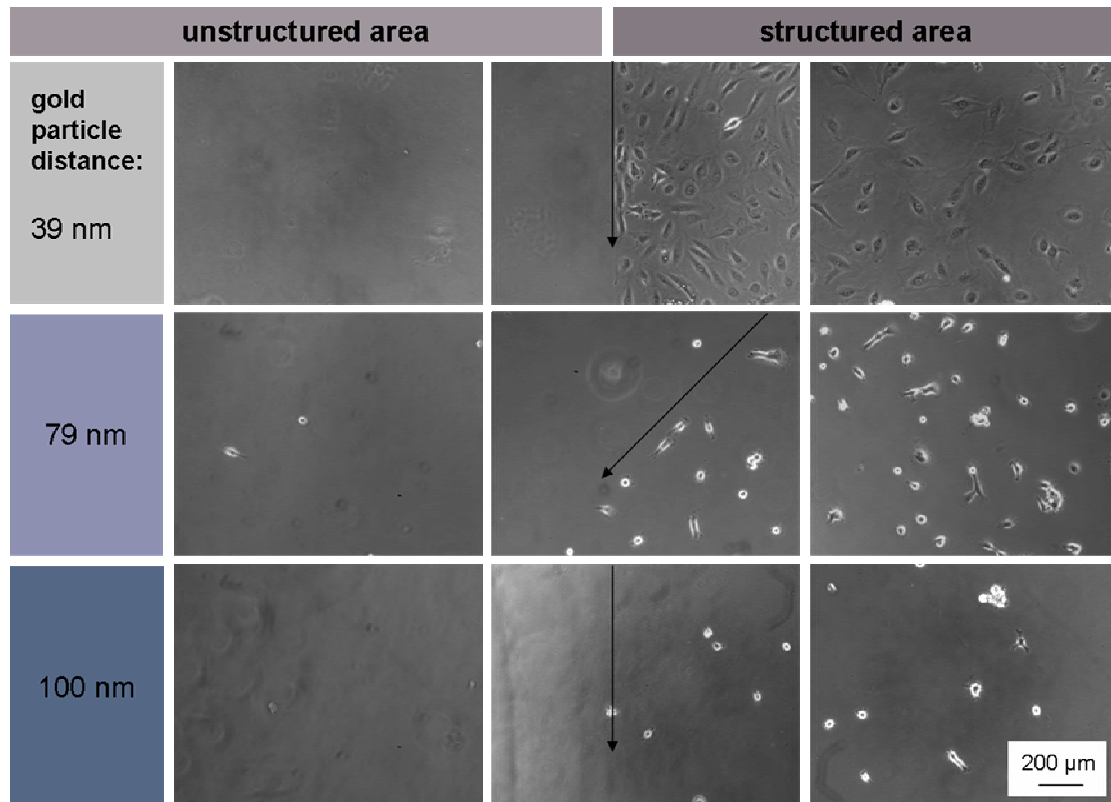


Fig. 70: Phase contrast images of fibroblasts on PEG 700 hydrogels after 24 h in culture . Cells did not grow on unstructured areas, but did grow on structured areas with RGD functionalized gold particles. The extent of growth differed, depending on the inter-particle distance. Arrows indicate the border of the nanostructured area.

Influence of different receptor ligands on cell growth

Bioactivation by means of chemical modifications of the artificial ECMs enables the specific tailoring of the chemical properties of the material, to certain cell types. This principle was demonstrated by comparing the rate of growth of various cell types, on substrates which differed in their biofunctionalization. Fig. 71 compares the behavior of REF WT-52 fibroblasts and PC 12-27 cells cultured on PEG hydrogels incubated with either c(RGDfK)-thiols or histidine-tagged L1 protein to activate the gold nanoparticles. As outlined in Sections III.2.2 and VII.1.2, the cyclic RGDfK sequence binds preferably to $\alpha_v\beta_3$ integrins, which are expressed at high levels by fibroblasts,

but only slightly expressed by PC 12-27 cells. PC 12-27 cells are known, rather, for their L1-mediated cell-cell contacts; in this respect, they also differ from fibroblasts (Sections III.2.3 and VII.1.2). In this cell culture assay, we therefore expected to be able to differentiate between the two cell types, based on differences in their growing behavior, which depended on the specific ligand presented by the gold particle. Indeed, REF WT-52 did not grow on L1-activated substrates, but grew normally on RGD-activated ones. In sharp contrast, PC 12-27 cells adhered to L1-activated substrates, and formed cell clusters mediated by the L1 protein. However, they were unable to adhere to the RGD-activated substrates. These cell experiments demonstrate the capability of the artificial ECM to preferentially target certain cell types by bioactivating the material adequately.

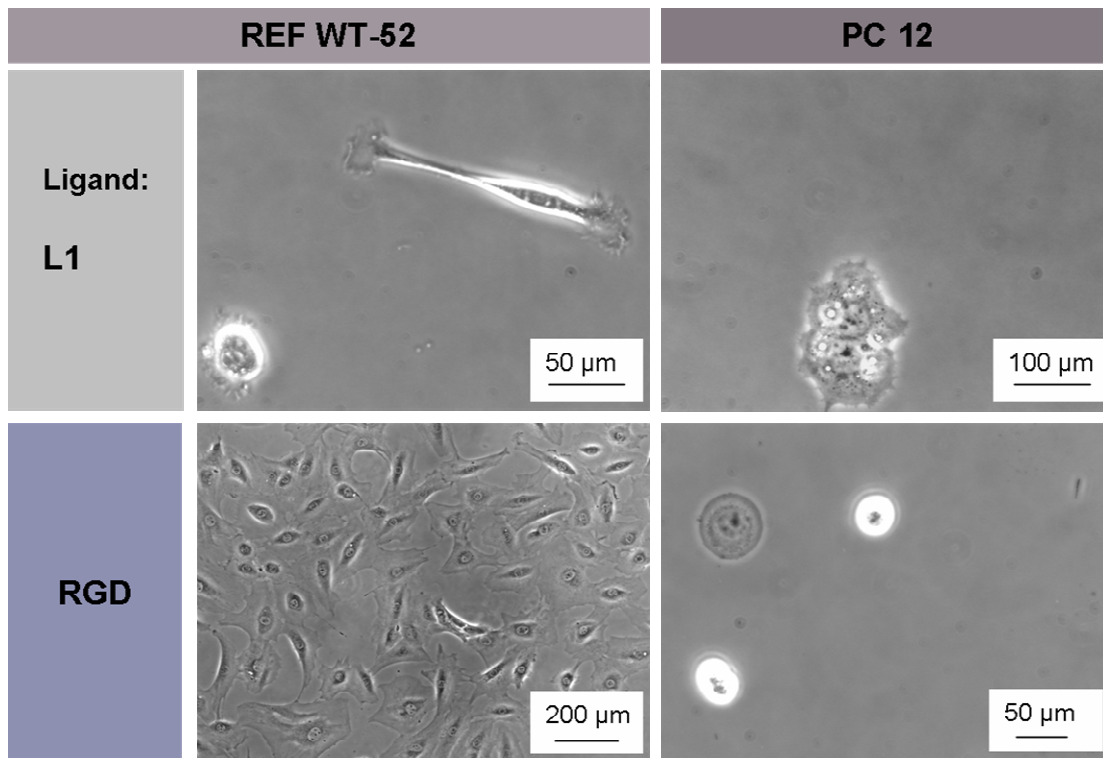


Fig. 71: Phase contrast images of REF WT-52 fibroblasts (left) and PC 12-27 cells (right) on gold nanopatterned PEG 700 hydrogels, incubated with protein L1 (top), or RGD peptides (bottom) after 24 h in culture. The inter-gold particle distance is 50 nm.

Influence of hydrogel rigidity on cell growth

The third crucial parameter of artificial ECMs concerns their mechanical properties; namely, their elasticity. The new transfer lithography technique enables the transfer of nanopatterns onto soft and organic materials. Using this type of lithography, it is now possible to nanopattern materials which are so soft that adhering cells can deform it, just as is the case for natural, hyaluronic acid-based ECMs (Sections III.1.2 and III.3.1).

To simply visualize the effect of substrate deformation by adhering cells, fibroblasts were seeded on micropatterned and RGD-functionalized PEG 20,000 hydrogels, the softest hydrogels hitherto developed for transfer lithography. The softness of such a hydrogel lies in the lower range of Young's moduli, a range typically preferred by various cell types. Fibroblasts, known to prefer stiffer surfaces for growth, are also expected to be capable of deforming such soft surfaces upon adhesion to them. As can be seen in the light microscope image shown in Fig. 72a, and schematically depicted for clarification in Fig. 72b, the fibroblast modifies the regular gold micropattern by differential deformation of the inter-particle distances.

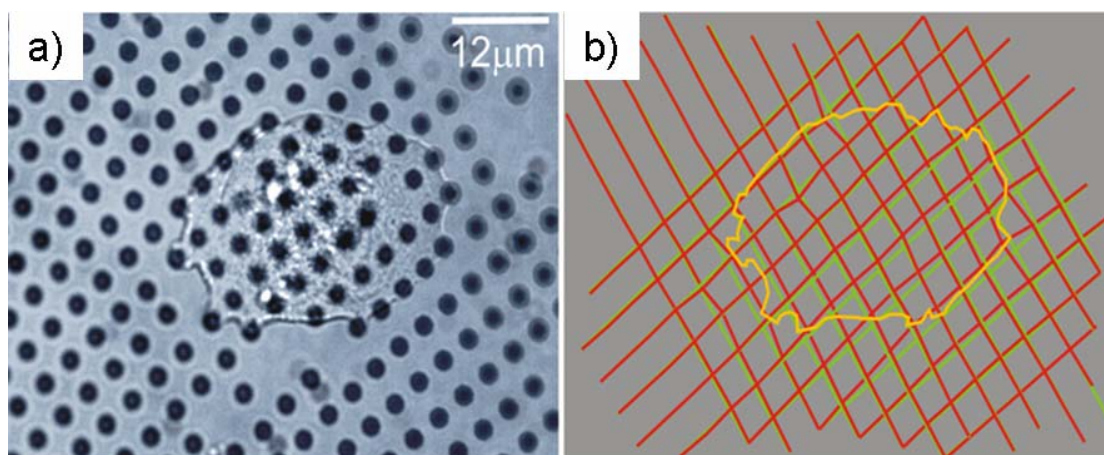


Fig. 72: (a) Light microscopy image of a fibroblast adhering to a soft PEG 20,000 hydrogel decorated with a gold micropattern. Regions to which the cell adheres are deformed. (b) Scheme to more clearly visualize the deformation shown in (a). Green lines indicate the original pattern, red lines the deformed pattern, and the yellow curve, the cell counter line.

As a proof of concept, fibroblasts were also seeded on RGD-functionalized gold nanopatterned PEG 20,000 hydrogels. Fig. 73 shows cryo-SEM images, revealing the strong deformation of the hydrogel surface by the adhering cells. The deformation provides evidence of direct, mechanical crosstalk between the cells and their environment, and mediated by the bioactivated gold pattern.

In principle, the mechanical stress to which the adhering cell subjects the surface can be quantified by the change in the inter-particle distance of the regular gold pattern. However, our preliminary experiments were carried out on substrates with insufficient regularity, caused by the use of a micellar solution of low quality for dipping the initial glass substrates. The same experiments on hydrogel substrates with improved regularity are currently underway.

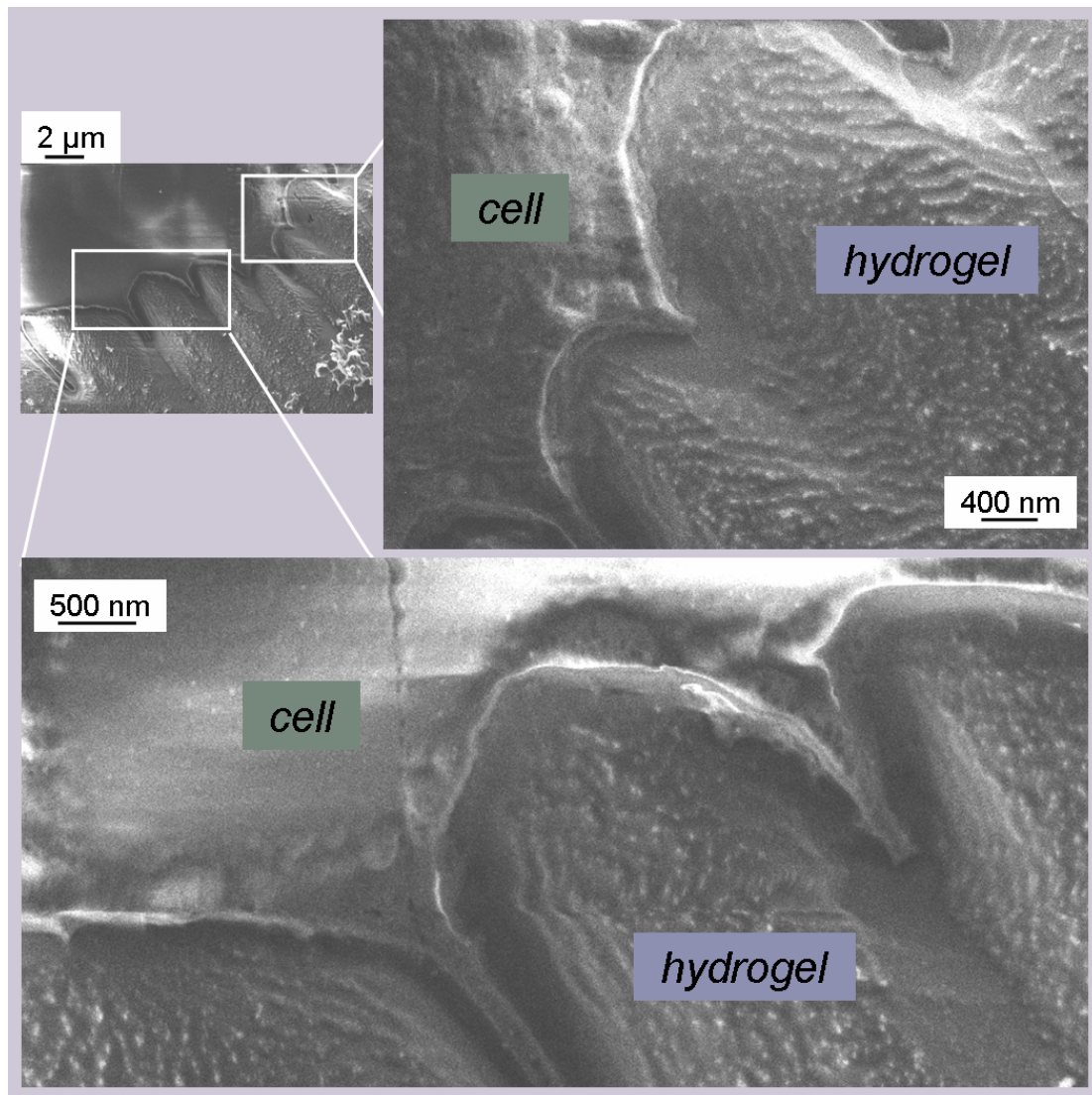


Fig. 73: Cryo-SEM images of fibroblasts cultured on PEG 20,000 hydrogels for 24 hours. Deformation of the soft hydrogel surface is clearly visible.

Cell cultures in hydrogel channels

Non-planar artificial ECMs such as microchannels, which can function as a cellular environment in three dimensions, have been developed by modifying the transfer lithography and chemical modification protocols of planar materials, as described in Chapter VI. Cell adsorption to the internal, curved side of the obtained microchannels was found, as expected (Fig. 74 a) and was tested herein with HeLa cells.

To biofunctionalize the channels, a solution of RGD was sucked into the channels with a syringe. The channels were then incubated for 1 h. After intensive rinsing with water, HeLa cells were seeded in the channels and cultured for 24 h. Fig. 74 b and c show images of the nanopatterned hydrogel tubes with cells adhered to them. The design of nanostructured tubes and their application to cell experiments suggest that

transfer nanolithography can serve as an adequate tool for the design of artificial, three-dimensional nanopatterned substrates for cell adhesion experiments.

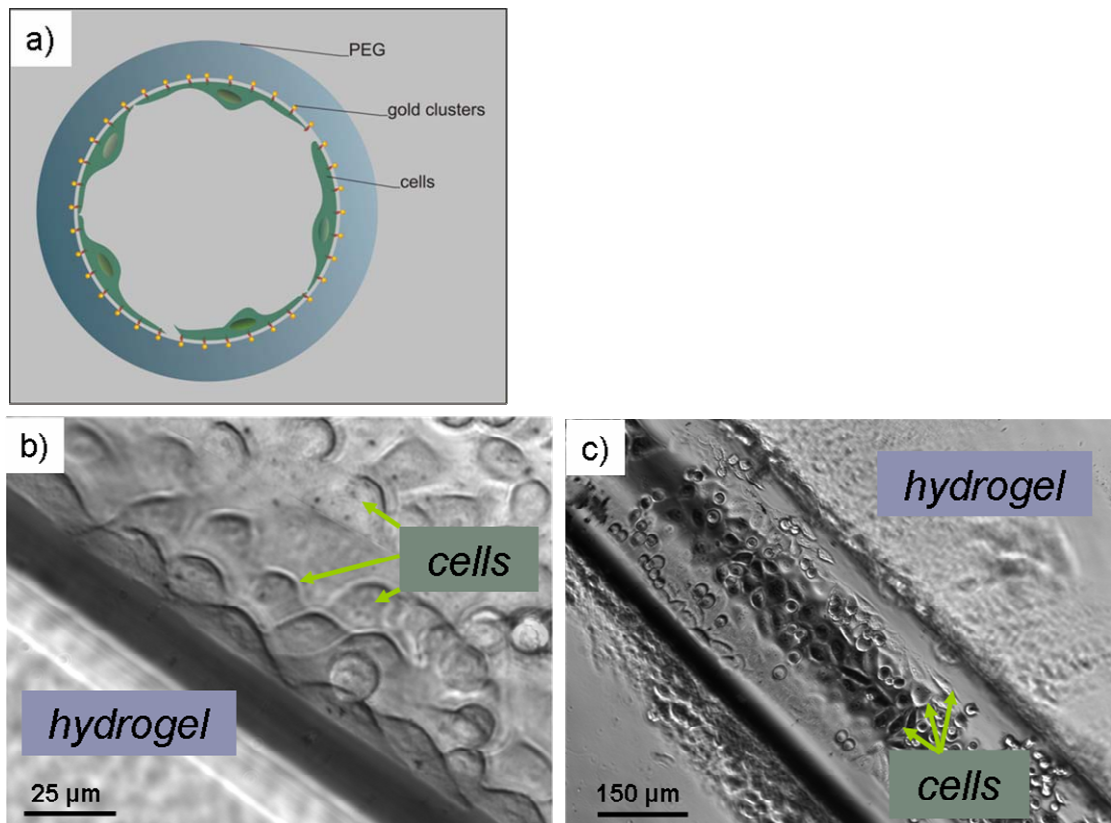


Fig. 74: Cell experiments on hydrogel microchannels. (a) Schematic drawing of fibroblasts adhering to the nanopatterned internal, curved channel side. (b-c) Light microscope image of the channel through the hydrogel. The transparent hydrogel enables internal observation of the cells, without physically opening the channel.

VIII.3. Conclusion

The major feature of the artificial ECM developed in this study is its modular architecture. The three components are the basic hydrogel, the gold nanopattern, and the subsequent modification of both to accomplish bioactivation. The adjustment of the properties of the ECM-mimicking material allows the investigation of specific cells, with regard to questions concerning their function. As a prerequisite for cell biology studies of this sort, the general applicability and functionality of the new three-component material was tested, and our findings described in this chapter.

First, cryo-SEM proved suitable for observing the cell-substrate interactions at a resolution at which single adhesion clusters on functionalized gold particles could be seen. Secondly, the materials utilized in the modules, including the newly-introduced molecules for chemical modifications, were not found to be cytotoxic. However, because cytotoxic reactants were used for some of the modification steps, extensive washing was required. Non-cytotoxicity was combined with a hydrogel whose inert

state endured, even over time, to guarantee a well-defined interaction pattern between the cell and the substrate. Thirdly, the functionality of the three different components was assessed. Results seen with different gold nanopatterns, as well as varying chemical modifications leading to bioactivation obtained with nanopatterned glass surfaces, were reproduced on corresponding hydrogel substrates; cell adhesion was also shown within hydrogel channels.

For the first time, cell adhesion to any nanopatterned polymeric material can now be studied. This includes hydrogels as soft as the natural cell environment, which can be designed so as to offer to the cell binding ligands with defined spacing. In this study, very soft gels were shown, in principle, to be manageable. Elasticities accessible by means of the polymerization and transfer lithography procedures lie within an appropriate order of magnitude for deformation by the adhering cells. For example, fibroblasts are known to preferentially grow on relatively stiff materials (Young's moduli higher than 3,000 Pa; see Section III.3.1). As expected, our experiments demonstrate that they do not deform stiff hydrogels (PEG 700), but do deform substrates with lower Young's moduli, (e.g., PEG 20,000 hydrogels) when adhering to them.

As a next step, adjustments to the properties of all three modules, with respect to cellular function, shall be combined. How does the cell react toward changes in the gold particle distance at different elasticities of the underlying hydrogel, and what is the associated degree of deformation of the substrate by the cell? How are these adhesion properties related to the bio-activation of the gold and hydrogel surfaces offered to the cell? What are the different adhesive forces acting on the various cell types, given a certain biofunctionalization of the adhesion sites? These and related questions may be answered in subsequent experiments which make use of our novel modular artificial ECMs.

IX. Conclusion and future plans

Cell function and behavior are tightly coupled to the interaction of the cell with its environment, the extracellular matrix (ECM). In order to understand and program cell function, it is necessary to design model systems which enable near-perfect control over the mechanical, structural, and chemical parameters which determine its properties.

This thesis aimed at the design of molecularly-defined cell matrices whose stiffness and cellular ligand presentation (both geometry and chemistry) could be controlled. The synthetic material employed in these studies was based on polyethylene glycol (PEG) but could be readily extended to different polymer systems. Ligand or signaling molecule presentation was accomplished either by binding molecules directly to the PEG hydrogels, or by patterning the hydrogel surface with gold nanoparticles. Patterning with gold nanoparticles was based on block copolymer micelle nanolithography transferred to PEG hydrogels. Each individual gold nanoparticle was a potential candidate for immobilizing a single biomolecule. The approach for biofunctionalized nanopatterned hydrogels presented herein also enabled the formation of quasi-three dimensional matrices such as hydrogel tubes.

The three modules, the hydrogel, the gold nanopattern, and the bioactivation, have been developed such that, in principle, they could be readily available within a range of bio-relevant properties, such as hydrogel elasticity or distance between gold particles at the nanoscale. A next step would be to further characterize and refine these modules, to optimize the artificial ECM in terms of its ability to mimic the functioning of the natural ECM, and its usefulness in analyzing cell behavior at the molecular level. To enhance the mechanical properties of the hydrogel, for example, dextrane could be copolymerized with the PEG hydrogel, in order to mimic the elastin present in the natural hyaluron ECM, thereby reducing its brittleness (for details, see Section III.1.2). For this purpose, dextrane molecules carrying methacrylate groups could be mixed with PEG macromers prior to photo-polymerization, resulting in the covalent incorporation of dextrane into the hydrogel network.

The basic material chosen for our artificial ECM, the PEG hydrogel, is not without problems regarding its handling in cell experiments and its examination by means of high-resolution light microscopy. Soft gels are difficult to hold, to transfer between surfaces, and to stretch in stretching experiments (see below). Thus far, nanopatterned and PEG-passivated glass substrates have been used for these kinds of cell studies; however, such substrates lose their biologically inert character in long-term experiments. A straightforward solution to this problem would be the chemical fixation of the substrates on glass cover slides or, to enable stretching, on PDMS films. This would require the preparation of hydrogels with thicknesses at the micrometer scale, and an appropriate fixation route. Developments along these lines involving the activation of glass or PDMS surfaces with an oxygen plasma and

subsequent silanization to bind the hydrogel, are already under way, and will be continued in the future.

Regarding the structural properties of the ECM, the periodicity of the gold structure following transfer to the hydrogel has yet to be quantified. Another issue which must be addressed concerns the embedding of the gold particles into the hydrogels. At what depth are the gold particles embedded into the gels; i.e., how accessible are they to cells wishing to adhere? Does the mechanical stability of the gold particle-hydrogel bond suffice to bear the stress load of cell adhesion clusters? AFM experiments will be performed to measure the surface profile around the embedded gold particles. The accessibility of the gold particles to cell adhesion receptors can also be more directly assessed by incubating the protein-functionalized, nanopatterned surface with gold particles carrying respective antibodies, and visualizing the gold particles, by means of cryo-SEM. The mechanical stability of the bond between the gold and the hydrogel will be further tested in cell experiments, by measuring the extent of defects in the nanopattern, caused by adhering cells eventually pulling single gold particles from the surface.

The chemical properties of the artificial ECM are, on the one hand, well-defined by the bio-functionalizing molecules, and on the other hand by the inertness of PEG to protein adsorption. However, these same properties might be altered during cell experiments, by either the cell and/or the cell medium. The adsorption of expressed ECM proteins such as fibronectin and collagen on the PEG surface remains to be characterized in terms of time scale, quantity and other associated changes in the cell-surface interaction. In addition, the diffusion behavior of proteins and nutrition molecules through the hydrogel meshwork remains to be elucidated. Proteins and other molecules both on the surface and within the gel could be analyzed by immunofluorescence staining of the respective ECM proteins, as well as by other means of detection.

Biofunctionalization was hitherto performed with selected peptides and proteins as a proof of concept; in the future, it will be extended to other biomolecules of interest. An important next step will be to combine two biofunctions, by chemically modifying both the gold particles and the hydrogel surface in between. In this way, the crosstalk between adhesion receptors targeted by receptor-binding molecules coupled to the gold, and other cell membrane receptors targeted by receptor-binding molecules coupled to the hydrogel, could be revealed. An obvious combination of two biofunctions for this purpose would be the RGD peptide bound to the gold particles, together with epidermal growth factor (EGF) proteins filling up the space on the hydrogel surface between the gold particles, or vice versa. Cell experiments using just such an artificial ECM with varying distances between the gold particles would reveal how the adhesion receptor clustering controlled by the nanopattern, influences the function of receptors for cell growth factors. Another application of the artificial ECM, making use of hydrogel softness, involves the design of surfaces specific for

neuronal tissue. Neuronal cells prefer a highly elastic environment for growth (see Section III.3.1) and express $\alpha_1\beta_3$ integrin receptors, which can be specifically addressed by the integrin-binding domain IKVAV. By coupling IKVAV to the gold nanopatterns found on the artificial ECM, the preferential distance of $\alpha_1\beta_3$ integrins for clustering at adhesion sites, and the softness of PEG hydrogels optimally supporting neurite growth, could be determined, and subsequently utilized for surfaces specifically tailored to neuron cell adhesion and growth. The resulting artificial ECM would be capable of promoting the growth of neurons while hampering, for example, fibroblast growth, thereby differentiating between cell types.

The formation of cell adhesion clusters is believed to be a pre-condition for the deformation of the ECM by the adhering cell. To test this hypothesis, artificial ECM substrates characterized by different ligand distances to control the formation of the adhesion clusters, and by different softness to vary the degree of deformation, shall be designed. Once they have formed adhesion clusters, fibroblasts presumably generate stronger forces acting on the substrate surfaces than do neurons, which would explain why fibroblasts, rather than neurons, prefer to grow on solid substrates. Furthermore, the degree of deformation of the surface could be analyzed as a function of substrate elasticities, in order to quantify the molecular forces generated by the cell at adhesion receptor clusters. The method of choice for this purpose would be cryo-scanning electron microscopy.

Another parameter influencing cell behavior, as yet unexamined, is the application of external forces onto the cell-ECM system. Hydrogel substrates can be stretched laterally, in order to subject the cell adhesion sites to mechanical stress. The dependence of adhesion receptor cluster formation on external force, and the resulting, albeit temporary, change in the gold particle distance could be investigated. Such studies would provide insights into the dynamics of cell adhesion clusters and cytoskeletal architecture which, *in vivo* as well as *in vitro*, are dynamically altered during tissue deformation and reorganization. Another *in vivo* scenario in which cells are mechanically stressed concerns the shear flow present in blood vessels, which acts on blood vessel cells such as erythrocytes, endothelial cells, or progenitor cells. Blood vessels, and the shear flow within them, could be mimicked by means of nanopatterned microchannels. In this manner, adhesion behavior and cell growth in blood vessel systems could be investigated, in order to understand, for example, the malfunctioning cell growth at stents interfaces (blood vessel implants).

In general, our next line of research will focus on the systematic screening of the different parameters c i.e., mechanical, structural and chemical properties – of the artificial ECM, including the examples described above. While structured surfaces at the microscale have been previously applied to cell experiments, our subsequent efforts will be aimed at addressing the functions of single adhesion molecules and clusters, in order to understand and to influence their assembly microscopically; i.e.,

at the nanoscale. The modular artificial ECM developed herein provides suitable tools for these purposes.

X. Materials

Chemicals

acryloylchloride	Sigma-Aldrich
cysteamine	Sigma-Aldrich
2-carboxyethylacrylate	Sigma-Aldrich
c[RGDfK(Ahx-Mpa)] and c[RGDfK(Ahx-Apa)] were kindly provided by Jörg Auernheimer and Prof. Horst Kessler, TU Munich.	
dithiobis(succinimidyl)propionate (DTSP)	Sigma-Aldrich
DMEM	Gibco
epoxyresin (Glycidether 100 or Epon 812)	Carl Roth
FBS	Gibco
His-tagged GFP was kindly provided by Dr. Thomas Surrey, EMBL Heidelberg	
His-tagged L1	R&D Systems
Horse Serum	Gibco
hydrogen peroxide p.a.	Merck
hydrogen tetrachloroaurate(III) trihydrate, 99.9%	Sigma-Aldrich
4-(2-hydroxyethoxy)phenyl-(2-hydroxy-2-propyl) ketone (Irgacure 2959)	Sigma-Aldrich
L-glutamine	Gibco
methanol	Sigma-Aldrich
N, N-Diisopropylethylamine (DIPEA)	Sigma-Aldrich
N-hydroxysuccinimide (NHS)	Sigma-Aldrich
N-(3-Dimethylaminopropyl)-N'-ethylcarbodiimide hydrochloride (EDAC)	Sigma-Aldrich
MilliQ water ($R \geq 18 M\Omega$)	Millipore
NiCl ₂	Sigma-Aldrich
N α ,N α -bis(carboxymethyl)-L-lysine (ANTA)	Sigma-Aldrich
PBS (sterile)	Gibco
PEG-DA (700)	Sigma-Aldrich
PEG-DA (other molecular weights), PEG (Mw 40,000 g/mol) dithiol was kindly provided by Prof. J. D. Ding, Fudan University, Shanghai, P.R. China	

poly(dimethyl siloxane) (PDMS) Sylgard 184	Dow Corning
polystyrene(x)-block-poly(2-vinylpyridine)(y)	(PolymerSource)
propenethiol	Fluka
sulphuric acid	Carl Roth
toluene, p.a.	Merck
trypsin-EDTA 2.5%	Gibco
trypan blue	Sigma-Aldrich

Materials

Cantilever (OMCL-AC 160TS-W2, OMCL-TR400PSA-HW)	Olympus
Glass cover slides	Carl Roth
Glass Fibers	Fiberlogix

Equipment

Atomic force microscope (MFP-3D)	Asylum Research
Cryo set up for SEM and sputter devices	Bal-Tec
Image acquisition CCD camera (AxioCam MRm)	Zeiss
Light microscope (Axiovert 25 or Axioplan 2)	Zeiss
objectives (10x/0.25 Ph1 A-plan or 20x/0.45 Ph2 A-plan)	Zeiss
Scanning electron microscope (Ultra 55)	Zeiss
Plasma (TEPLA E-100)	PVA TePLA
UV light (wavelength 366 nm, intensity 1200 $\mu\text{w}/\text{cm}^2$)	Carl Roth

XI. Acknowledgments

The research for this thesis was encouraged and supported by a number of people, to whom I would like to express my gratitude.

First and foremost, I would like to thank Prof. Dr. Joachim Spatz, for manifold reasons. I was privileged to join his group as a diploma student at the University of Heidelberg, and to continue my studies into the behavior of cells at gold-patterned surfaces as a Ph.D. student. I thank Joachim for his suggestion that I extend the technique of gold nanolithography to polymer materials, as a step toward the design and construction of artificial ECMs. It was his steady support of my plans to carry out part of my research at Fudan University, Shanghai, China, that finally enabled me to do so. He backed my efforts at all time, in Heidelberg and in Stuttgart, as well as long-distance, during the time I spent in Shanghai. Our discussions were always instructive, stimulating, and motivating. Along with his support, came the freedom to follow my own ideas.

As stated above, this work was partially carried out in collaboration with Prof. Jiandong Ding and his group at Fudan University, Shanghai, P. R. China. I thank Prof. Ding for accepting me into his group as a guest researcher, and for his helpful advice. I also gratefully acknowledge the warm welcome and great support by his group.

I am most thankful to the entire Biophysical Chemistry Department at the University of Heidelberg, both current and former members, for their ongoing and essential support, particularly during my stays at Fudan University, and including the many probes sent over to Shanghai. In that connection, I would especially like to name Alexandre Micoulet, Ada Cavalcanti-Adam, Jacques Blümmel, Jens Ulmer, Marco Arnold, and Roman Glass.

I also wish to express my appreciation to the members of the Department of New Materials and Biosystems at the Max-Planck-Institute for Metals Research in Stuttgart. All were very supportive, in and amongst the reconstruction work in the newly set-up laboratories. Here, I would specifically like to thank Raquel Martin, Marco Schwieder, Francesca Corbellini, and Ralf Kemkemer.

This research could never have been carried out as such, without the contributions of many of my colleagues on the experimental side. With Francesca Corbellini, we worked on the coupling of L1 and related cell experiments. Nicole Rauch helped me to carry out the elasticity measurements of hydrogels of different macromer lengths. Nadine Perschmann optimized the preparation of the nanopatterned hydrogel channels, and performed cell experiments in the channels. Julia Schölermann contributed to the development of the transfer lithography technique, and to the hydrogel characterizations. Nanostructures were prepared by Sabine Oberhansel. I am indebted to my co-workers, for contributing in one form or another to my thesis, for

our fruitful collaborations, for the stimulating discussions, and for providing an excellent working atmosphere.

I sincerely thank my parents, for giving me the opportunity to follow my interests and concentrate on my studies, and for encouraging and backing me all along.

Finally, I thank my wife, Frauke Gräter, for the great times we have had during the past ten years together in Tübingen, Heidelberg and Shanghai, Göttingen and Stuttgart. Her neverending humor, energy, and creativity helped me to endure the difficulties of study, and energized our shared existence.

XII. Bibliography

- ¹ B. T. Estes, J. M. Gimble, F. Guilak. Mechanical signals as regulators of stem cell fate. *Curr Top Dev Biol.* 60 (2004) 91-126.
- ² J. S. Park, J. S. Chu, C. Cheng, F. Chen, D. Chen, S. Li. Differential effects of equiaxial and uniaxial strain on mesenchymal stem cells. *Biotechnol Bioeng.* 88 (2004) 359-368.
- ³ T. Okano-Uchida, T. Himi, Y. Komiya, Y. Ishizaki. Cerebellar granule cell precursors can differentiate into astroglial cells, *Proc Natl Acad Sci.*, 101 (2004) 1211-1216.
- ⁴ P. C. Georges, W. J. Miller, D. F. Meaney, E. S. Sawyer, P. A. Janmey. Matrices with compliance comparable to that of brain tissue select neuronal over glial growth in mixed cortical cultures. *Biophys J.* 90 (2006) 3012-3018.
- ⁵ M. Cehreli, S. Sahin, K. Akca. Role of mechanical environment and implant design on bone tissue differentiation: current knowledge and future contexts. *J Dent.* 32 (2004) 123-132.
- ⁶ S. P. Massia, M. M. Holecko, G. R. Ehteshami. In vitro assessment of bioactive coatings for neural implant applications. *J Biomed Mater Res A.* 68 (2004) 177-186.
- ⁷ A. V. Tutter, G. A. Baltus, S. Kadam. Embryonic stem cells: a great hope for a new era of medicine. *Curr Opin Drug Discov Devel.* 2 (2006) 169-175
- ⁸ A. K. Moore, I. R. Lemischka. Stem cells and their niches. *Science.* 311 (2006) 1880-1885.
- ⁹ W. N. E. van Dijk-Wolthuis, P. van de Wetering, W. L. J. Hinrichs, L. J. F. Hofmeyer, R. M. J. Liskamp, D. J. A. Crommelin, and W. E. Hennink. A Versatile Method for the Conjugation of Proteins and Peptides to Poly[2-(dimethylamino)ethyl methacrylate]. *Bioconjugate Chem.*, 10 (1999) 687-692
- ¹⁰ C. Ploetz, E. I. Zycband. D. E. Birk. Collagen fibril assembly and deposition in the developing dermis: segmental deposition in extracellular compartments. *J. Struct. Biol.*, 106 (1991) 73-81
- ¹¹ C. H. Streuli, M. J. Bissell. Expression of extra cellular matrix components is regulated by substratum. *J. Cell Biol.*, 110 (1990) 1405-1415
- ¹² E. Ruoslahti, B. Oerbrink. Common principles in cell adhesion. *Exp. Cell Res.*, 227 (1996) 1-11.
- ¹³ H. M. Blau, D. Baltimore. Differentiation requires continuous regulation. *J. Cell Biol.*, 112 (1991) 781-783.
- ¹⁴ K. Salchert, U. Streller, T. Pompe, N. Herold, M. Grimmer, C. Werner. In vitro reconstitution of fibrillar collagen type I assemblies at reactive polymer surfaces. *Biomacromolecules* 5 (2004) 1340-1350
- ¹⁵ J. D. Watson, K. Roberts, M. Raff, J. Lewis, D. Brau, B. Alberts. *Molekularbiologie der Zelle* 3. Aufl. (1995) VCH Weinheim. 1165
- ¹⁶ D. R. Moshier (Hgb). *Fibronectin*. Academic Press (1988). New York
- ¹⁷ E. Ruoslahti, M. D. Pierschbacher. New perspectives in cell adhesion: RGD and integrins. *Science*, 238 (1987) 491-497
- ¹⁸ K. M. Yamada, D. W. Kennedy. Dualistic nature of adhesive protein function: fibronectin and its biologically active peptide fragments can autoinhibit fibronectin function. *J. Cell. Biol.*, 24 (1984) 99

- ¹⁹ M. D. Pierschbacher, E. Ruoslahti. Cell attachment activity of fibronectin can be duplicated by small synthetic fragments of the molecule. *Nature*, 30 (1984) 309
- ²⁰ M. Pfaff, K. Tangemann, B. Müller, M. Gurrath, G. Müller, H. Kessler, R. Timpl, J. Engel. Selective recognition of cyclic RGD peptides of NMR defined conformation by alpha IIb beta 3, alpha V beta 3, and alpha 5 beta 1 integrins. *J. Biol. Chem.*, 269 (1994) 20233
- ²¹ G. Baneyx, L. Baugh, V. Vogel. Fibronectin extension and unfolding within cell matrix fibrils controlled by cytoskeletal tension. *Proc Natl Acad Sci U S A.* 99 (2002) 5139-43.
- ²² G. Baneyx, L. Baugh, V. Vogel. Coexisting conformations of fibronectin in cell culture imaged using fluorescence resonance energy transfer. *Proc Natl Acad Sci U S A.* 98 (2001) 14464-8.
- ²³ S. E. D'Souza, M. H. Ginsberg, E. F. Plow. Arginyl-glycyl-aspartic acid (RGD): a cell adhesion motif. *Trends Biochem. Sci.*, 21 (1991) 246
- ²⁴ T. Pompe, L. Renner, C. Werner. Nanoscale features of fibronectin fibrillogenesis depend on protein-substrate interaction and cytoskeleton structure. *Biophys. J.*, 88 (2005) 527-534.
- ²⁵ R. Martin, M. E. Ackerman, T. Volberg, B. Geiger, E. Ruoslahti, D. Hanein. Unraveling The Early Steps in Fibronectin Fiber Formation. *J. Mol. Biol.* in print.
- ²⁶ M. Cohen, E. Klein, B. Geiger, L. Addadi. Organization and adhesive properties of the hyaluronan pericellular coat of chondrocytes and epithelial cells. *Biophys. J.*, 85 (2003) 1996–2005.
- ²⁷ M. Cohen, Z. Kam, L. Addadi, B. Geiger. Dynamic study of the transition from hyaluronan- to integrin-mediated adhesion in chondrocytes. *EMBO J.* 25 (2006) 302-11.
- ²⁸ D. W. Urry, T. Hugel, M. Seitz, H. E. Gaub, L. Sheiba, J. Dea, J. Xu, T. Parker. Elastin: a representative ideal protein elastomer. *Philos Trans R Soc Lond B Biol Sci.* 357 (2002) 169-84.
- ²⁹ M. V. Nermut, N. Green, P. Eason, S. S. Yamada, K. M. Yamada. Electron microscopy and structural model of human fibronectin receptor. *EMBO J.*, 7 (1988) 4093–4099.
- ³⁰ J. P. Xiong, T. Stehle, B. Diefenbach, R. Zhang, R. Dunker, D. Scott, A. Joachimiak, S. L. Goodman, M. A. Arnaout. Crystal structure of the extra cellular segment of integrin $\alpha V\beta 3$. *Science*, 294 (2001) 339–345.
- ³¹ U. Hersel, C. Dahmen, H. Kessler. RGD Modified Polymers: Biomaterials for Stimulated Cell Adhesion *Biomaterials*, 24 (2003) 4385-4415
- ³² M. Kim, C. V. Carman, T. A. Springer, Bidirectional transmembrane signaling by cytoplasmic domain separation in integrins. *Science*, 301 (2003) 1720–1725.
- ³³ J. Takagi, B. M. Petre, T. Walz, T. A. Springer. Global conformational rearrangements in integrin extra cellular domains in outside-in and inside-out signaling. *Cell*, 110 (2002) 599–611.
- ³⁴ R. Li, C. R. Babu, J. D. Lear, A. J. Wand, J. S. Bennett, W. F. DeGrado. Oligomerization of the integrin $\alpha IIb\beta 3$: roles of the transmembrane and cytoplasmic domains. *Proc. Natl. Acad. Sci. U. S. A.*, 98 (2001) 12462–12467.
- ³⁵ R. Li, N. Mitra, H. Gratkowski, G. Vilaire, R. Litvinov, C. Nagasami, J. W. Weisel, J. D. Lear, W. F. DeGrado, J. S. Bennett. Activation of integrin $\alpha IIb\beta 3$ by modulation of transmembrane helix associations. *Science*, 300 (2003) 795–798.
- ³⁶ J. C. Adams. Cell-matrix contact structures. *Cell. Mol. Life Sci.*, 58 (2001) 371–392.

- ³⁷ I. I. Singer, S. Scott, D. W. Kawka, D. M. Kazazis, J. Gailit, E. Ruoslahti. Cell surface distribution of fibronectin and vitronectin receptors depends on substrate composition and extra cellular matrix accumulation. *J. Cell Biol.*, 106 (1998) 2171–2182.
- ³⁸ N.J. Boudreau, P.L. Jones. Extra cellular matrix and integrin signalling: the shape of things to come. *Biochem. J.*, 339 (1999) 481
- ³⁹ D. Riveline, E. Zamir, N. Q. Balaban, U. S. Schwarz, T. Ishizaki, S. Narumiya, Z. Kam, B. Geiger, A. D. Bershadsky. Focal Contacts as Mechanosensors: Externally Applied Local Mechanical Force Induces Growth of Focal Contacts by an mDial-dependent and ROCK-independent Mechanism. *The Journal of Cell Biology*, 153 (2001) 1175–1185
- ⁴⁰ D. Stopak, A. K. Harris. Connective tissue morphogenesis by fibroblast traction. I. Tissue culture observations. *Dev. Biol.*, 90 (1982) 383–398
- ⁴¹ T. Yeung, P. C. Georges, L. A. Flanagan, B. Marg, M. Ortiz, M. Funaki, N. Zahir, W. Ming, V. Weaver, P. A. Janmey. Effects of Substrate Stiffness on Cell Morphology, Cytoskeletal Structure, and Adhesion. *Cell Motility and the Cytoskeleton*, 60 (2005) 24–34
- ⁴² P. C. Georges, W. J. Miller, D. F. Meaney, E. Sawyer, P. A. Janmey. Matrices with compliance comparable to that of brain tissue select neuronal over glial growth in mixed cortical cultures. *Biophys J.*, (2006) 1529
- ⁴³ P. C. Georges, P. A. Janmey. Cell type-specific response to growth on soft materials. *Journal of Applied Physiology*, 98 (2005) 1547–1553
- ⁴⁴ R. J. Pelham, Y. Wang. Fibroblasts and epithelial cells. *Proc. Natl. Acad. Sci.*, 94 (1997) 13661
- ⁴⁵ D. E. Ingber. Mechanosensation through integrins: Cells act locally but think globally. *PNAS*, 100 (2003) 1472–1474
- ⁴⁶ U. S. Schwarz, N. Q. Balaban, D. Riveline, A. Bershadsky, B. Geiger, S. A. Safran, Calculation of Forces at Focal Adhesions from Elastic Substrate Data: The Effect of Localized Force and the Need for Regularization. *Biophysical Journal*, 83 (2002) 1380–1394
- ⁴⁷ M. A. Wozniak, R. Desai, P. A. Solski, C. J. Der, P. J. Keely. ROCK-generated contractility regulates breast epithelial cell differentiation in response to the physical properties of a three-dimensional collagen matrix. *The Journal of Cell Biology*, 163 (2003) 583–595
- ⁴⁸ G. H. Altman, R. L. Horan, I. Martin, J. Farhadi, P. R. H. Stark, V. Volloch, J. C. Richmond, G. Vunjak-Novakovic, D. L. Kaplan. Cell differentiation by mechanical stress. *FASEB J.*, 16 (2002) 270
- ⁴⁹ K. Endlich. Podocytes respond to mechanical stress in vitro. *J. Am. Soc. Nephrol.*, 12 (2001) 413–422
- ⁵⁰ O. Akhouayri, M. Lafage-Proust, A. Rattner, N. Laroche, A. Caillot-Augusseau, C. Alexandre, L. Vico. Effects of Static or Dynamic Mechanical Stresses on Osteoblast Phenotype Expression in Three-Dimensional Contractile Collagen Gels. *Journal of Cellular Biochemistry*, 76 (1999) 217–230
- ⁵¹ H. Shina, K. Zygourakis, M. C. Farach-Carson, M. J. Yaszemski, A. G. Mikos. Attachment, proliferation, and migration of marrow stromal osteoblasts cultured on biomimetic hydrogels modified with an osteopontin-derived peptide. *Biomaterials*, 25 (2004) 895–906
- ⁵² C. Chung, R. Firtel. Signaling pathways at the leading edge of chemotaxing cells. *J Muscle Res Cell Motil.* 23 (2002) 773–779

- ⁵³ A. Kasza, M. Kowanetz, K. Poslednik, B. Witek, T. Kordula, A. Koj. Epidermal growth factor and pro-inflammatory cytokines regulate the expression of components of plasminogen activation system in U373-MG astrocytoma cells. *Cytokine*, 16 (2001) 187-190
- ⁵⁴ M. Arnold, E. A. Cavalcanti-Adam, R. Glass, J. Blümmel, W. Eck, M. Kantelechner, H. Kessler, J. P. Spatz. Activation of Integrin Function by Nanopatterned Adhesive Interfaces. *Chem. Phys. Chem.*, 5 (2004) 383-388
- ⁵⁵ B. Wojciak-Stothard, A. Curtis, W. Monaghan, K. MacDonald, C. Wilkinson. Guidance and activation of murine macrophages by nanometric scale topography. *Exp. Cell Res.*, 233 (1996) 426-435
- ⁵⁶ J. Y. Wong, A. Velasco, P. Rajagopalan, Q. Pham. Directed Movement of Vascular Smooth Muscle Cells on Gradient-Compliant Hydrogels. *Langmuir*, 19 (2003) 1908-1913
- ⁵⁷ S. Jungbauer, R. Kemkemer, H. Gruler, D. Kaufmann, J. P. Spatz. Cell shape normalization, dendrite orientation, and melanin production of normal and genetically altered (haploinsufficient NF1)-melanocytes by micro-structured substrate interactions. *Chem. Phys. Chem.*, 23 (2004) 85-92.
- ⁵⁸ D. Lehnert, B. Wehrle-Haller, C. David, U. Weiland, C. Ballestrem, B. A. Imhof, M. Bastmeyer. Cell behavior on micro patterned substrata: limits of extra cellular matrix geometry for spreading and adhesion. *Journal of Cell Science*, 117 (2004) 41-52
- ⁵⁹ I. Gotman. Characteristics of metals used in implants. *J. Endourol.*, 11 (1997) 383-389.
- ⁶⁰ J. P. Fisher, D. Dean, P. S. Engel, A. G. Mikos. Photoinitiated polymerization of biomaterials. *Annu. Rev. Mater. Res.*, 31 (2001) 171-181
- ⁶¹ V. Fainerman, E. Lucassen-Reynders, R. Miller. Description of the adsorption behaviour of proteins at water/fluid interfaces in the framework of a two-dimensional solution model. *Adv. Colloid Interface Sci.*, 106 (2003) 237-259
- ⁶² M. Bergkvist, J. Carlsson, S. Oscarsson. Surface-dependent conformations of human plasma fibronectin adsorbed to silica, mica, and hydrophobic surfaces, studied with use of Atomic Force Microscopy. *J. Biomed. Mater. Res. A*, 64 (2003) 349-356
- ⁶³ L. Baugh, V. Vogel. Structural changes of fibronectin adsorbed to model surfaces probed by fluorescence resonance energy transfer. *J. Biomed. Mater. Res. A*, 69 (2004) 525-534
- ⁶⁴ R. Siegel, P. Harder, R. Dahint, M. Grunze, F. Josse, M. Mrksich, G. Whitesides. On-line detection of nonspecific protein adsorption at artificial surfaces. *Anal. Chem.*, 69 (1997) 3321-3328
- ⁶⁵ A. Garcia, M. Vega, D. Boettiger. Modulation of cell proliferation and differentiation through substrate-dependent changes in fibronectin conformation. *Mol. Biol. Cell*, 10 (1999) 785-798
- ⁶⁶ L. Renner, B. Jørgensen, M. Markowski, K. Salchert, C. Werner, T. Pompe. Control of fibronectin displacement on polymer substrates to influence endothelial cell behaviour. *J. Mater. Sci. Mater. Med.*, 15 (2004) 387-390
- ⁶⁷ N. Tooney, M. Mosesson, D. Amrani, J. Hainfeld, J. Wall. Solution and surface effects on plasma fibronectin structure. *J. Cell Biol.*, 97(1983) 1686-1692
- ⁶⁸ D. Ryan, B. A. Parviz, V. Linder, V. Semetey, S. K. Sia, J. Su, M. Mrksich, G. M. Whitesides. Patterning Multiple Aligned Self-Assembled Monolayers Using Light. *Langmuir*, 20 (2004) 9080-9088

- ⁶⁹ S. M. Cutlera, A. J. Garciab. Engineering cell adhesive surfaces that direct integrin $\alpha 5\beta 1$ binding using a recombinant fragment of fibronectin. *Biomaterials*, 24 (2003) 1759-1770
- ⁷⁰ J. Groll, K. Albrecht, P. Gasteier, S. Riethmueller, U. Ziener, M. Moeller. Nanostructured Ordering of Fluorescent Markers and Single Proteins on Substrates. *Chem. Bio. Chem.*, 6 (2005) 1782-1787
- ⁷¹ N. Levit-Binnun, A. B. Lindner, O. Zik, Z. Eshhar, E. Moses. Quantitative detection of protein arrays. *Anal. Chem.*, 75 (2003) 1436-1441
- ⁷² E. Diamandis, T. Christopoulos. The biotin-(strept)avidin system: principles and applications in biotechnology. *Clin. Chem.*, 37 (1991) 625-636.
- ⁷³ G. Hermanson. *Bioconjugate Techniques*, (1996) 570-592.
- ⁷⁴ M. Mrksich, C. Chen, Y. Xia, L. Dike, D. Ingber, G. Whitesides. Controlling cell attachment on contoured surfaces with self-assembled monolayers of alkanethiolates on gold. *Proc. Natl. Acad. Sci. U S A*, 93 (1996) 10775-10778
- ⁷⁵ Y. Ito, M. Kajihara, Y. Imanishi. Materials for enhancing cell adhesion by immobilization of cell-adhesive peptide. *J. Biomed. Mater. Res.*, 25 (1991) 1325-1337
- ⁷⁶ J. Groll, T. Ameringer, J. P. Spatz, M. Moeller. Ultrathin Coatings from Isocyanate-Terminated Star PEG Prepolymers: Layer Formation and Characterization. *Langmuir*, 21 (2005) 1991-1999
- ⁷⁷ A. L. Gonzalez, A. S. Gobin, J. L. West, L. V. McIntire, C. W. Smith. Integrin Interactions with Immobilized Peptides in Polyethylene Glycol Diacrylate Hydrogels. *Tissue Engineering*, 10 (2004) 1775-1786
- ⁷⁸ A. S. Hoffman. Hydrogels for biomedical applications. *Advanced Drug Delivery Reviews* 43 (2002) 3-12
- ⁷⁹ Photopolymerizable hydrogels for tissue engineering applications, Kytai Truong Nguyen, Jennifer L. West*, *Biomaterials* 23 (2002) 4307-4314
- ⁸⁰ D. Campoccia, P. Doherty, M. Radice, P. Brun, G., Abatangelo, D.F. Williams, Semisynthetic resorbable materials from hyaluronan esterification, *Biomaterials*, 19 (1998) 2101-2127.
- ⁸¹ O. Wichterle, D. Lim, Hydrophilic gels in biologic use, *Nature*, 185 (1960) 117.
- ⁸² B. Muller. Photocrosslinked polymers. Ciba-Geigy Corporation. US Patent, (1995) 286,035
- ⁸³ B. Muller. Photocrosslinked polymers. Ciba Vision Corporation. US Patent, (1996) 678,437
- ⁸⁴ P. Kingshott, H. J. Griesser. Surfaces that resist bioadhesion. *Current Opinion in Solid State and Materials Science*, 4 (1999) 403-412
- ⁸⁵ J. Kim, J. G. Kim, D. Kim, Y. H. Kim. Preparation and Properties of PEG Hydrogel from PEG Macromonomer with Sulphonate End Group *Journal of Applied Polymer Science*, 96 (2005) 56-61
- ⁸⁶ S. H. Kim, C. C. Chu. Synthesis and characterization of dextran-methacrylate hydrogels and structural study by SEM. *J. Biomed. Mater. Res.*, 49 (2000) 517-27
- ⁸⁷ R. S. Kane, S. Takayama, E. Ostuni, D. E. Ingber, G. M. Whitesides. Patterning proteins and cells using soft lithography. *Biomaterials*, 20 (1999) 2363-2376
- ⁸⁸ J. Ulmer. Quantitative Measurements of Force Distribution in Single and Multi Cellular Systems. Dissertation, Universitaet Heidelberg, Juli 2005

- ⁸⁹ G. A. Silva, C. Czeisler, K. L. Niece, E. Beniash, D. A. Harrington, J. A. Kessler, S. I. Stupp. Selective Differentiation of Neural Progenitor Cells by High-Epitope Density Nanofibers. *Science*, 303 (2004) 1352-1355
- ⁹⁰ R. Glass, M. Möller J. P. Spatz. Block copolymer micelle nanolithography. *Nanotechnology*, 14 (2003) 1153-1160
- ⁹¹ L. G. Griffith, G. Naughton. Tissue engineering--current challenges and expanding opportunities. *Science*. 295 (2002) 1009-14.
- ⁹² E. Ruoslahti. RGD and other recognition sequences for integrins. *Annu. Rev. Cell. Dev. Biol.*, 12 (1996) 697-715
- ⁹³ D. L. Hern, J. A. Hubbell. Incorporation of adhesion peptides into nonadhesive hydrogels useful for tissue resurfacing. *J. Biomed. Mater. Res.*, 39 (1998) 266-276
- ⁹⁴ M. Mrksich, G. Whitesides. Using self-assembled monolayers to understand the interactions of man-made surfaces with proteins and cells. *Annu. Rev. Biophys. Biomol. Struct.*, 25 (1996) 55-78
- ⁹⁵ W. S. Dillmore, M. N. Yousaf, M. Mrksich. A photochemical method for patterning the immobilization of ligands and cells to self-assembled monolayers. *Langmuir*, 20 (2004) 7223-7231
- ⁹⁶ D. J. Irvine, A. M. Mayes, L. G. Griffith. Nanoscale clustering of RGD peptides at surfaces using Comb polymers. 1. Synthesis and characterization of Comb thin films. *Biomacromolecules*. 2 (2001) 85-94.
- ⁹⁷ D. J. Irvine, A. V. Ruzette, A. M. Mayes, L. G. Griffith. Nanoscale clustering of RGD peptides at surfaces using comb polymers. 2. Surface segregation of comb polymers in polylactide. *Biomacromolecules* 2 (2001) 545-56.
- ⁹⁸ L. G. Griffith, M. A. Swartz. Capturing complex 3D tissue physiology in vitro. *Nat Rev Mol Cell Biol*. 7 (2006) 211-24.
- ⁹⁹ S. J. Bryant, Charles, R. Nuttelmann, K. S. Anseth. Cytocompatibility of UV and visible light photoinitiating systems on cultured NIH/3T3 fibroblasts in vitro. *J. Biomater. Sci. Polymer*, 11 (2000) 439-457
- ¹⁰⁰ J. E. Elliott, J. W. Anseth, C. N. Bowman. Kinetic modeling of the effect of solvent concentration on primary cyclization during polymerization of multifunctional monomers *Chemical Engineering Science* 56 (2001) 3173-3184
- ¹⁰¹ F. M. Andreopoulos, E. J. Beckman, A. J. Russell. Light-induced tailoring of PEG-hydrogel properties. *Biomaterials*, 19 (1998) 1343-1352
- ¹⁰² S. J. Bryant, K. S. Anseth. Hydrogel properties influence ECM production by chondrocytes photoencapsulated in poly(ethylene glycol) hydrogels. *J. Biomed. Mater. Res.* 59 (2002) 63-72
- ¹⁰³ R. J. Russell, A. C. Axel, K. L. Shields, M. V. Pishko. Mass transfer in rapidly photopolymerized poly(ethylene glycol) hydrogels used for chemical sensing. *Polymer*, 42 (2001) 4893-4901
- ¹⁰⁴ E. Asmussen, A. Peutzfeldt. Influence of selected components on crosslink density in polymer structures. *Eur. J. Oral. Sci.*, 108 (2001) 282-285
- ¹⁰⁵ B. S. Kim, J. S. Hrkach, R. Langer. Biodegradable photo-crosslinked poly(ether-ester) networks for lubricious coatings. *Biomaterials*, 21 (2000) 259-265

- ¹⁰⁶ P. van de Wetering, A. T. Metters, R. G. Schoenmakers, J. A. Hubbell Poly(ethylene glycol) hydrogels formed by conjugate addition with controllable swelling, degradation, and release of pharmaceutically active proteins. *Journal of Controlled Release*, 102 (2005) 619– 627
- ¹⁰⁷ R. E. Mahaffy, C. K. Shih, F. C. MacKintosh, J. Käs. Scanning Probe-Based Frequency-Dependent Microrheology of Polymer Gels and Biological Cells. *Physical Review Letters*, 85 (2000) 880-883
- ¹⁰⁸ S. Lin-Gibson, S. Bencherif, J. A. Cooper, S. J. Wetzel, J. M. Antonucci, B. M. Vogel, F. Horkay, N. R. Washburn. Synthesis and Characterization of PEG Dimethacrylates and Their Hydrogels. *Biomacromolecules*, 5 (2004) 1280-1287
- ¹⁰⁹ T. Canal, N. A. Peppas. Correlation between mesh size and equilibrium degree of swelling of polymeric networks. *J. Biomed. Mater. Res.* 23 (1989) 1183–1193
- ¹¹⁰ E.W. Merrill et al. Partitioning and discussion of solutes in hydrogels of poly(ethylene oxide). *Biomaterials* 14 (1993) 1117-1126.
- ¹¹¹ P. J. Flory. Principles of polymer chemistry. Ithaca, NY. Cornell University Press, (1953)
- ¹¹² K. S. Anseth, C. N. Bowman, L. B. Peppas. Mechanical properties of hydrogels and their experimental determination. *Biomaterials*, 17 (1996) 1647-1657
- ¹¹³ M. Radmacher, J. P. Cleveland, M. Fritz, H. G. Hansma, P. K. Hansma. *Biophys. J.*, 66 (1994) 2159
- ¹¹⁴ F. Benmouna, D. Johannsmann. Viscoelasticity of Gelatin Surfaces Probed by AFM Noise Analysis *Langmuir*, 20 (2004) 188-193
- ¹¹⁵ Y. Tseng, T. P. Kole, D. Wirtz. *Biophys. J.*, 83 (2002) 3162
- ¹¹⁶ M. Antonietti, C. Göltner. Superstructures of functional colloids: chemistry on the nanometer scale. *Angew. Chem. Int. Edit. Engl.*, 36 (1996) 911-928
- ¹¹⁷ P Alivisatos, P. F. Barbara, A. W. Castleman, J. Chang, D. A. Dixon, M. L. Klein, G. L. Mclendon, J. S. Miller, M. A. Ratner, P. J. Rossky, S. I. Stupp, M. E. Thompson. From molecules to materials: current trends and future directions. *Adv. Mater.*, 10 (1998) 1297-1336
- ¹¹⁸ S. A. Harfenist, S. D. Cambron, E. W. Nelson, S. M. Berry, A. W. Isham, M. M. Crain, K. M. Walsh, R. S. Keynton, R. W. Cohn. Direct Drawing of Suspended Filamentary Micro- and Nanostructures from Liquid Polymers. *Nano-Letters* 4 (2004) 1931-1937
- ¹¹⁹ M. Li, J. D. Glawe, H. Green, D. K. Mills, M. J. McShane, B. K. Gale. Effect of High-Aspect-Ratio Micro-structures on Cell Growth and Attachment. *Microtechnologies in Medicine and Biology*, 1st Annual International Conference (2000) 531-536
- ¹²⁰ G.A. Somorjai and Y.G. Borodko. Research in nanosciences – Great opportunity for catalysis science. *Catal. Lett.* 76 (2001)
- ¹²¹ K. B. Lee, S. J. Park, C. A. Mirkin, J. C. Smith, M. Mrksich. Protein nanoarrays generated by dip-pen nanolithography. *Science* 295 (2002) 1702-1705
- ¹²² L. Yan, X. M. Zhao, G. M. Whitesides. Patterning a Preformed, Reactive SAM Using Microcontact Printing. *J. Am. Chem. Soc.*, 120 (1998) 6179-6180
- ¹²³ Y. N. Xia, G. M. Whitesides. Soft Lithography. *Angew. Chem. Int. Ed. Engl.*, 37 (1998) 550-575

- ¹²⁴ E. Delamarche, A. Bernard, H. Schmid, B. Michel, H. Biebuyck. Patterned delivery of immunoglobulins to surfaces using microfluidic networks. *Science*, 276 (1997) 779-781
- ¹²⁵ E. Delamarche, A. Bernard, H. Schmid, A. Bietsch, B. Michel, H. Biebuyck. Microfluidic Networks for Chemical Patterning of Substrates: Design and Application to Bioassays. *J. Am. Chem. Soc.*, 120 (1998) 500-508
- ¹²⁶ H. D. Dörfler. *Grenzflächen und Kolloid-disperse Systeme*. Springer-Verlag Heidelberg, (2002)
- ¹²⁷ J. P. Spatz, S. Sheiko, M. Möller. Substrate-induced lateral micro-phase separation of a diblock copolymer. *Adv. Mater.*, 8 (1996) 513-517
- ¹²⁸ A. P. Gast. Block copolymers at interfaces. NATO ASI Series, Series C: Mathematical and Physical Sciences 303 (1990) 311-312
- ¹²⁹ B. Chu. Structure and dynamics of block copolymer colloids. *Langmuir*, 11 (1995) 414-421
- ¹³⁰ M. Moffitt, K. Khougaz, A. Eisenberg. Micellization of Ionic Block Copolymers. *Accounts Chem. Res.*, 29 (1996) 95-102
- ¹³¹ Z. Gao, X. F. Zhong, A. Eisenberg. Chain dynamics in coronas of ionomer aggregates. *Macromolecules*, 27 (1994) 794-802
- ¹³² S. Förster, M. Zisenis, E. Wenz, M. Antonietti. Micellization of strongly segregated block copolymers. *J. Chem. Phys.*, 104 (1996) 9956-9970
- ¹³³ J. Perrin. Brownian movement and molecular reality. *Annales de Chimie et de Physique* 18 (1909) 5-114
- ¹³⁴ J. P. Spatz, S. Mößmer, M. Möller. Mineralization of gold nano-particles in a block copolymer microemulsion. *Chem. Eur. J.*, 2 (1996) 1552-1555
- ¹³⁵ H. W. Deckman, J. H. Dunsmuir. Natural lithography. *Appl. Phys. Lett.*, 41 (1982) 377-379
- ¹³⁶ A. S. Dimitrov, K. Nagayama. Continuous convective assembling of fine Particles into two-dimensional arrays on solid surfaces. *Langmuir*, 12 (1996) 1303-1311
- ¹³⁷ N. Denkov, O. Velev, P. Kralchevski, I. Ivanov, H. Yoshimura, K. Nagayama. Mechanism of formation of two-dimensional crystals from latex particles on substrates. *Langmuir*, 8 (1992) 3183-3190
- ¹³⁸ N. Denkov, O. Velev, P. Kralchevski, I. Ivanov, H. Yoshimura, K. Nagayama. Two-dimensional crystallization. *Nature*, 361 (1993) 26
- ¹³⁹ V. Paunov, P. Kralchevsky, N. Denkov, K. Nagayama. Lateral capillary forces between floating submillimeter particles. *J. Colloid Interface Sci.*, 157 (1993) 100-112
- ¹⁴⁰ G. Kästle, H. Boyen, F. Weigl, G. Lengel, T. Herzog, P. Ziemann, S. Riethmüller, O. Mayer, C. Hartmann, J. Spatz, M. Möller, M. Ozawa, F. Banhart, M. Garnier, P. Ölhafen. Micellar nanoreactors-preparation and characterization of hexagonally ordered arrays of metallic nanodots. *Adv. Funct. Mater.*, 13 (2003) 853-861
- ¹⁴¹ Y. Xia, J. Rogers, K. Paul, G. Whitesides. Unconventional Methods for Fabricating and Patterning Nanostructures. *Chem. Rev.*, 99 (1999) 1823

- ¹⁴² Verfahren zur Herstellung einer Anordnung von einer Vielzahl von Säulen und von fadenförmigen Strukturen an einer Grenzfläche und deren Anwendung. German Patent Applikation, (2004) DE 10 2004 043908 A1
- ¹⁴³ R. G. Nuzzo, B. R. Zegarski, L. H. Dubois. Fundamental Studies of the Chemisorption of Organosulphur Compounds on Au(111). Implications for Molecular Self-Assembly on Gold Surfaces. *J. Am. Chem. Soc.*, 109 (1987) 733-740
- ¹⁴⁴ A. Ulman. Formation and Structure of Self-Assembled Monolayers. *Chem. Rev.* 96 (1996) 1533-1554
- ¹⁴⁵ M. A. Bryant, J. E. Pemberton. Surface Raman scattering of selfassembled monolayers formed from 1-alkanethiols: Behavior of films at Au and comparison to Ag. *J. Am. Chem. Soc.*, 113 (1991) 8284
- ¹⁴⁶ F. Mirkhalaf, D. J. Schiffrin. Surface spectroscopy and electrochemical characterisation of metal dithizonates covalently attached to gold by a self-assembled cysteamine monolayer. *J. Chem. Soc.*, 94 (1998) 1321-1327
- ¹⁴⁷ J. Blümmel. Entwicklung biofunktionalisierter Nanostrukturen an Grenzflächen zur Untersuchung der Kinetik des molekularen Motorproteins Eg5. Dissertation, Ruprecht-Karls-Universität Heidelberg, (2005)
- ¹⁴⁸ D. Schwendel, R. Dahint, S. Herrwerth, M. Schloerholz, W. Eck, M. Grunze. Temperature Dependence of the Protein Resistance of Poly- and Oligo(ethylene glycol)-Terminated Alkanethiolate Monolayers. *Langmuir*, 17 (2001) 5717-5720
- ¹⁴⁹ M. Pfaff. Recognition sites of RGD-dependent integrins. (1997) 101–121
- ¹⁵⁰ M. Pierschbacher, E. Ruoslahti. Influence of stereochemistry of the sequence Arg-Gly-Asp-Xaa on binding specificity in cell adhesion. *J. Biol. Chem.*, 262 (1987) 17294–17298
- ¹⁵¹ M. Aumailley, M. Gurrath, G. Müller, J. Calvete, R. Timpl, H. Kessler. Arg-Gly-Asp constrained within cyclic pentapeptides. Strong and selective inhibitors of cell adhesion to vitronectin and laminin fragment P1. *FEBS Lett.*, 291 (1991) 50–54
- ¹⁵² M. Gurrath, G. Mueller, H. Kessler, M. Aumailley, R. Timpl. Conformation/activity studies of rationally designed potent anti-adhesive RGD peptides. *Eur. J. Biochem.*, 210 (1992) 911–921
- ¹⁵³ R. Haubner, R. Gratias, B. Diefenbach, S. Goodman, A. Jonczyk, H. Kessler. Structural and functional aspects of RGD-containing cyclic pentapeptides as highly potent and selective integrin $\alpha V\beta 3$ antagonists. *J. Am. Chem. Soc.*, 118 (1996) 7461–7472
- ¹⁵⁴ M. Kantlehner, P. Schaffner, D. Finsinger, J. Meyer, A. Jonczyk, B. Diefenbach, B. Nies, G. Hölzemann, S. Goodman, H. Kessler. Surface coating with cyclic RGD peptides stimulates osteoblast adhesion and proliferation as well as bone formation. *Chem. Bio. Chem.* 1 (2000) 107–114
- ¹⁵⁵ B. Jeschke, J. Meyer, A. Jonczyk, H. Kessler, P. Adamietz, N. Meenen, M. Kantlehner, C. Goepfert, B. Nies. RGD-peptides for tissue engineering of articular cartilage. *Biomaterials* 23 (2002) 3455–3463
- ¹⁵⁶ D. Davenport, J. Nicol. Luminescence in hydromedusae. *Proc. R. Soc. London Series B - Biol. Sci.*, 144 (1995) 399–411
- ¹⁵⁷ R. Y. Tsien. The green fluorescent protein. *Ann. Rev. Biochemistry*, 67 (1998) 509–544

Hiermit erkläre ich an Eides statt, dass ich die vorliegende Arbeit selbständig und ohne unerlaubte Hilfsmittel angefertigt habe.

Stuttgart, den 06. Juni 2006

Stefan Gräter